Daya Bay 原子炉ニュートリノ実験における反電子ニュートリノ消失の精密測定

中島　康博

ローレンス・バークレー国立研究所

2013年10月8日

京都大学

Outline

- Introduction
- Daya Bay experiment
- Current data sets
- **Spectrum analysis**
  - Challenges and improvements
  - Oscillation parameter extraction
- Summary

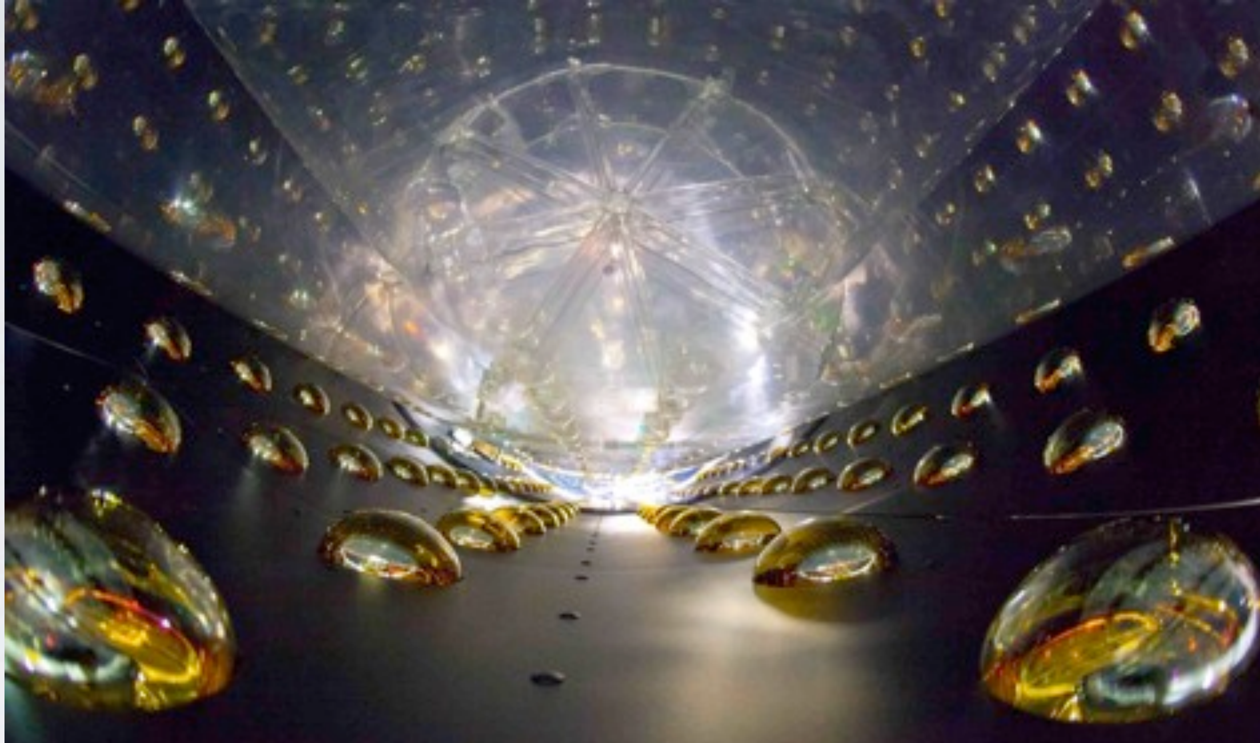

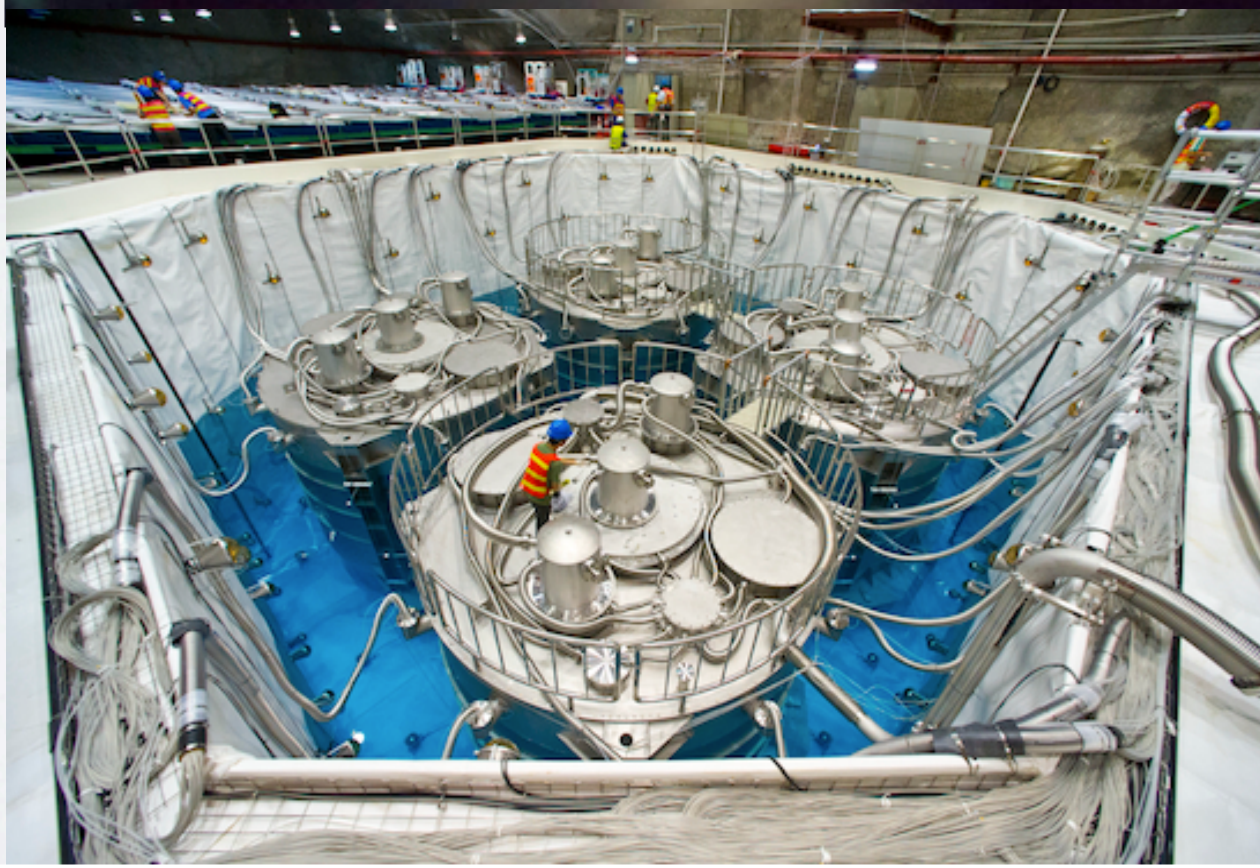

Neutrino Mixing

- Neutrino flavor (weak) eigenstates and mass eigenstates are mixed

$$|\nu_\alpha\rangle = \sum_i U_{\alpha i} |\nu_i\rangle$$

Weak eigenstate (α = e, μ, τ) — Mass eigenstate (i = 1, 2, 3) — MNS mixing matrix

- Neutrinos change their flavor as they travel (neutrino oscillation)
- Natural interferometer to explore fundamental nature of neutrinos

Two neutrino case: $P(\nu_\alpha \to \nu_\beta) = |\langle \nu_\beta | \nu(t) \rangle|^2 = \sin^2 2\theta \sin^2 \left(\Delta m^2 \frac{L}{4E} \right)$

Amplitude ($\sin^2 2\theta$) **Frequency** ($\Delta m^2 \frac{L}{4E}$)

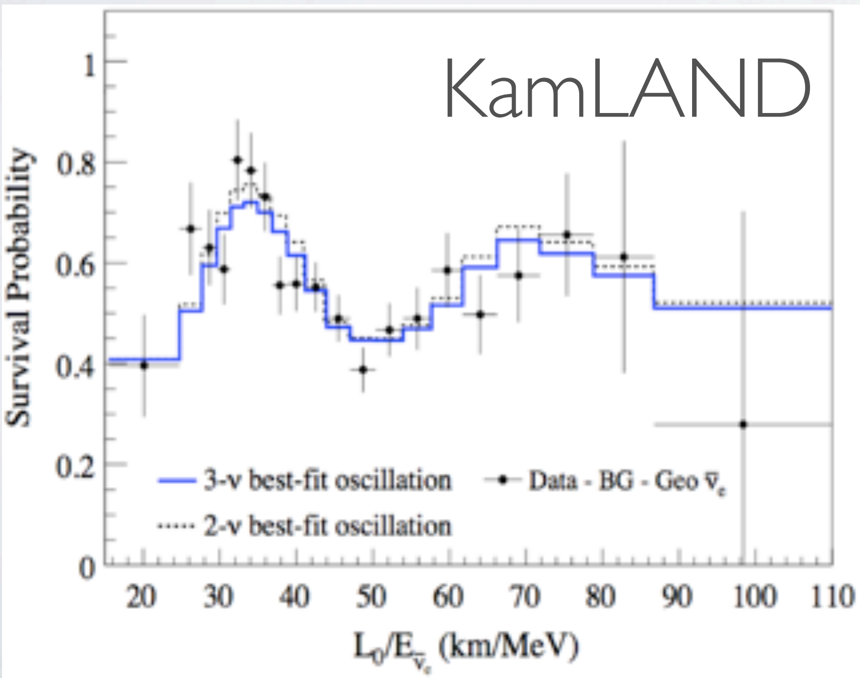

θ	**: mixing angle**
Δm^2	**: mass squared difference**
L	: the distance traveled
E	: the energy of neutrino

Neutrino Mixing

All the three angles are finally observed!

$c_{ij} \equiv \cos\theta_{ij}$ and $s_{ij} \equiv \sin\theta_{ij}$

$$U = \begin{pmatrix} 1 & 0 & 0 \\ 0 & c_{23} & s_{23} \\ 0 & -s_{23} & c_{23} \end{pmatrix} \times \begin{pmatrix} c_{13} & 0 & s_{13}e^{-i\delta} \\ 0 & 1 & 0 \\ -s_{13}e^{i\delta} & 0 & c_{13} \end{pmatrix} \times \begin{pmatrix} c_{12} & s_{12} & 0 \\ -s_{12} & c_{12} & 0 \\ 0 & 0 & 1 \end{pmatrix}$$

$\theta_{23} \approx 45^o$
Atmospheric ν
Accelerator ν

$\theta_{13} \sim 9^o$
First >5σ observation at Daya Bay (2012)

$\theta_{12} \approx 35^o$
Solar ν
Long-Baseline Reactor ν

- Open questions:
  - Is there CP-violation in neutrino sector?
  - What is mass hierarchy?
  - Are there any other type of neutrinos?

Precise measurement of mixing angle is a key to answer those questions.

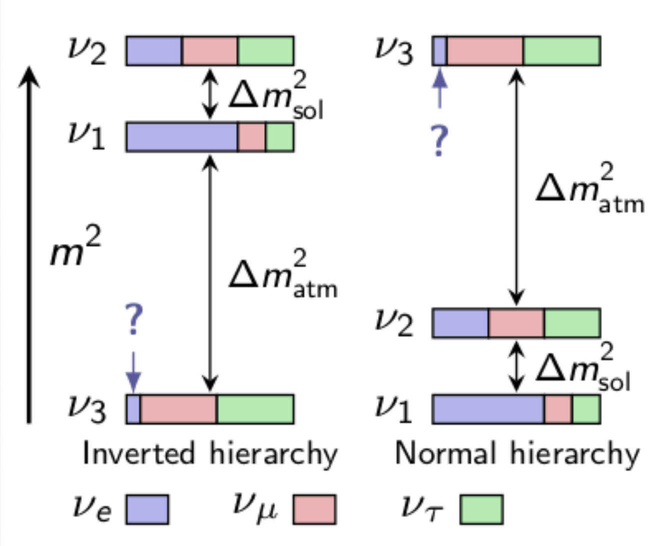

Reactor Antineutrinos

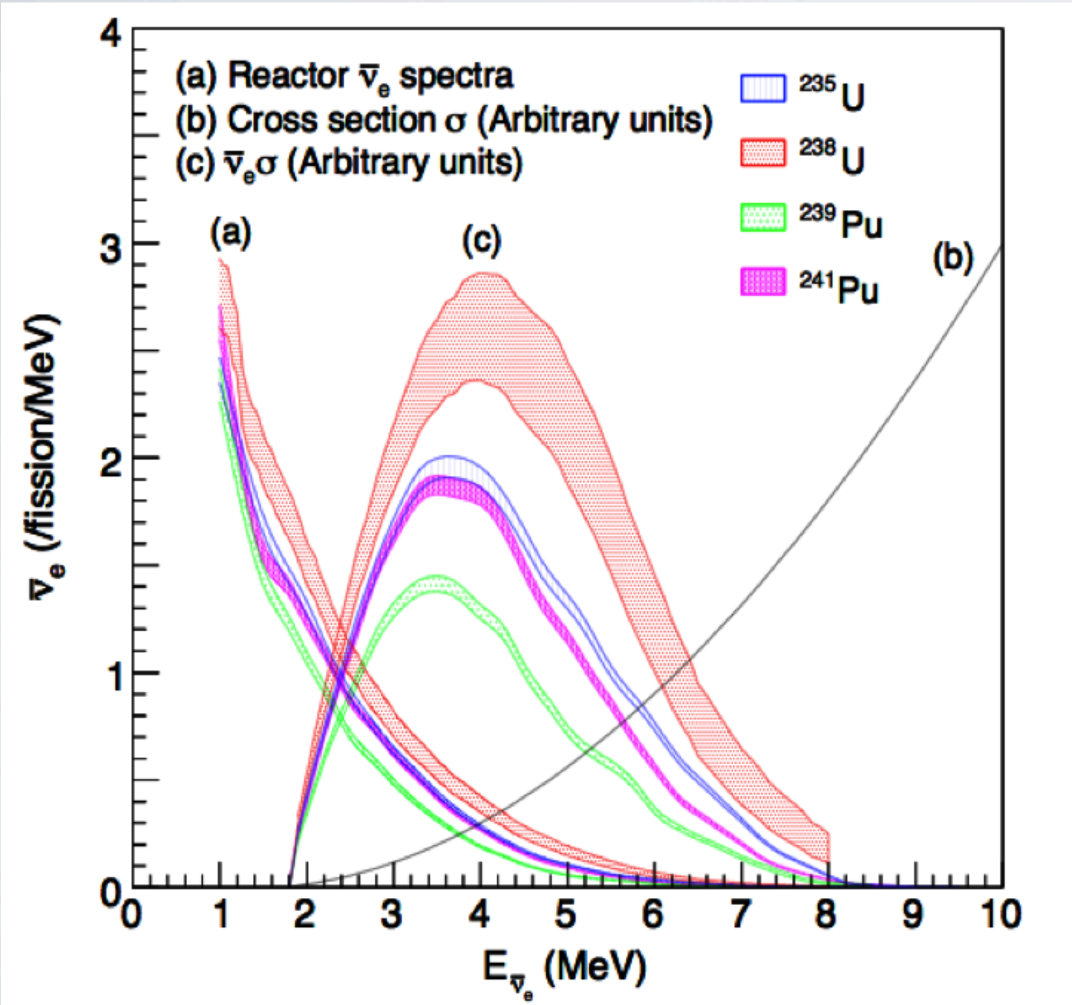

- Most powerful man-made source of antineutrinos, and it's free
- Nuclear fission release:
  - 6 antineutrinos/fission
  - Typically ~10^{20} fissions/second
- Detected through inverse beta decay
- Broad spectrum with mean energy of ~4 MeV

Reactor Neutrino Oscillation

$$P(\overline{\nu}_e \to \overline{\nu}_e) = 1 - \sin^2 2\theta_{13} \sin^2\left(\Delta m^2_{ee} \frac{L}{4E}\right) - \cos^4\theta_{13} \sin^2 2\theta_{12} \sin^2\left(\Delta m^2_{21} \frac{L}{4E}\right)$$

$$\Delta m^2_{ee} \simeq \Delta m^2_{32} \simeq \Delta m^2_{31}$$

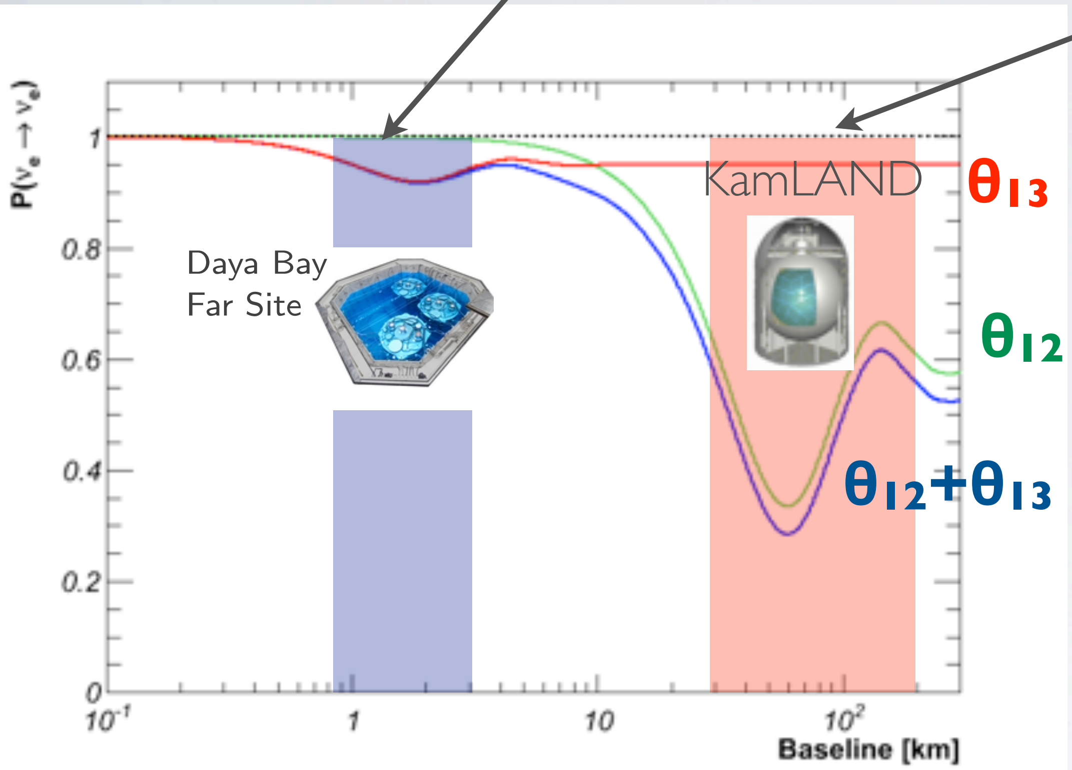

Survival probability at 1.6 km

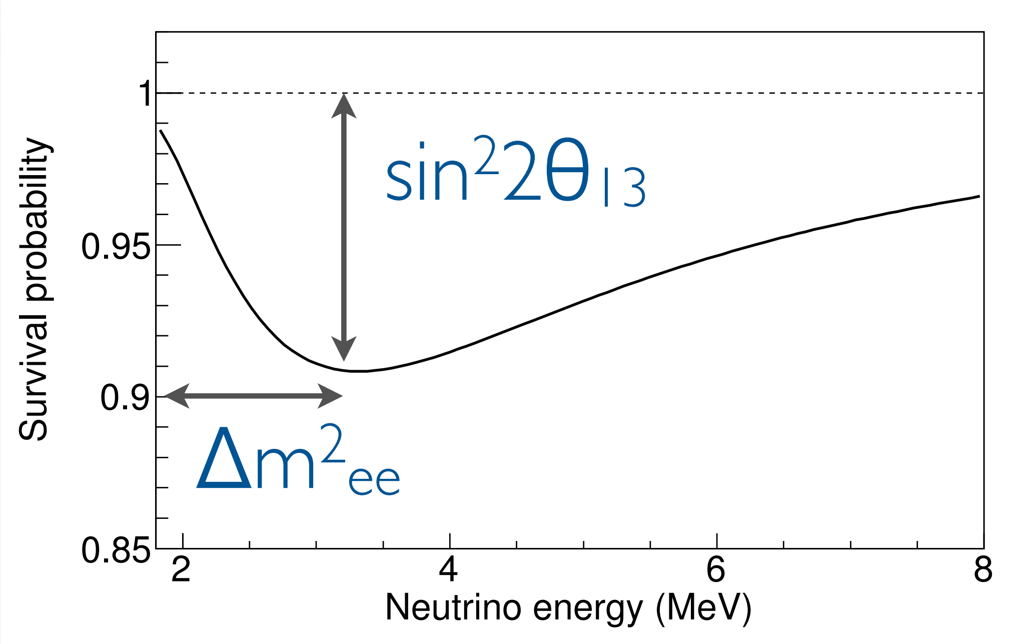

Characteristic deficit at ~2 km due to θ_{13} and Δm^2_{ee}

First established by Daya Bay (2012)

Now moving towards precision measurement!

Complementarity

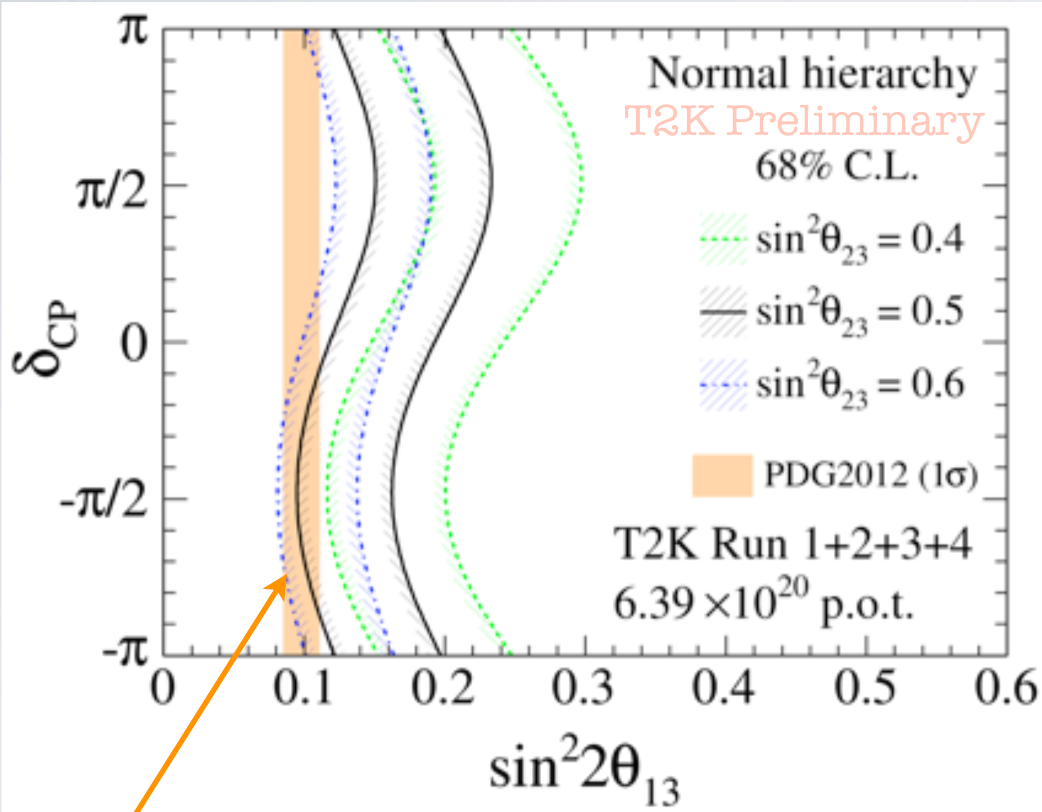

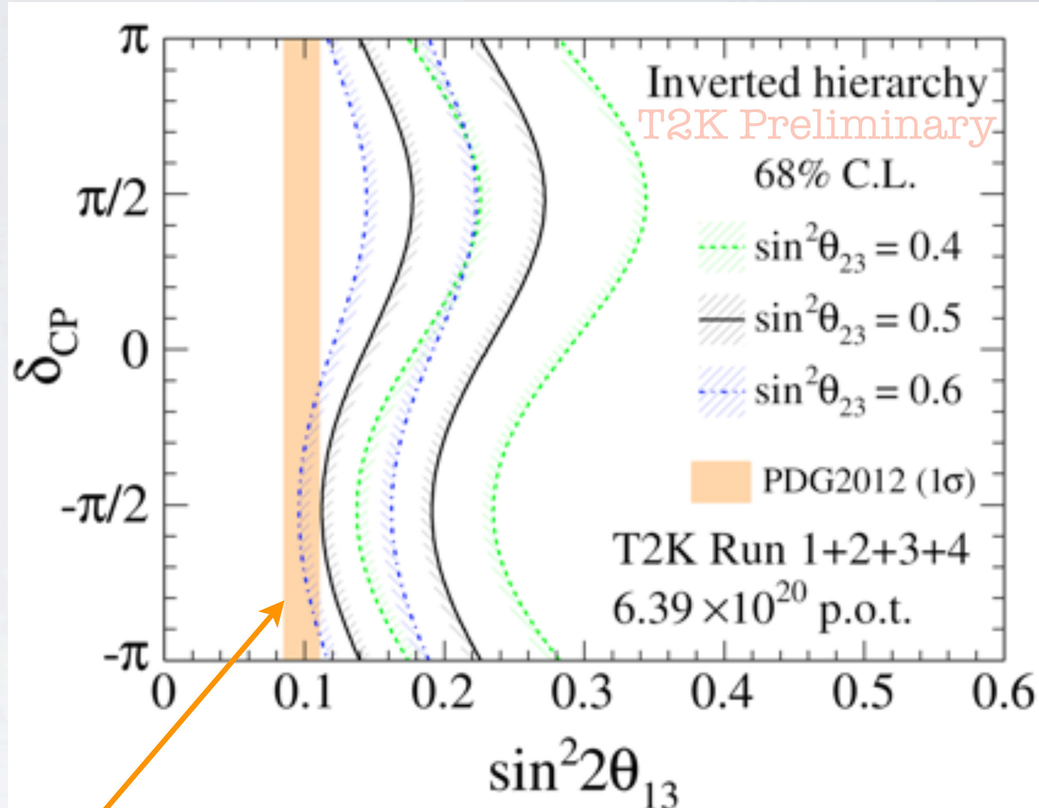

$\sin^2 2\theta_{13}$ results from reactor experiments
(Dominated by Daya Bay)

M. Wilking @EPS-HEP2013

Precise measurement of $\sin^2 2\theta_{13}$ is an essential ingredient for resolving CP violation and mass hierarchy

Daya Bay Experiment

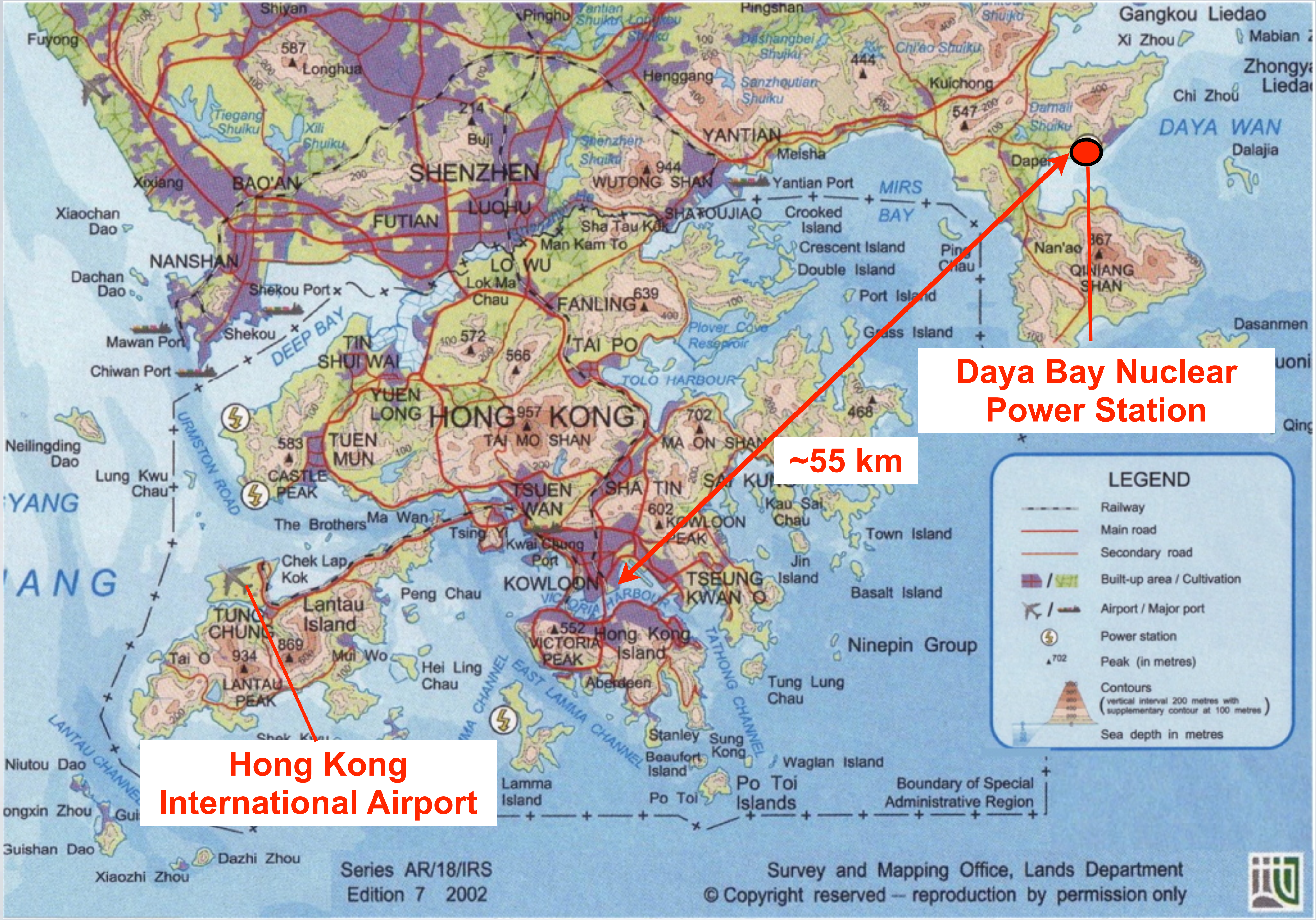
Daya Bay Nuclear Power Station
~55 km
Hong Kong International Airport
HONG KONG
SHENZHEN
DAYA WAN
LEGEND
Railway
Main road
Secondary road
Built-up area / Cultivation
Airport / Major port
Power station
Peak (in metres)
Contours
Sea depth in metres
Boundary of Special Administrative Region
Series AR/18/IRS
Edition 7 2002
Survey and Mapping Office, Lands Department
© Copyright reserved – reproduction by permission only

Daya Bay:
A Powerful Neutrino Source at an Ideal Location

Daya Bay Collaboration

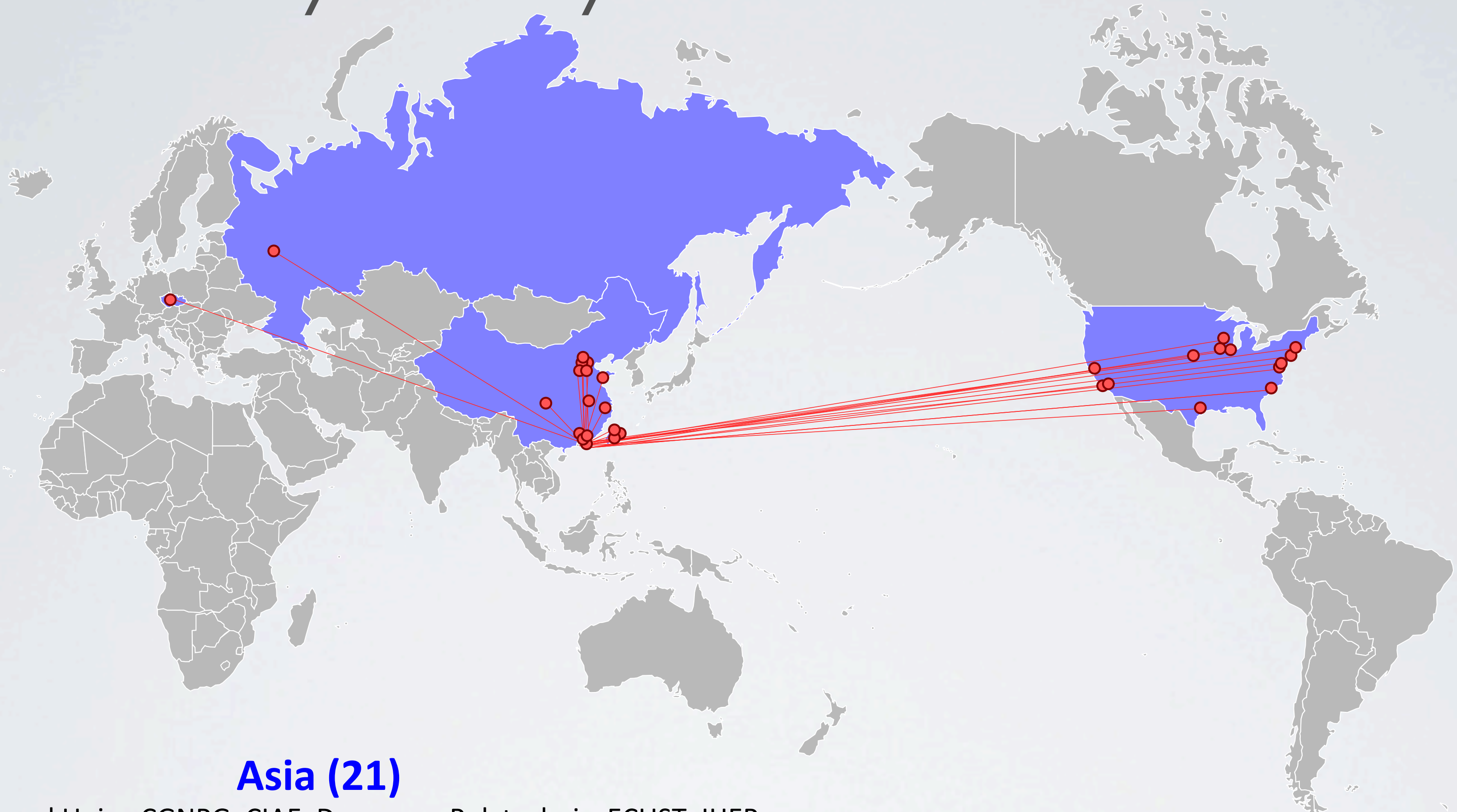

Asia (21)

Beijing Normal Univ., CGNPG, CIAE, Dongguan Polytechnic, ECUST, IHEP, Nanjing Univ., Nankai Univ., NCEPU, Shandong Univ., Shanghai Jiao Tong Univ., Shenzhen Univ., Tsinghua Univ., USTC, Xian Jiaotong Univ., Zhongshan Univ.,
Chinese Univ. of Hong Kong, Univ. of Hong Kong,
National Chiao Tung Univ., National Taiwan Univ., National United Univ.

Europe (2)

Charles University, JINR Dubna

North America (17)

Brookhaven Natl Lab, CalTech, Illinois Institute of Technology, Iowa State, Lawrence Berkeley Natl Lab, Princeton, Rensselaer Polytechnic, Siena College, UC Berkeley, UCLA, Univ. of Cincinnati, Univ. of Houston, UIUC, Univ. of Wisconsin, Virginia Tech, William & Mary, Yale

~230 collaborators from 40 institutions

Strategy for Precise Measurement

Relative measurement with functionally identical detectors

Most of uncertainty from detector response and absolute flux cancel

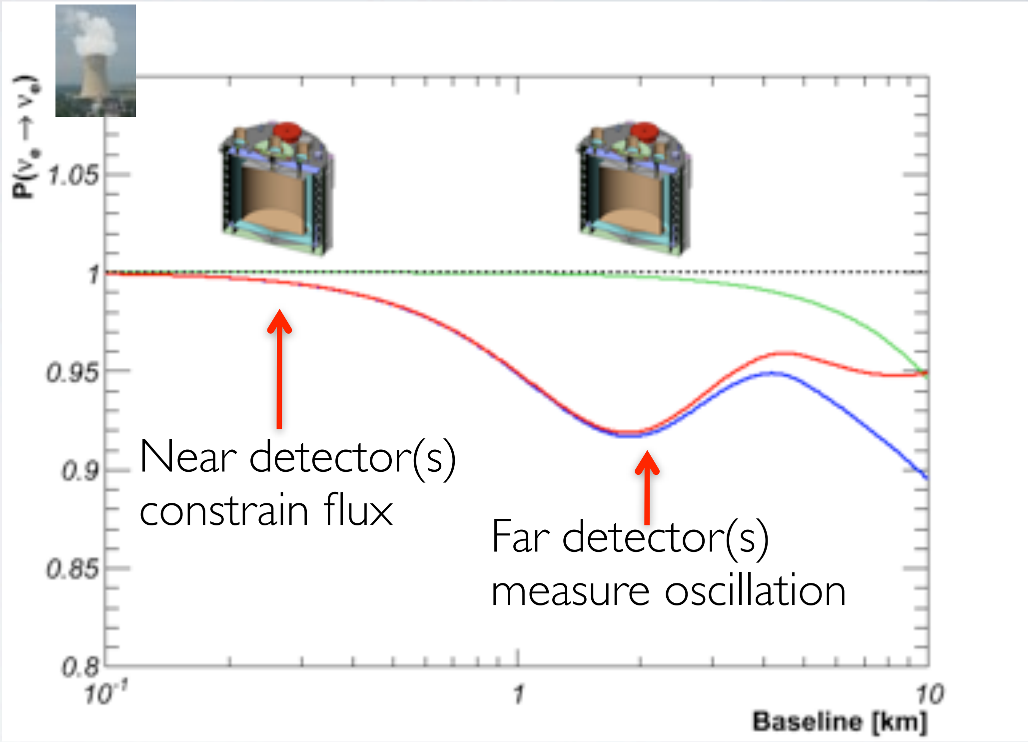

Far/Near ν_e Ratio

Distances from reactor

Oscillation deficit

$$\frac{N_\mathrm{f}}{N_\mathrm{n}} = \left(\frac{N_\mathrm{p,f}}{N_\mathrm{p,n}}\right)\left(\frac{L_\mathrm{n}}{L_\mathrm{f}}\right)^2\left(\frac{\epsilon_\mathrm{f}}{\epsilon_\mathrm{n}}\right)\left[\frac{P_\mathrm{sur}(E,L_\mathrm{f})}{P_\mathrm{sur}(E,L_\mathrm{n})}\right]$$

Detector Target Mass

Detector efficiency

Experiment Layout

Far hall measures oscillation

Two near halls constrain reactor flux

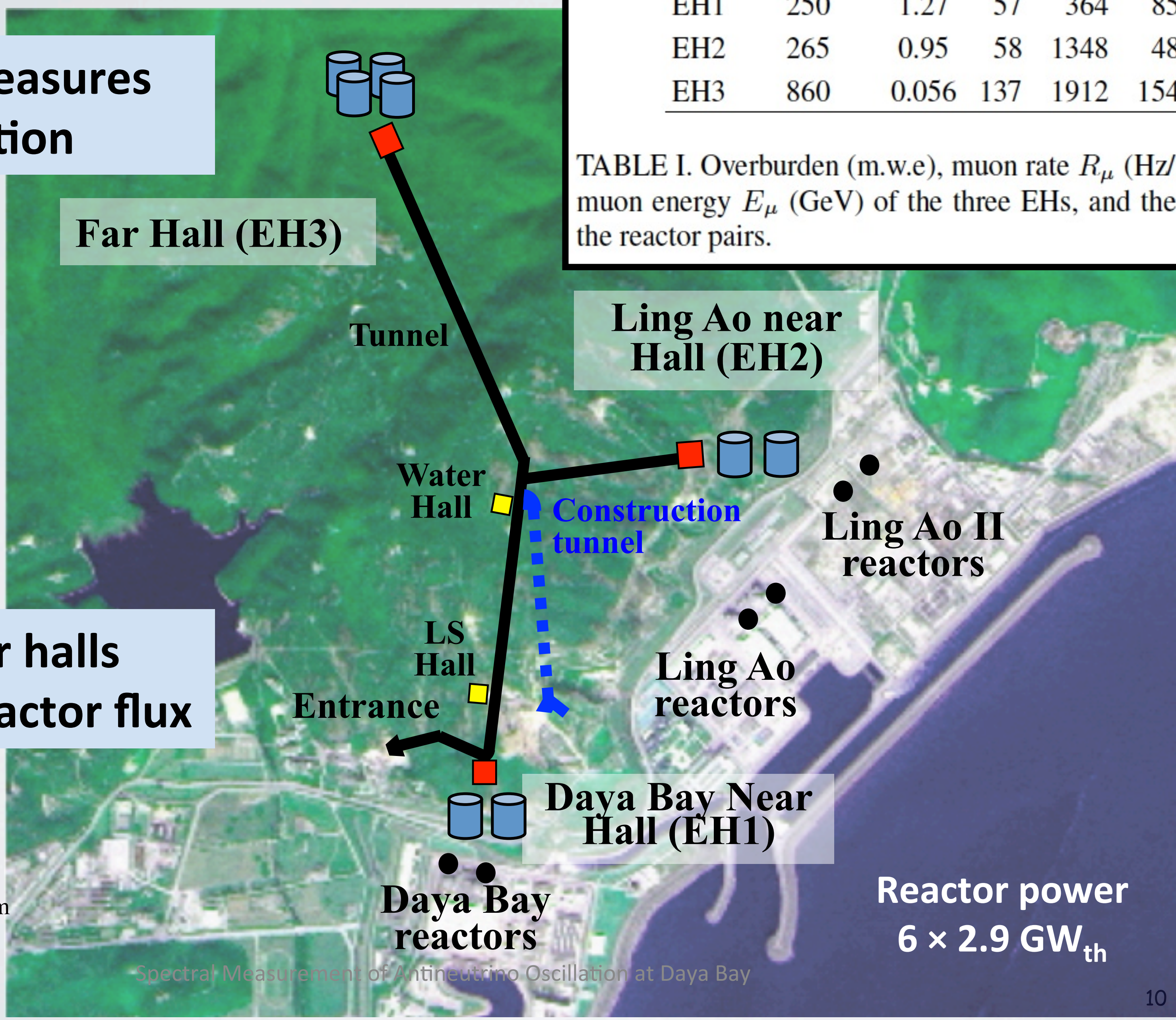

	Overburden	R_μ	E_μ	D1,2	L1,2	L3,4
EH1	250	1.27	57	364	857	1307
EH2	265	0.95	58	1348	480	528
EH3	860	0.056	137	1912	1540	1548

TABLE I. Overburden (m.w.e), muon rate R_μ (Hz/m^2), and average muon energy E_μ (GeV) of the three EHs, and the distances (m) to the reactor pairs.

Daya Bay Advantages

Ideal baseline

- Detector locations optimized to known parameter space of Δm^2_{ee}
- Better sensitivity to both θ_{13} and Δm^2_{ee}

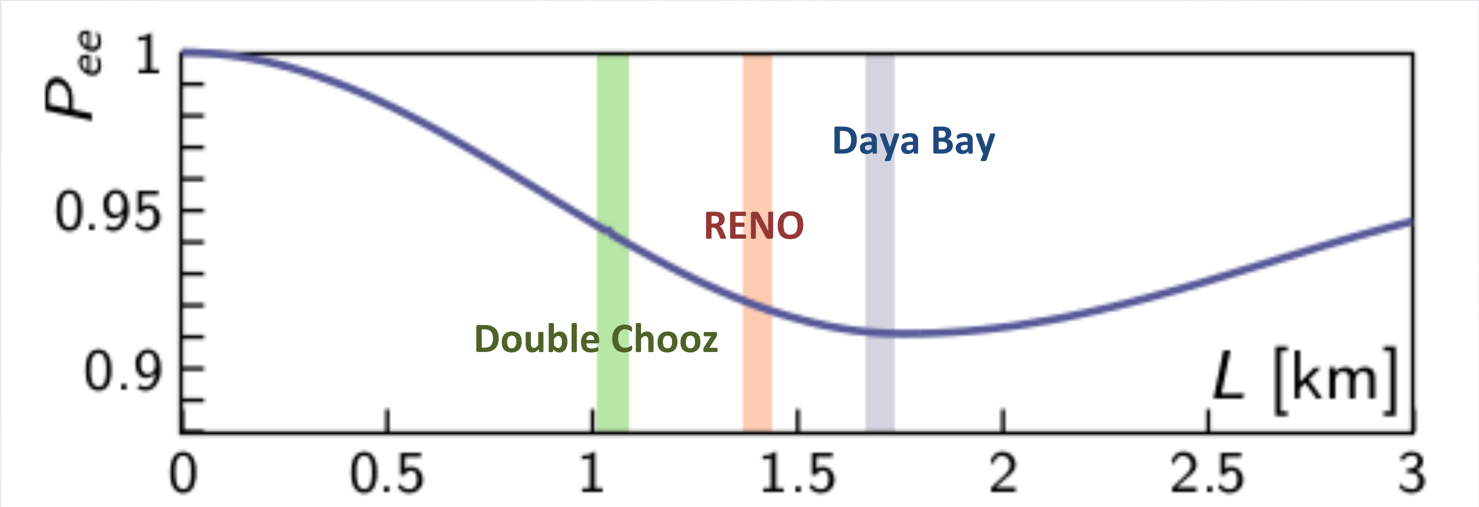

Stronger, bigger, and deeper

	Reactor [GW_{th}]	Target [tons]	Depth [m.w.e]
Double Chooz	8.6	16 (2 × 8)	300, 120 (far, near)
RENO	16.5	32 (2 × 16)	450, 120
Daya Bay	17.4	160 (8 × 20)	860, 250
	Large Signal		Low Background

Daya Bay Detector

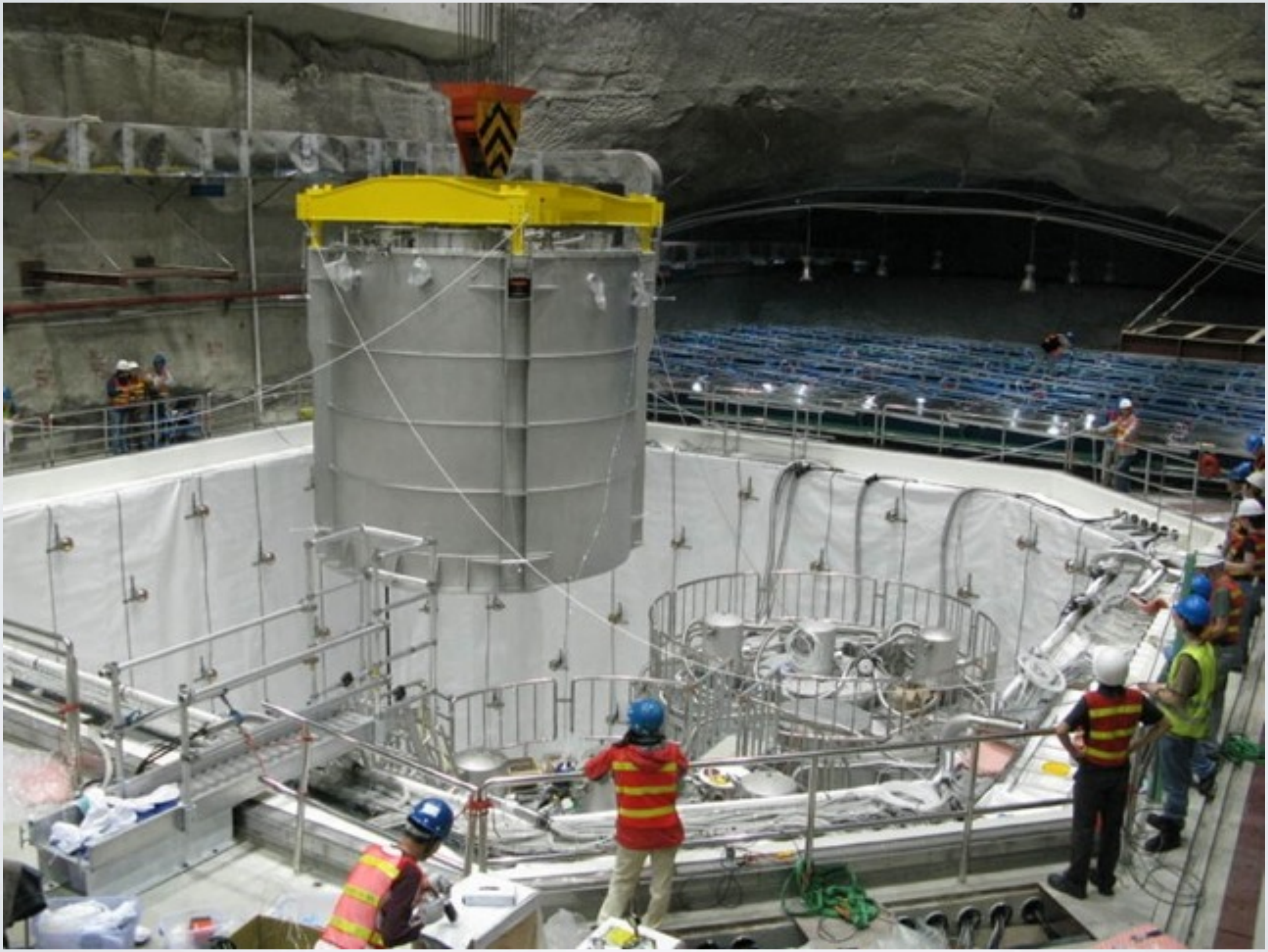

Detection Method

Antineutrinos are detected via inverse beta decay reaction

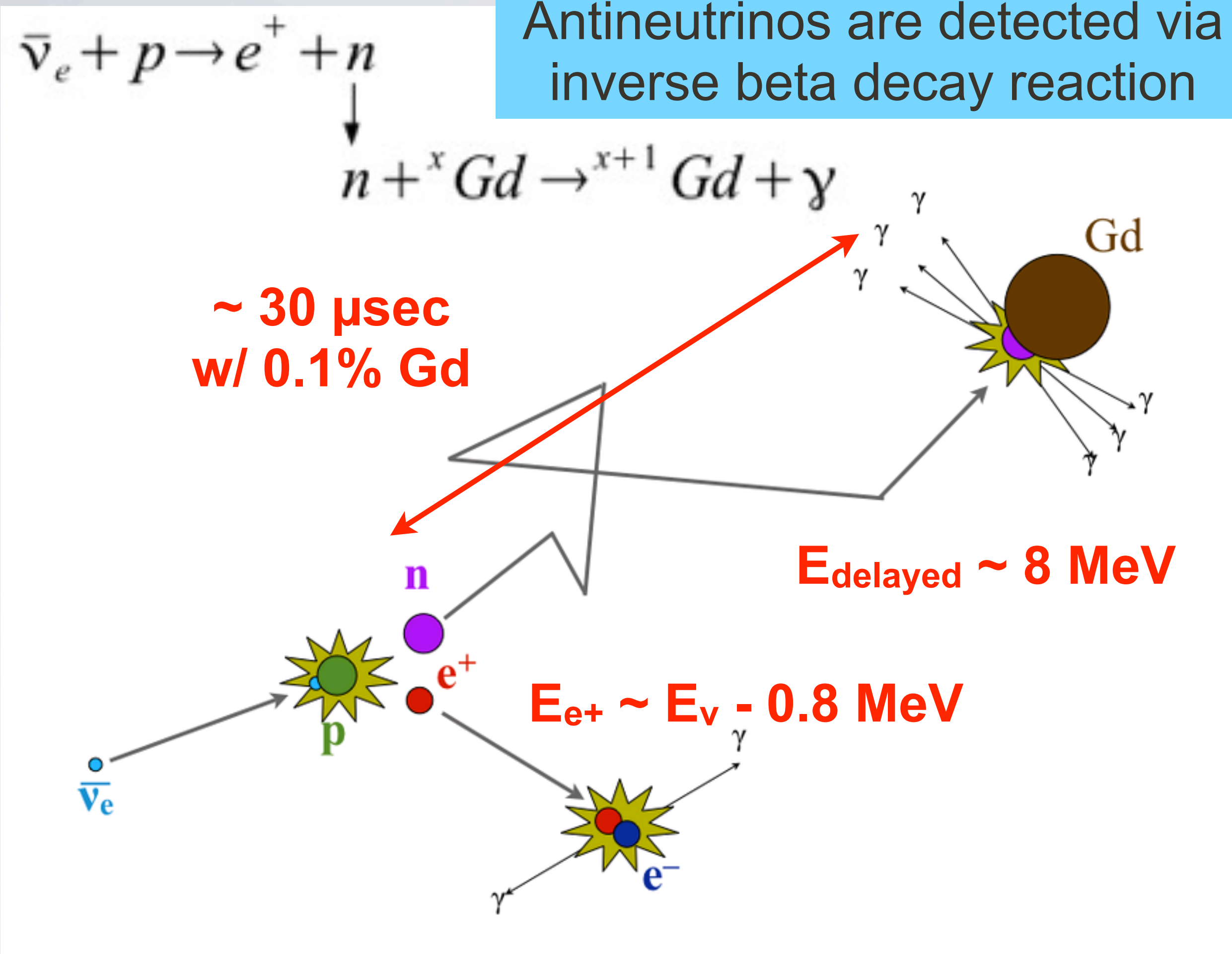

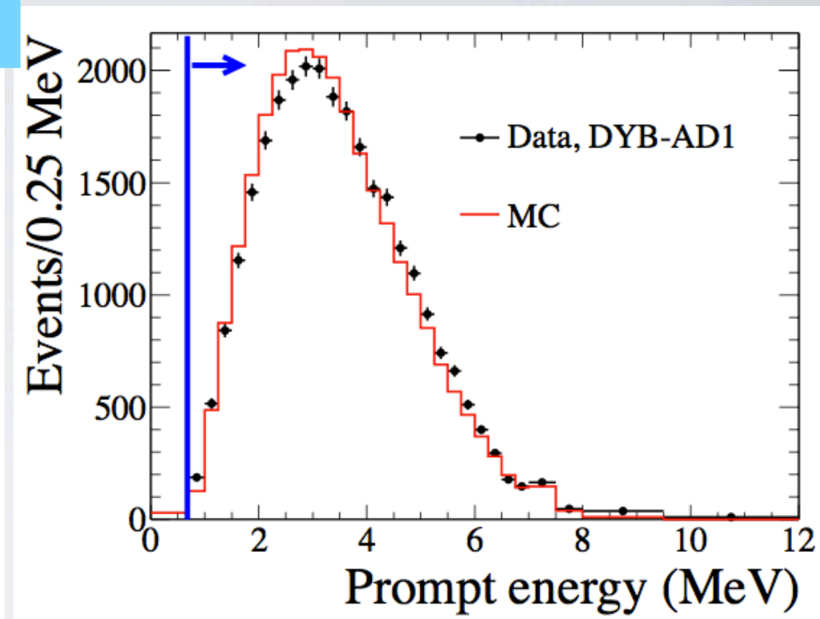

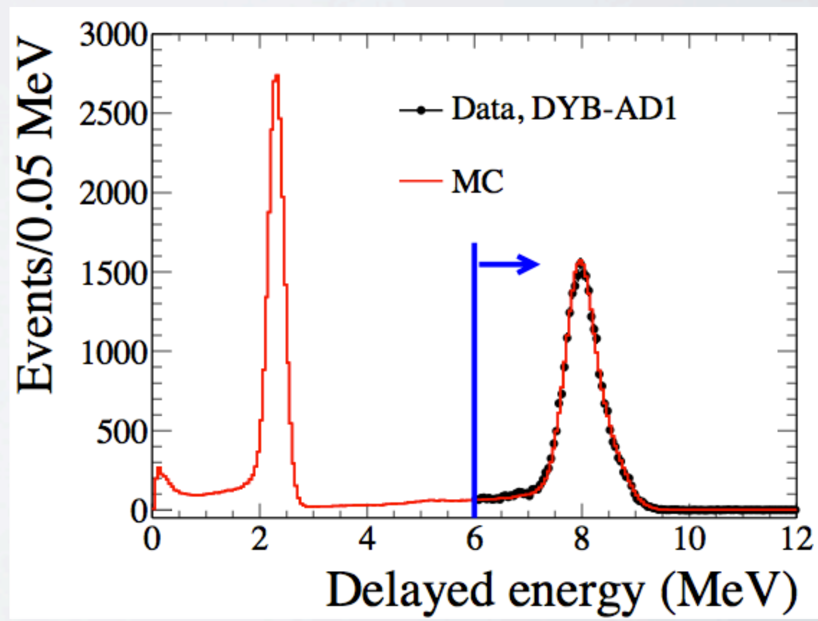

Prompt + Delayed coincidence

- Prompt positron: carries antineutrino energy
- Delayed neutron capture: efficiently tag antineutrino signal

Antineutrino Detector

- 8 functionally identical detectors
- Three-zone cylindrical modules:

Zone	Mass	Liquid	Purpose
Inner acrylic vessel	20 t	Gd-doped liquid scintillator	**Anti-neutrino target**
Outer acrylic vessel	22 t	Liquid scintillator	Gamma catcher (from target zone)
Stainless steel vessel	40 t	Mineral Oil	Radiation shielding

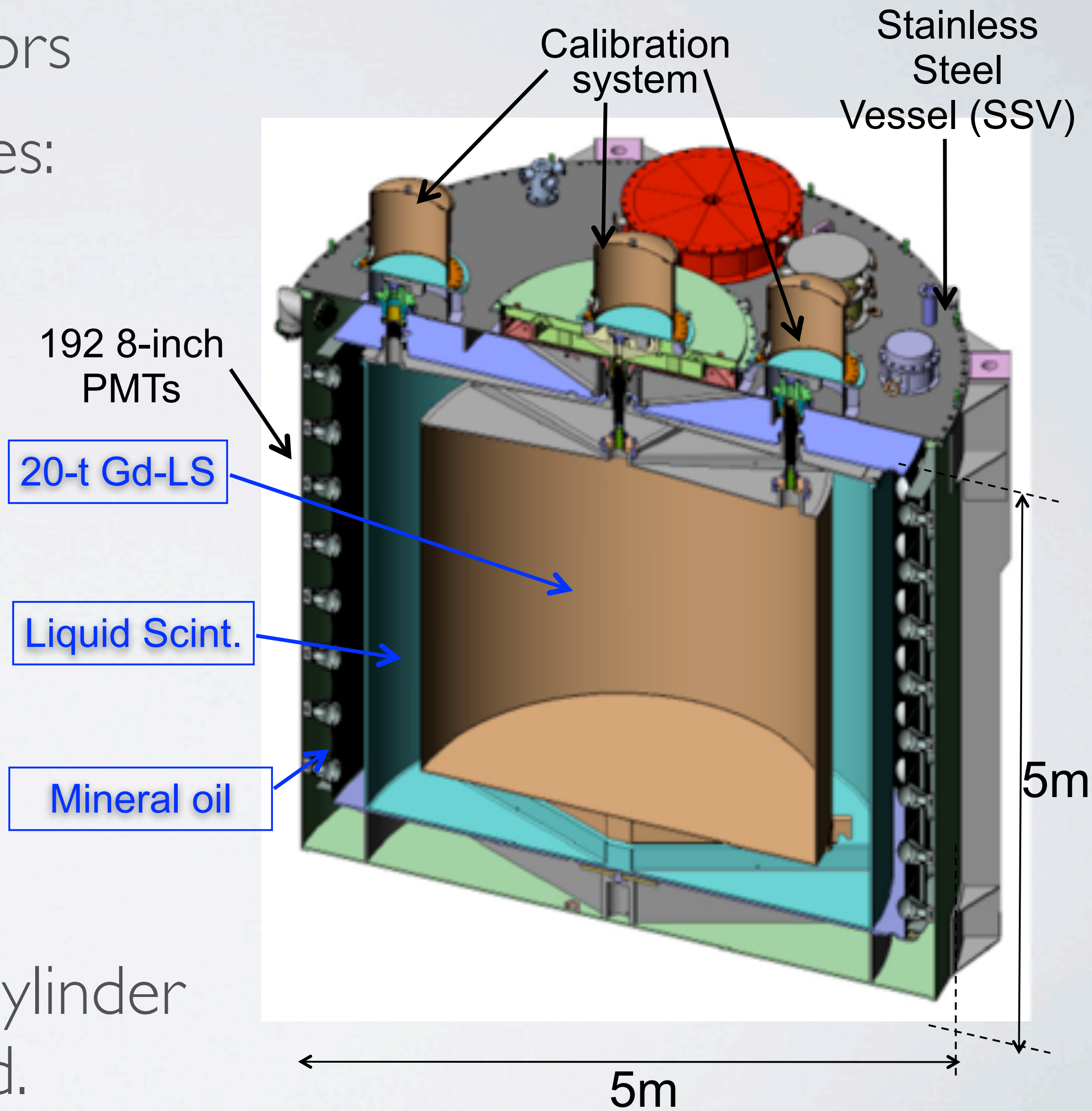

- Reflectors at top/bottom of cylinder are used to increase light yield.

Calibration System

- Three Automated Calibration Units (ACUs) per detector.
- Deploy sources along the z-axis
- Three sources + LED in each ACU, on a turn table.
  - ^{68}Ge (γ, 2 x 0.511 MeV)
  - ^{60}Co (γ, 2.506 MeV)
  - ^{241}Am-^{13}C (n, 8MeV)
  - LED for timing and gain calibration
- Temporary special calibration sources:
  - γ: ^{137}Cs(0.622 MeV), ^{54}Mn(0.835 MeV), ^{40}K (1.461 MeV)
  - n: ^{241}Am-^{9}Be, ^{239}Pu-^{13}C

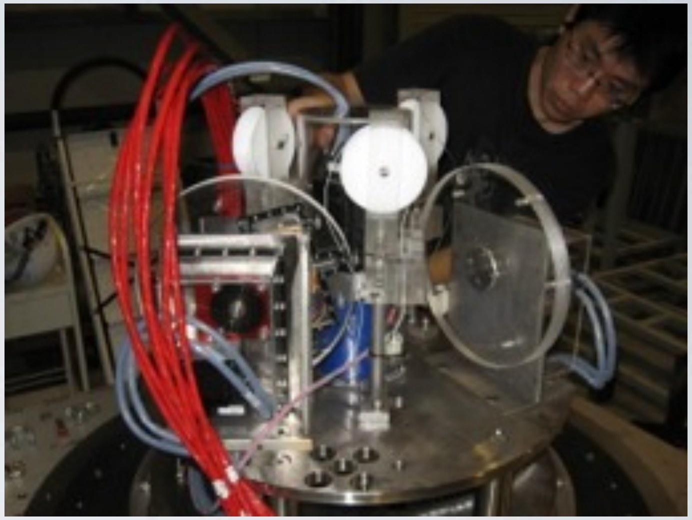

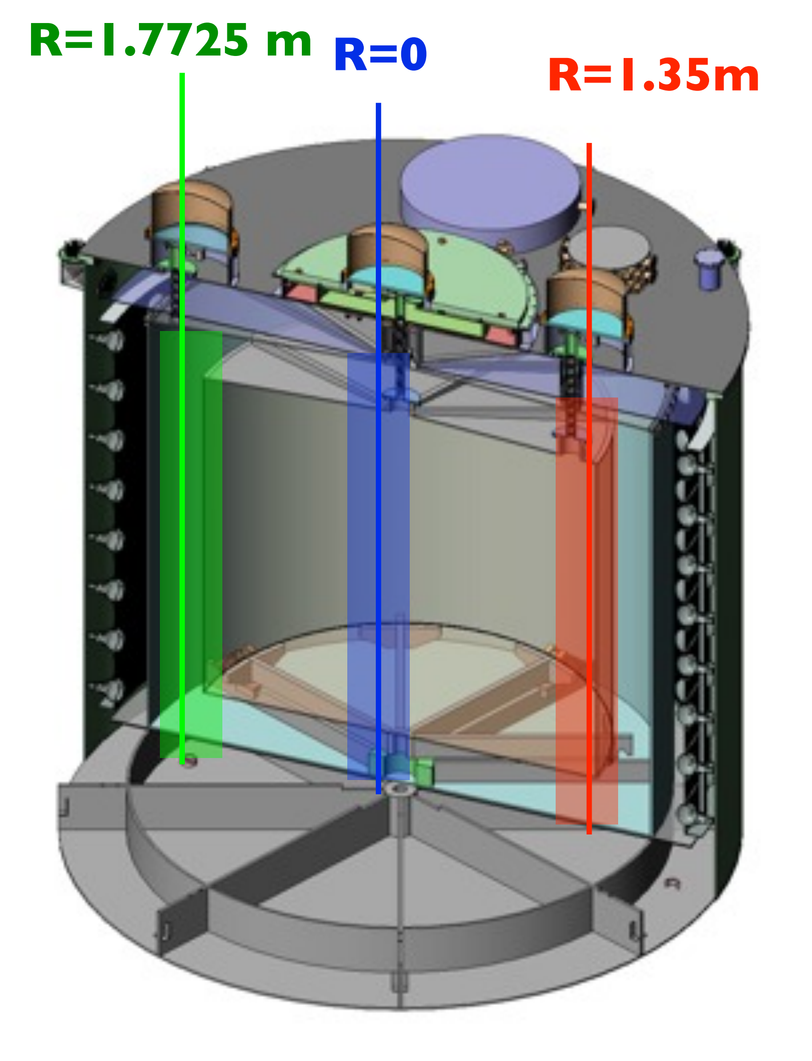

Muon Tagging System

- 2.5 meter thick two-section water shield
  - Cherenkov detector to tag cosmic ray muons.
  - Shield for neutrons and gammas from surrounding materials.
- RPC
  - Covers water pool to provide further muon tagging.

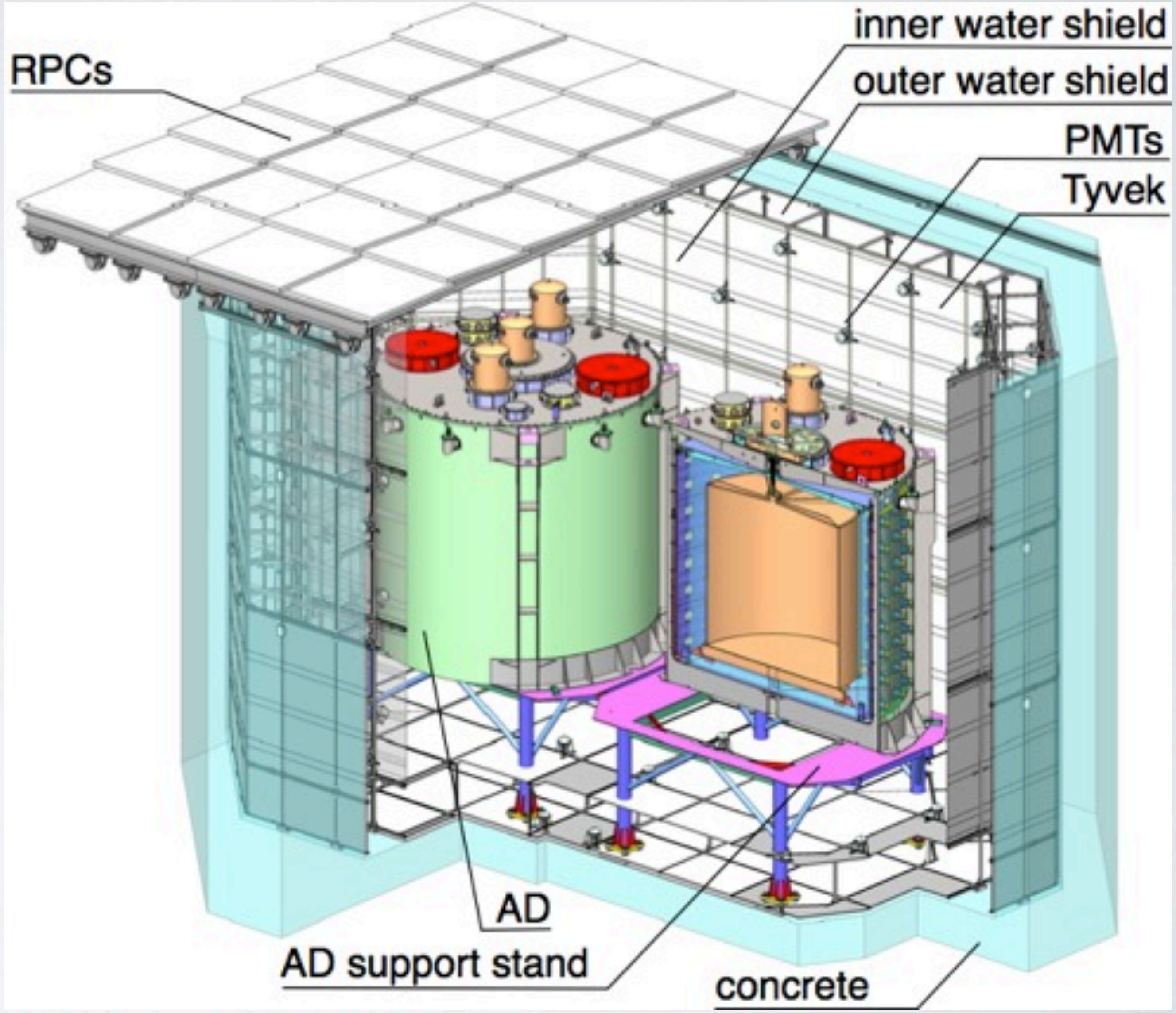

Data Set

Data sets

Two detector comparison [1202.6181]

- 90 days of data, Daya Bay near only
- NIM A **685** (2012), 78-97

First oscillation analysis [1203:1669]

- 55 days of data, 6 ADs near+far
- PRL **108** (2012), 171803

Improved oscillation analysis [1210.6327]

- 139 days of data, 6 ADs near+far
- CP C **37** (2013), 011001

Spectral Analysis

- 217 days, complete 6 AD period
- 55% more statistics than CPC result

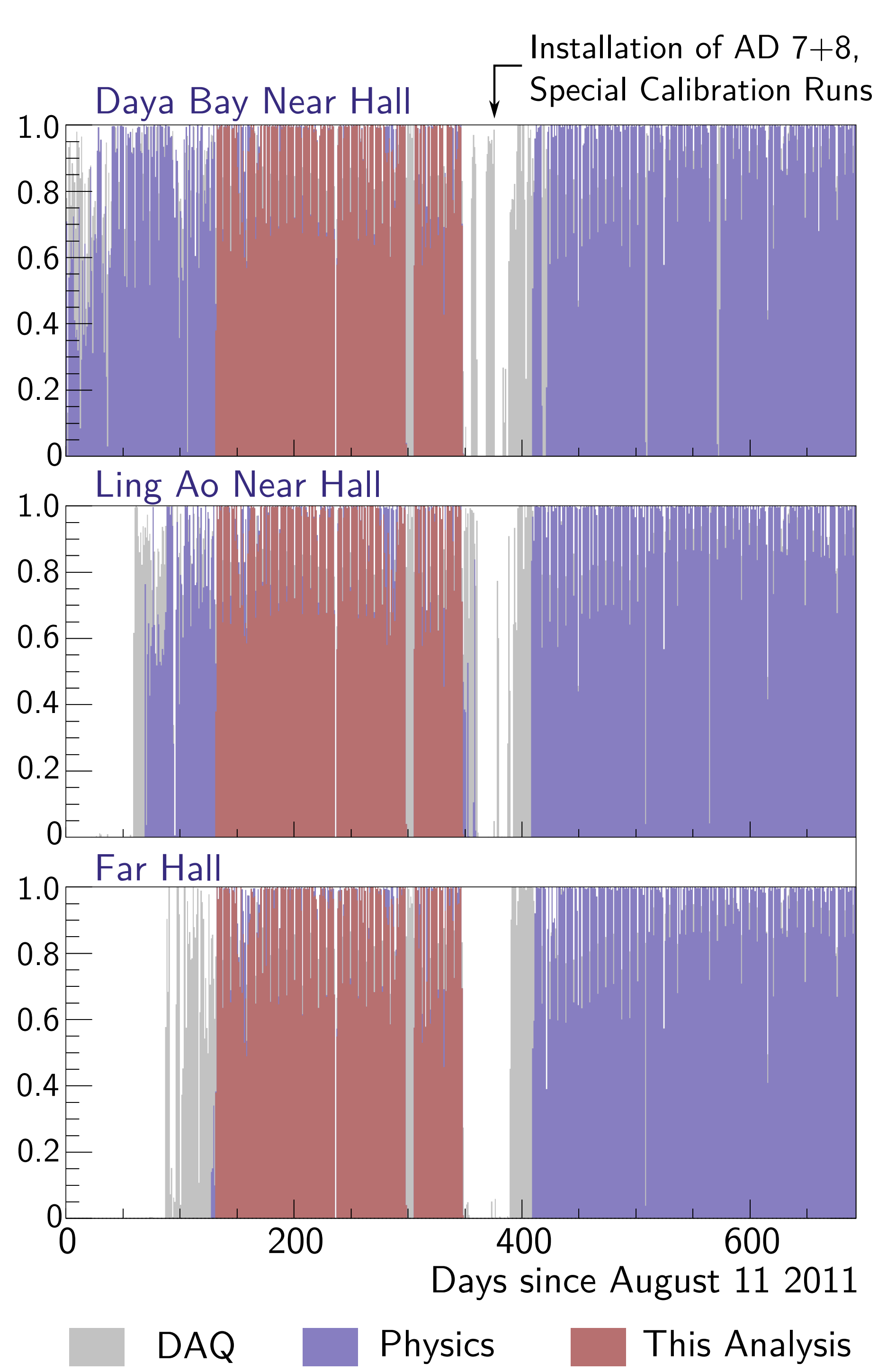

Antineutrino Selection

① Reject spontaneous PMT light emission ("flashers")

② Prompt positron:
0.7 MeV < Ep < 12 MeV

③ Delayed neutron:
6.0 MeV < Ed < 12 MeV

④ Neutron capture time:
1 μs < t < 200 μs

⑤ Muon veto:

- Water pool muon (>12 hit PMTs): Reject [-2μs; 600μs]
- AD muon (>3000 photoelectrons): Reject [-2 μs; 1400μs]
- AD shower muon (>3×10^5 p.e.): Reject [-2 μs; 0.4s]

⑥ Multiplicity:

- No additional prompt-like signal
  400μs before delayed neutron
- No additional delayed-like signal
  200μs after delayed neutron

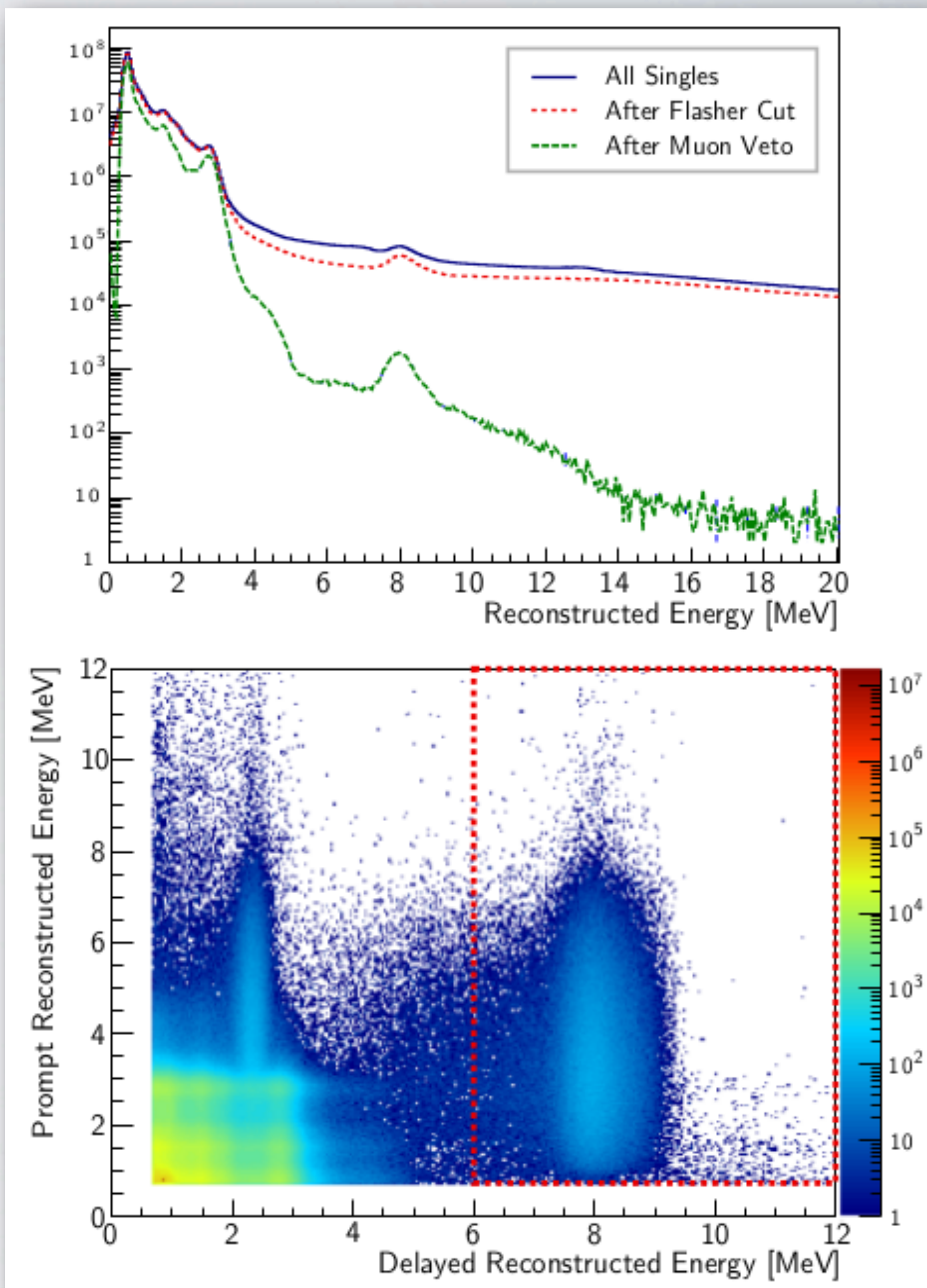

Antineutrino Rate vs. Time

Detected rate strongly correlated with reactor flux expectations

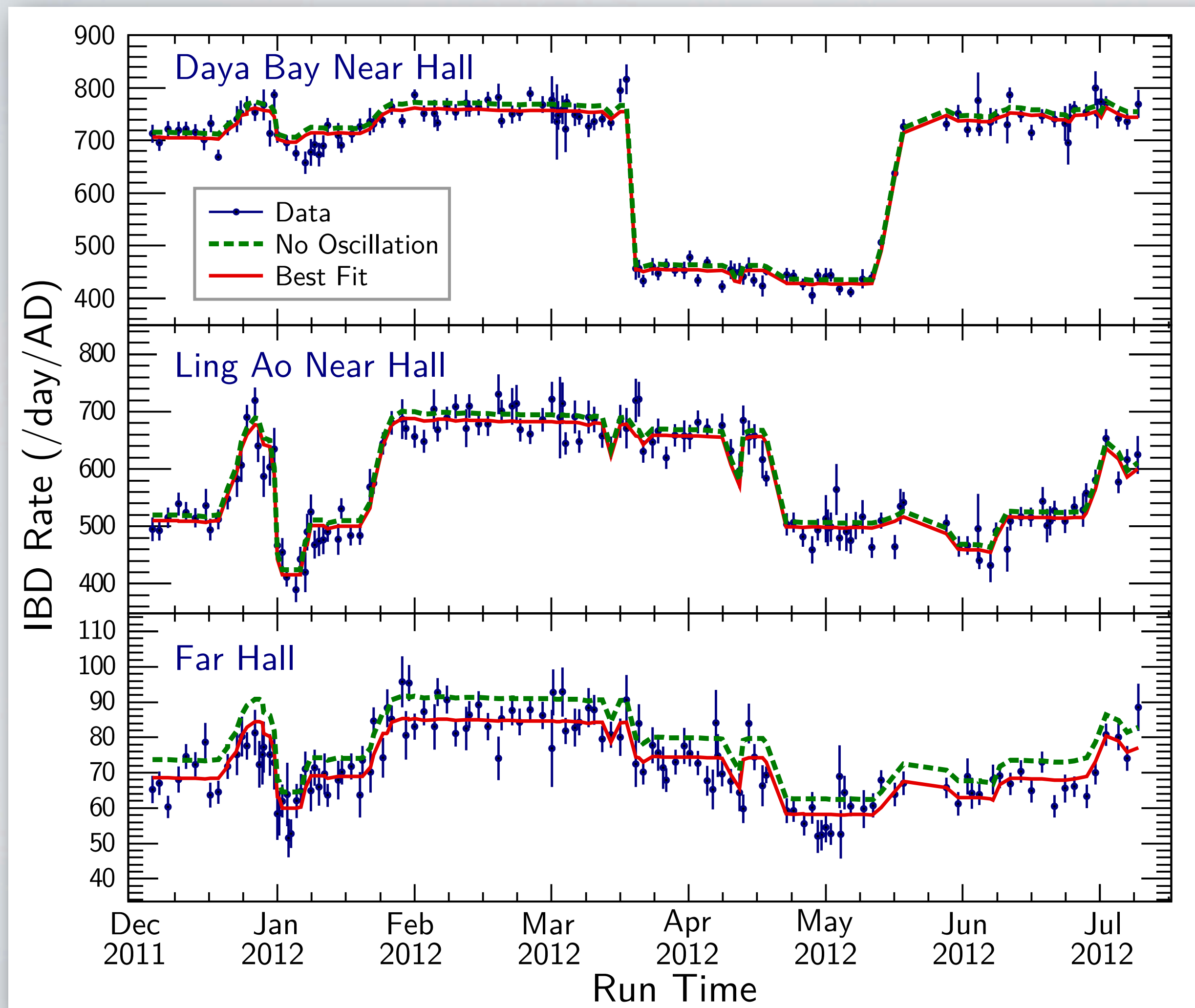

- Absolute normalization determined by fit to data
- Normalization within a few percent of expectations

Signal and Background Summary

	Near Halls			Far Hall		
	AD1	**AD2**	**AD3**	**AD4**	**AD5**	**AD6**
IBD candidates	101290	102519	92912	13964	13894	13731
DAQ live time (day)	191.001		189.645		189.779	
Efficiency	0.7957	0.7927	0.8282	0.9577	0.9568	0.9566
Accidentals (/day/AD)*	9.54±0.03	9.36±0.03	7.44±0.02	2.96±0.01	2.92±0.01	2.87±0.01
Fast neutron (/day/AD)*	0.92±0.46		0.62±0.31		0.04±0.02	
^{8}He/^{9}Li (/day/AD)*	2.40±0.86		1.20±0.63		0.22±0.06	
Am-C corr. (/day/AD)*	0.26±0.12					
^{13}C(α, n)^{16}O (/day/AD)*	0.08±0.04	0.07±0.04	0.05±0.03	0.04±0.02	0.04±0.02	0.04±0.02
IBD rate (/day/AD)*	**653.30 ± 2.31**	**664.15 ± 2.33**	**581.97 ± 2.07**	**73.31 ± 0.66**	**73.03 ± 0.66**	**72.20 ± 0.66**

* Corrected for the efficiency of the muon veto and multiplicity cuts

Collected more than 300k antineutrino interactions

- Consistent rates for side-by-side detectors
- Uncertainties still dominated by statistics

Oscillation Analysis

Initial results

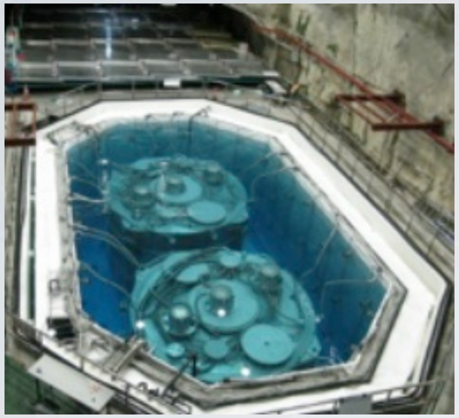

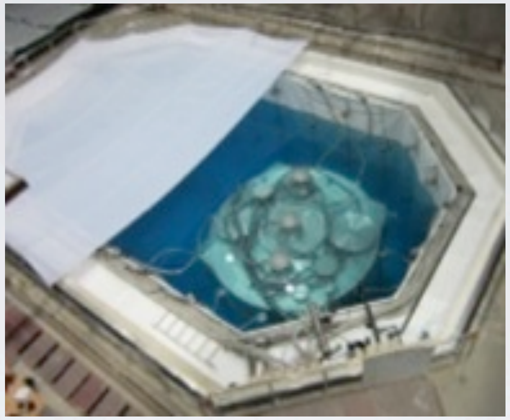

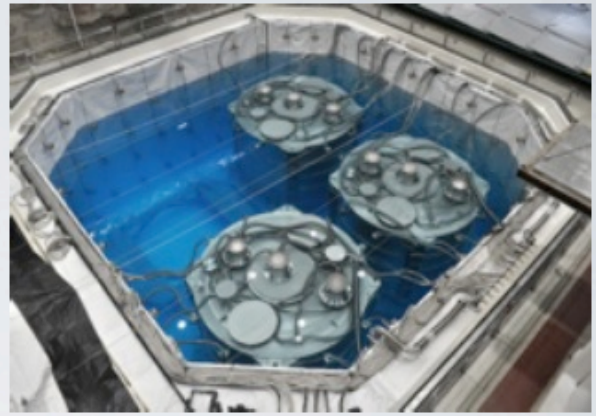

Based on 55 days of data with 6 ADs, discovered disappearance of reactor $\overline{\nu}_e$ at short baseline in March 2012. [PRL **108**, 171803]

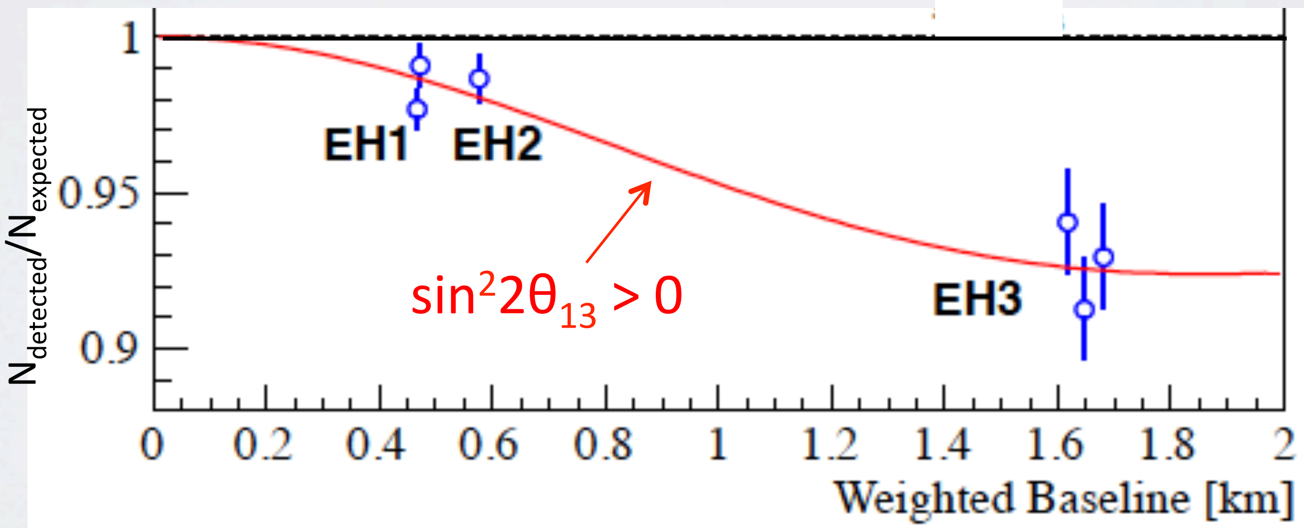

Obtained the most precise value of θ_{13} in Jun. 2012:

$$\sin^2 2\theta_{13} = 0.089 \pm 0.010 \pm 0.005$$ [CPC **37**, 011001]

Rate Only Analysis

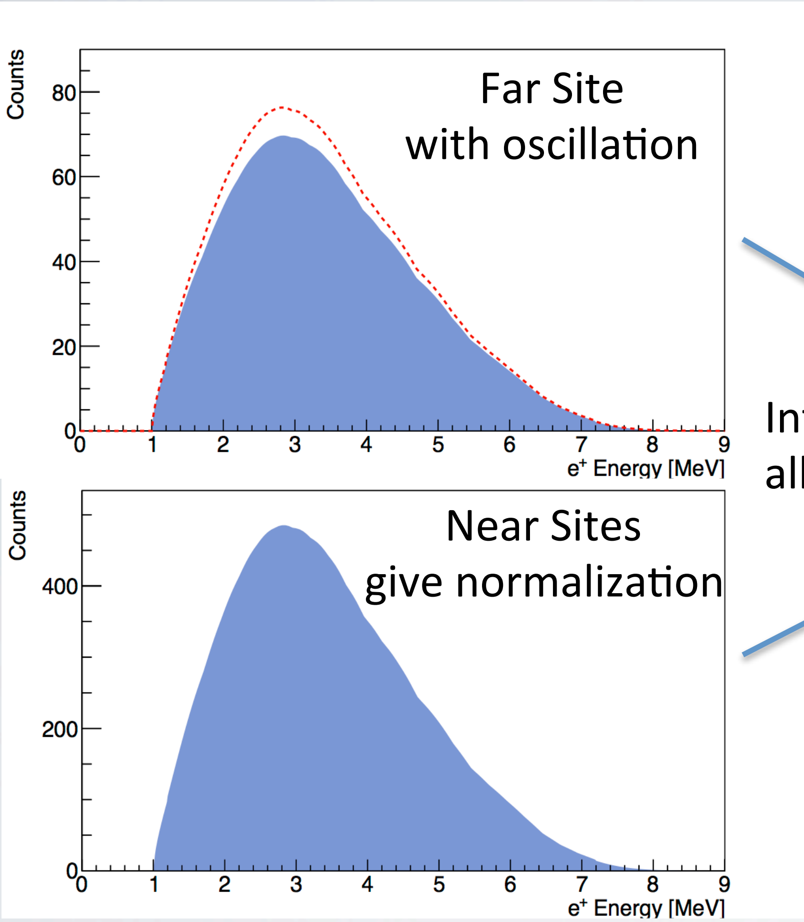

Integrate
all energies

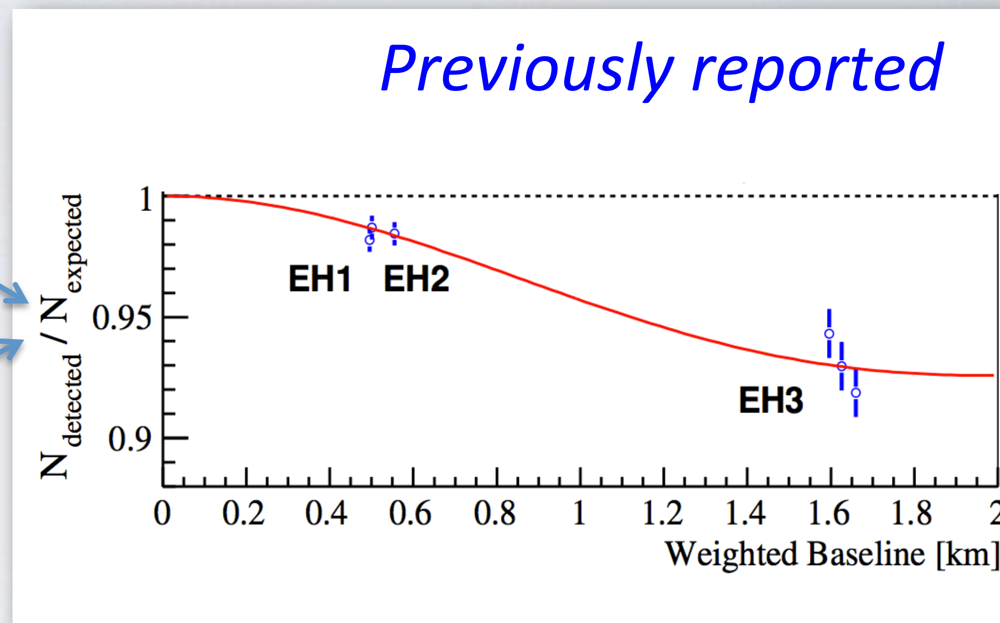

$$\frac{N_{\text{far}}}{N_{\text{near}}} = \frac{N_{\text{protons,far}}}{N_{\text{protons,near}}} \frac{1/L_{\text{far}}^2}{1/L_{\text{near}}^2} \frac{\epsilon_{\text{far}}}{\epsilon_{\text{near}}} \frac{\int_{E_{\text{min}}}^{E_{\text{max}}} P_{ee}(E, L_{\text{far}}; \theta_{13}, \Delta m^2_{ee})\sigma(E)\Phi(E)dE}{\int_{E_{\text{min}}}^{E_{\text{max}}} P_{ee}(E, L_{\text{near}}; \theta_{13}, \Delta m^2_{ee})\sigma(E)\Phi(E)dE}$$

Advantage: Fewer systematic uncertainties

Disadvantages: Less sensitive. Unable to constrain Δm^2_{ee}

Rate + Shape Analysis

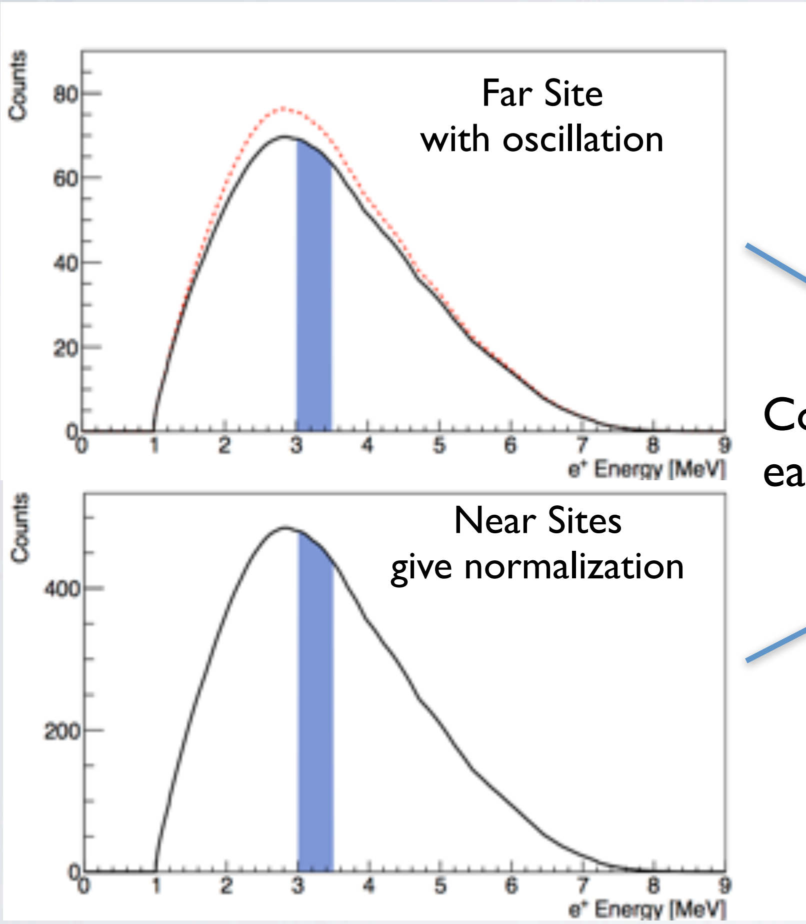

Compare each energy

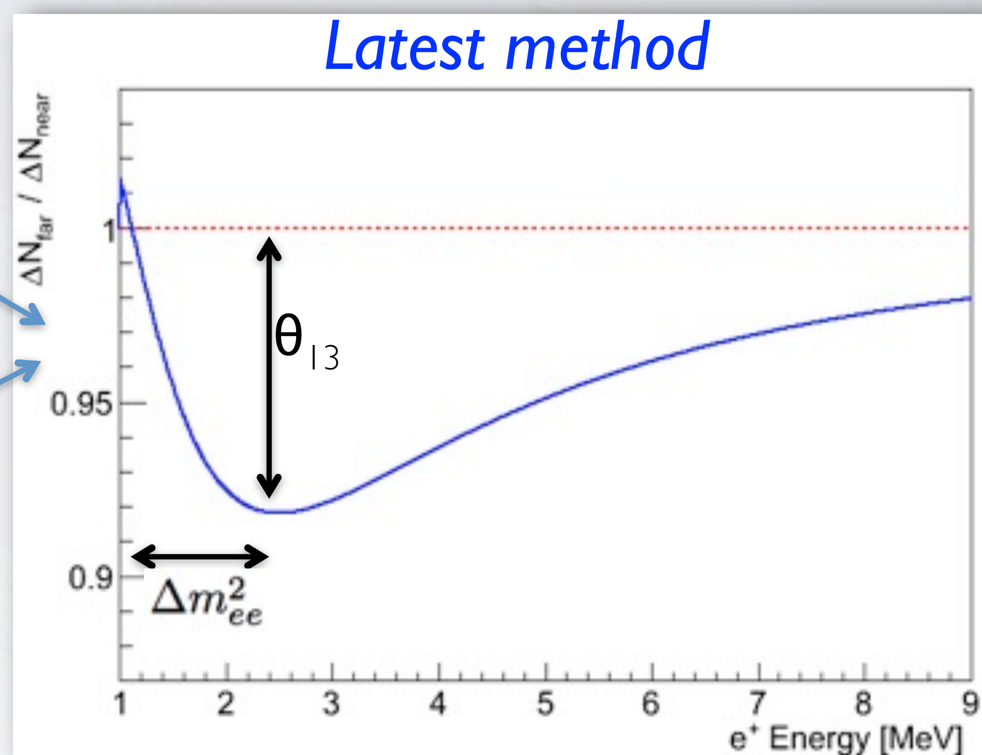

$$\frac{\frac{dN_{\text{far}}}{dE}}{\frac{dN_{\text{near}}}{dE}} = \frac{N_{\text{protons,far}}}{N_{\text{protons,near}}} \frac{1/L^2_{\text{far}}}{1/L^2_{\text{near}}} \frac{\epsilon_{\text{far}}}{\epsilon_{\text{near}}} \frac{P_{ee}(E, L_{\text{far}}; \theta_{13}, \Delta m^2_{ee})\sigma(E)\Phi(E)}{P_{ee}(E, L_{\text{near}}; \theta_{13}, \Delta m^2_{ee})\sigma(E)\Phi(E)}$$

Advantages: Gain sensitivity from energy dependence. Constrain Δm^2_{ee}.

Disadvantages: Require detailed understanding of detector response

Challenges for the spectrum shape analysis

- Understanding of background rate and shape
- Understanding of the detector response
  - Energy resolution
  - Energy scale
  - Effect of inactive volume (acrylic vessel)

Challenges for the spectrum shape analysis

- **Understanding Background rate and shape**
- Understanding of the detector response
  - Energy resolution
  - Energy scale
  - Effect of inactive volume (acrylic vessel)

Understanding Background Rate and Shape

	Near Halls				Far Hall	
	AD1	AD2	AD3	AD4	AD5	AD6
IBD candidates	101290	102519	92912	13964	13894	13731
DAQ live time (day)	191.001		189.645		189.779	
Efficiency	0.7957	0.7927	0.8282	0.9577	0.9568	0.9566
Accidentals (/day/AD)*	9.54±0.03	9.36±0.03	7.44±0.02	2.96±0.01	2.92±0.01	2.87±0.01
Fast neutron (/day/AD)*	0.92±0.46		0.62±0.31		0.04±0.02	
^{8}He/^{9}Li (/day/AD)*	2.40±0.86		1.20±0.63		0.22±0.06	
Am-C corr. (/day/AD)*			0.26±0.12			
^{13}C(α, n)^{16}O (/day/AD)*	0.08±0.04	0.07±0.04	0.05±0.03	0.04±0.02	0.04±0.02	0.04±0.02
IBD rate (/day/AD)*	**653.30 ± 2.31**	**664.15 ± 2.33**	**581.97 ± 2.07**	**73.31 ± 0.66**	**73.03 ± 0.66**	**72.20 ± 0.66**

Two worst contributors to background uncertainty at the far hall

^{8}He/^{9}Li Backgrounds

Directory measured by fitting the distribution of IBD candidates vs. time since muon

β-n decay:
- Prompt: β-decay
- Delayed: neutron capture

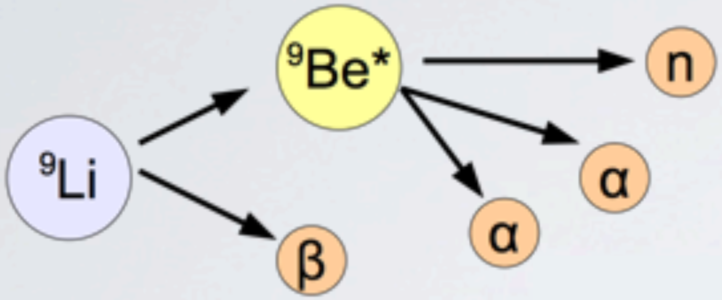

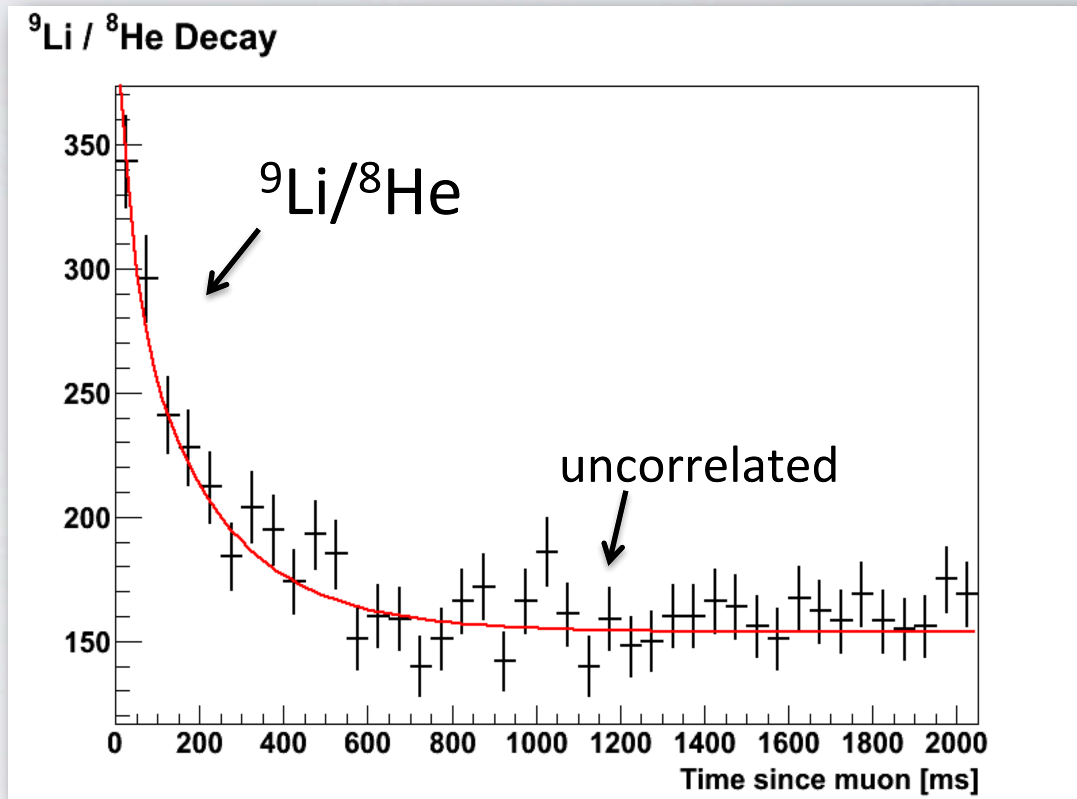

^{9}Li: $\tau_{1/2}$ = 178 ms, Q = 13.6 MeV

^{8}He: $\tau_{1/2}$ = 119 ms, Q = 10.6 MeV

- Generated by cosmic rays
- Long-lived
- Mimic antineutrino signal

Analysis muon veto cuts control B/S to ~0.3±0.1%

$^{8}He/^{9}Li$ Backgrounds

- Simulated $^{8}He/^{9}Li$ spectra including neutron and alpha contributions
- Benchmarked with external data
- Uncertainty in shape is conservatively estimated by varying $^{9}Li/(^{9}Li+^{8}He)$ ratio and detector response model

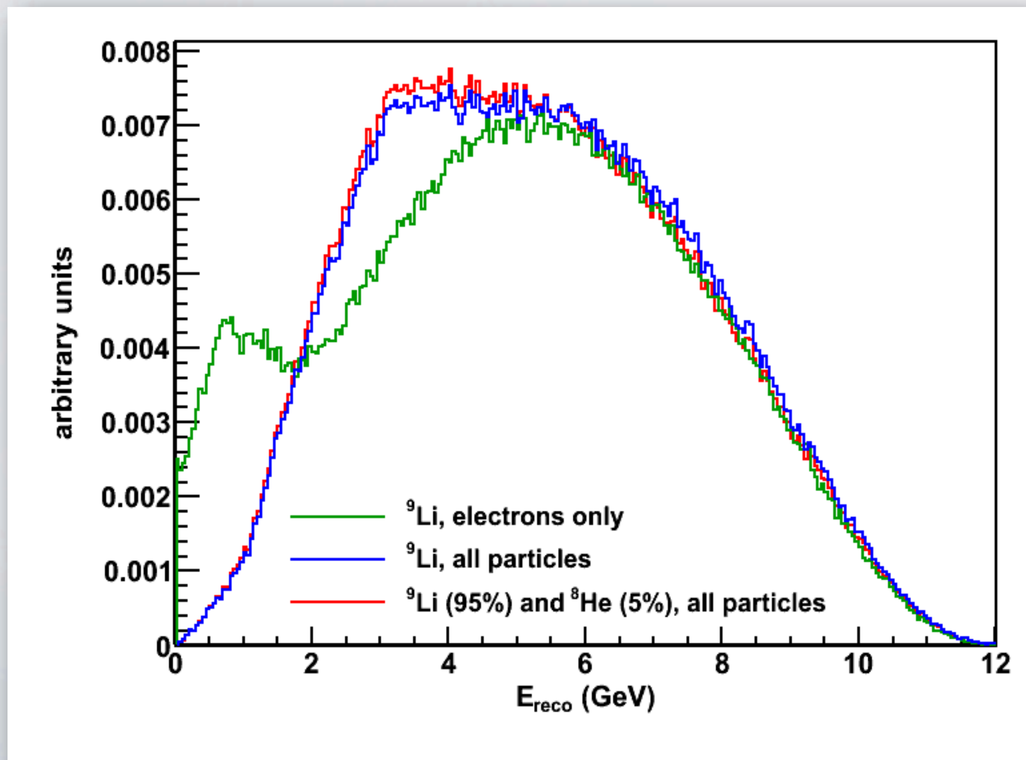

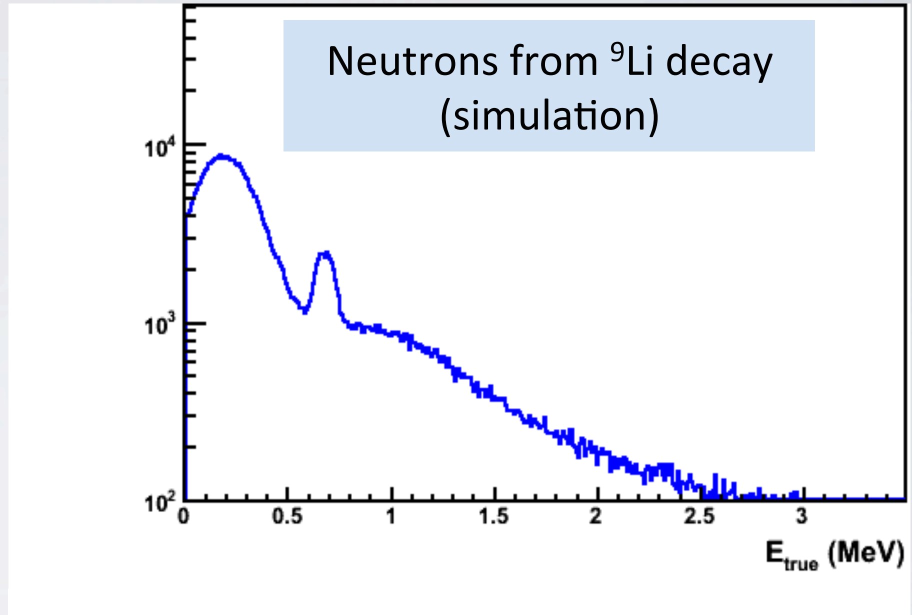

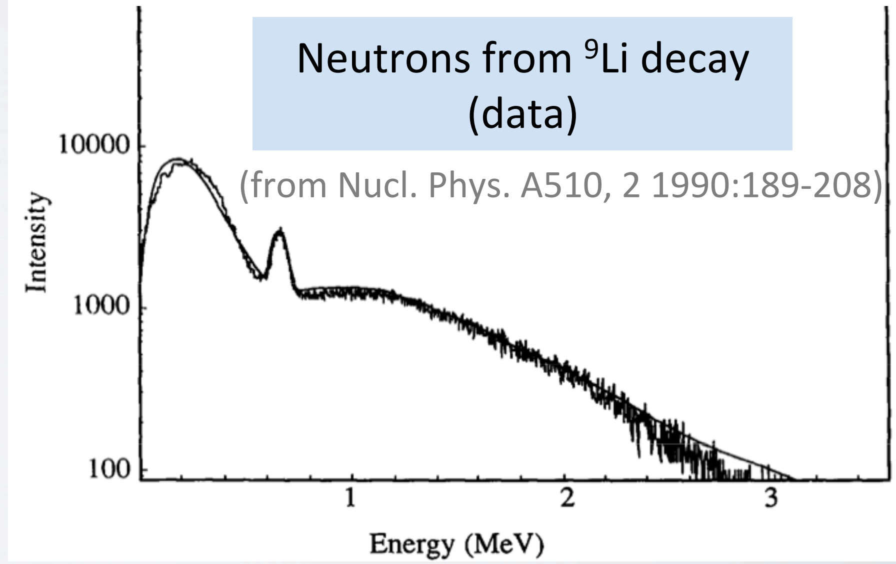

^{241}Am-^{13}C Background

Subtle background from our calibration source

- ^{241}Am-^{13}C source produces ~0.75 Hz neutron via ^{13}C(α,n)^{16}O
- Neutron interact with steel to produce fake prompt-delayed pair

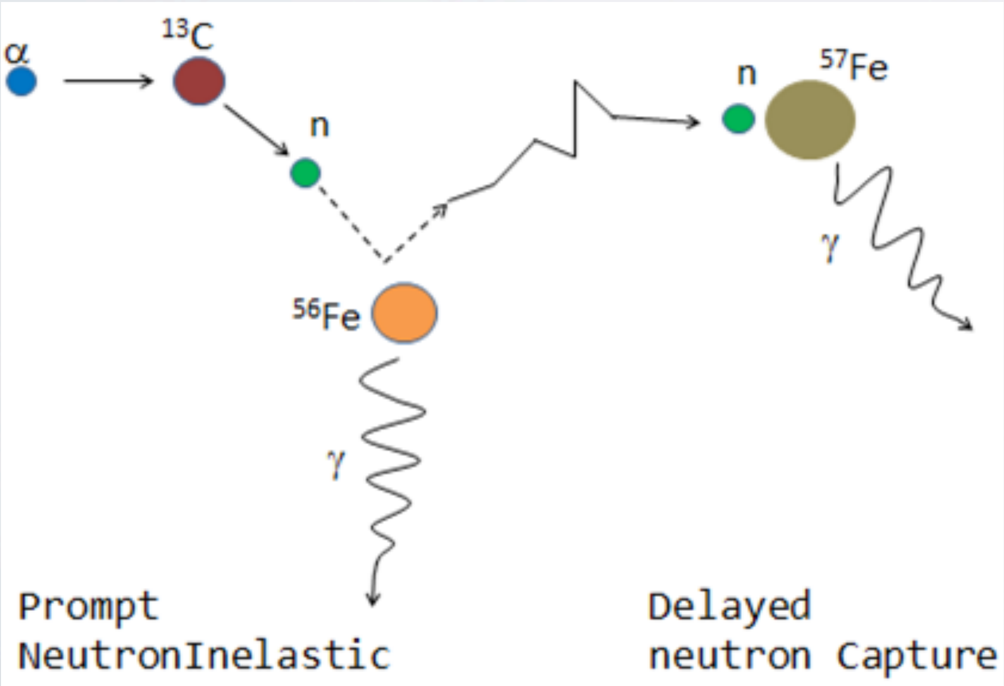

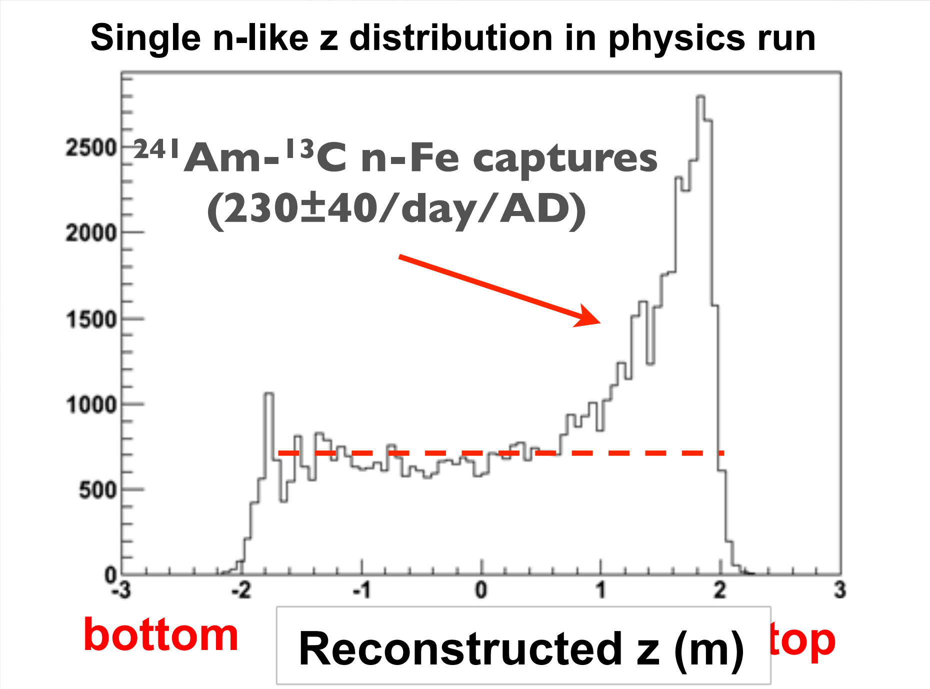

- Background rate expected to be small: 0.2-0.3/day/module (MC)
- Yet, one of the largest source of systematic uncertainty from backgrounds

^{241}Am-^{13}C Background

A special x80 stronger ^{241}Am-^{13}C source placed on the AD

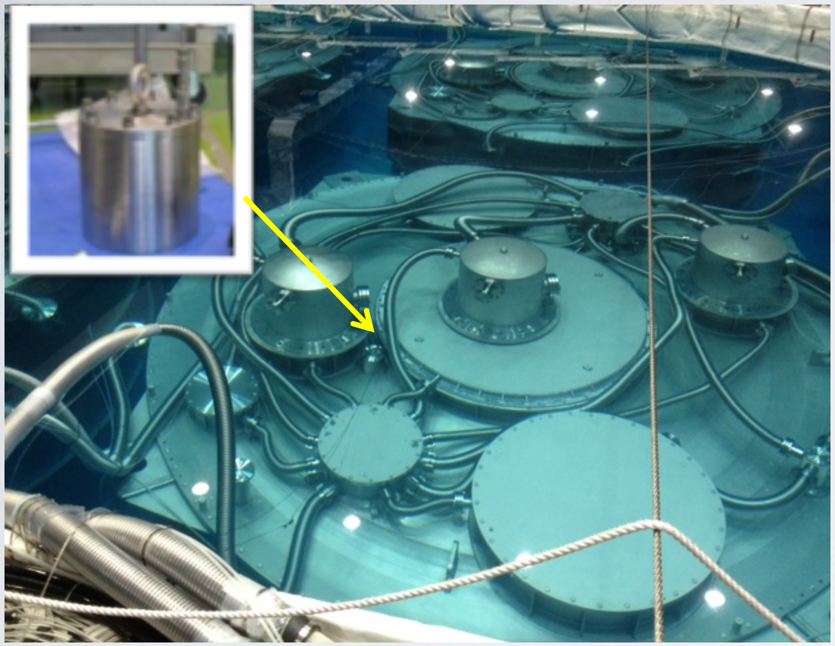

Single n-like

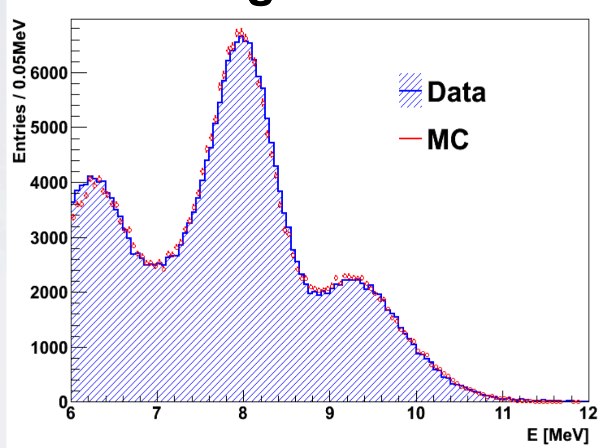

Correlated prompt spectrum

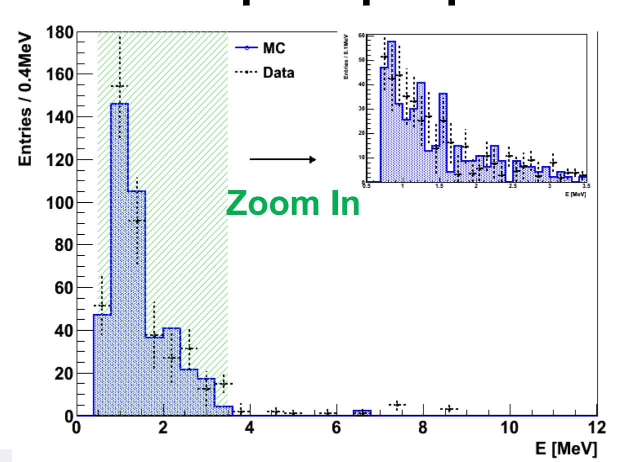

Used special strong source data to benchmark and correct MC simulation

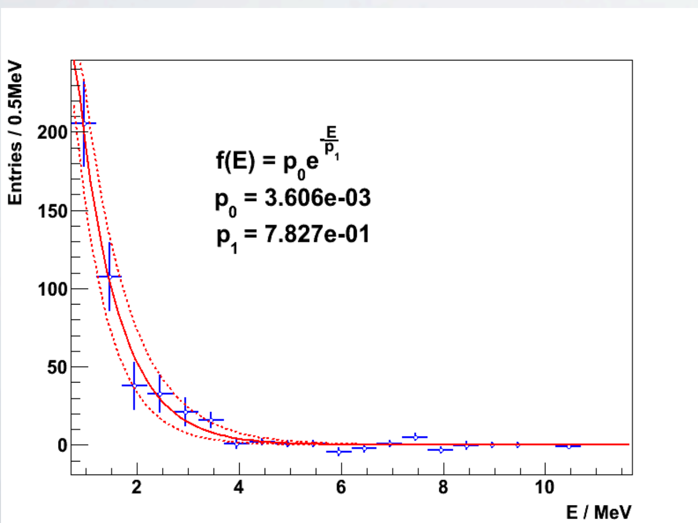

Estimation for physics data:

- Rate: 0.26/day/module (45% uncertainty)
- Spectrum: exponential (15% uncertainty)

Factor 2 reduced from the previous analysis

Removed 2 of 3 sources in far detectors to reduce future backgrounds.

Challenges for the spectrum shape analysis

- Understanding Background rate and shape
- **Understanding of the detector response**
  - Energy resolution
  - Energy scale
  - Effect of inactive volume (acrylic vessel)

Understanding of Detector Response

Particle Energy E_{true}

↓

Energy Deposited in Scintillator E_{dep}

↓

Energy Converted to Visible Light E_{vis}

↓

Reconstructed Energy E_{rec}

Energy Losses in Acrylic

Acrylic vessels non-scintillating

- Induce shape distortion
- Correction from MC

Energy Resolution

- Light production
- Light collection
- PMT/electronics response

Two major sources of non-linearity. Difficult to decouple !

1: Scintillator Response

- Quenching effects
- Cherenkov radiation

2: Readout Electronics

- Charge collection efficiency decreases with visible light

Acrylic Vessel / Energy Resolution

Energy loss in the acrylic vessel distorts spectrum

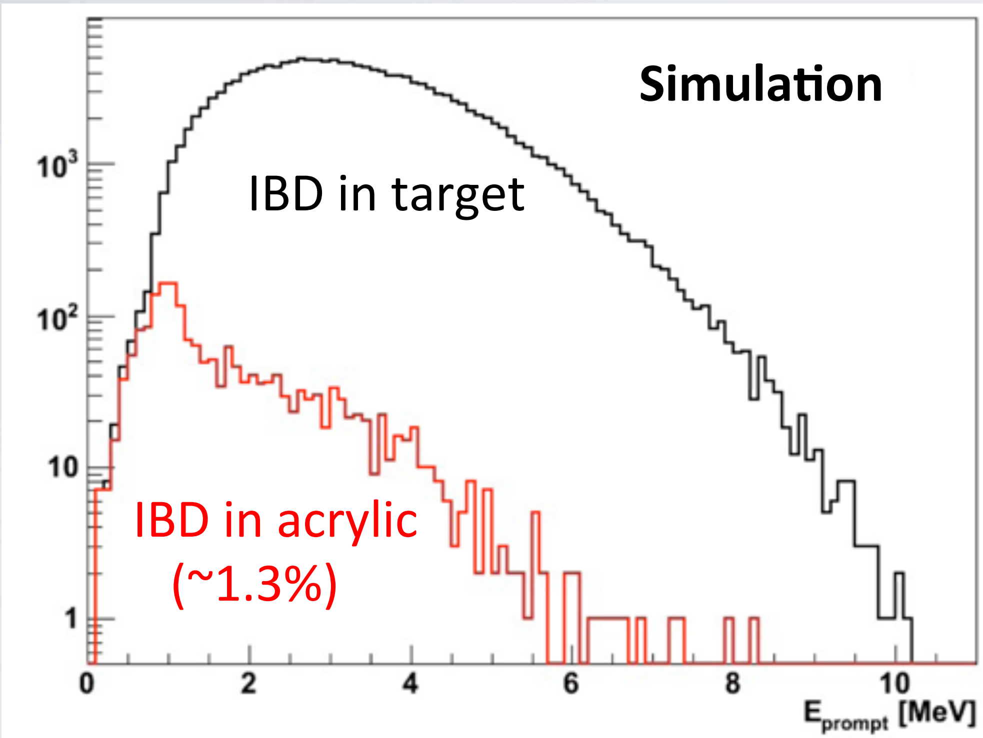

Modeled using MC simulation

Energy resolution

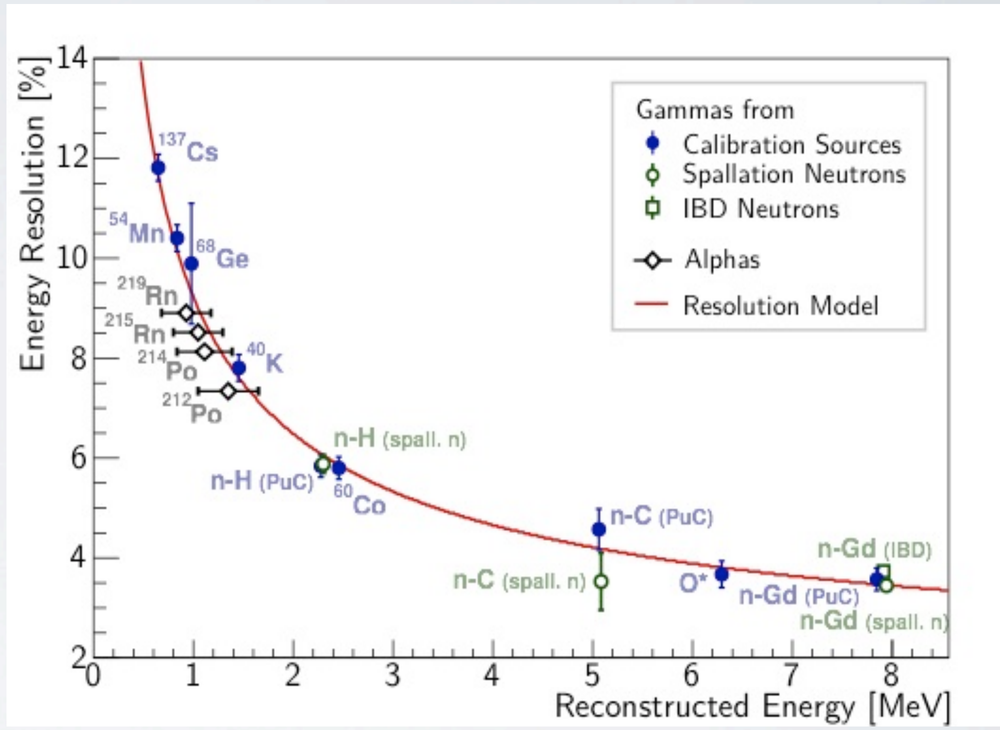

$$\frac{\sigma_E}{E} = \sqrt{a^2 + \frac{b^2}{E} + \frac{c^2}{E^2}}$$

Contributions from:

- a : Spacial/temp. resolution (E)
- b : Photon statistics (E)
- c : Dark noise (const:)

Calibrated primarily using mono-energetic gamma sources

Constraining Non-Linearity Parameters

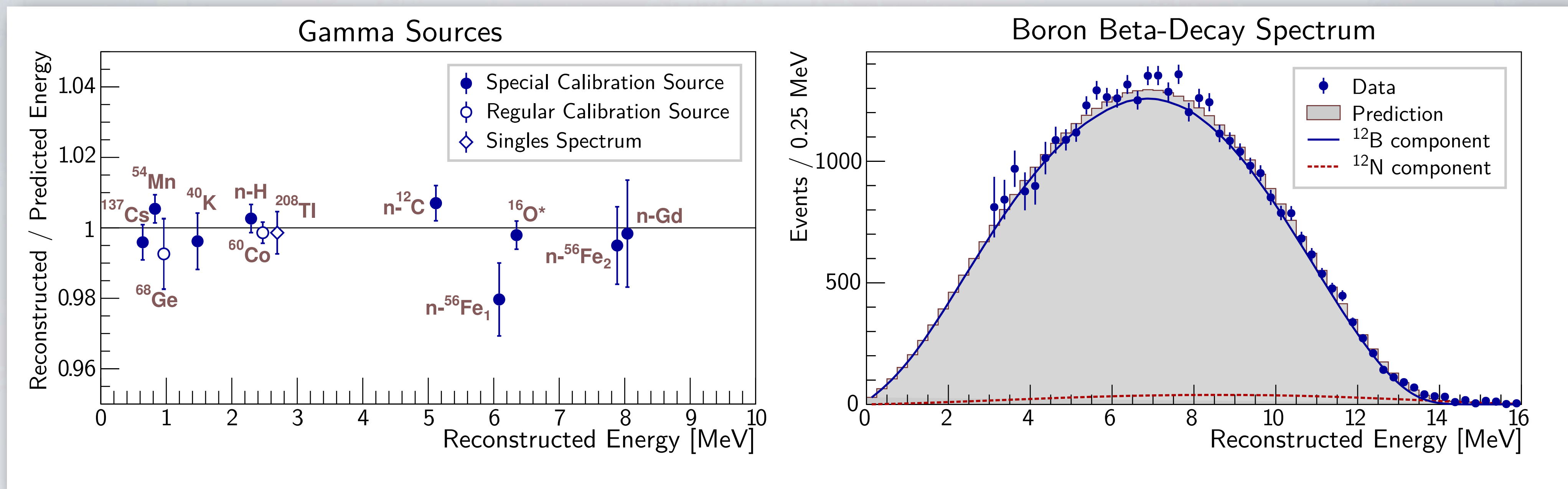

Full detector calibration data

1. Monoenergetic gamma lines from various sources
   - Radioactive calibration sources, employed regularly: ^{68}Ge, ^{60}Co, ^{241}Am-^{13}C and during special calibration periods: ^{137}Cs, ^{54}Mn, ^{40}K, ^{241}Am-^{9}Be, Pu-^{13}C
   - Singles and correlated spectra in regular physics runs (^{40}K, ^{208}Tl, n capture on H)
2. Continuous spectrum from ^{12}B produced by muon spallation inside the scintillator

Standalone measurements

- Scintillator quenching measurements using neutron beams and Compton e^-
- Calibration of readout electronics with flash ADC

Final Positron Energy Non-Linearity response

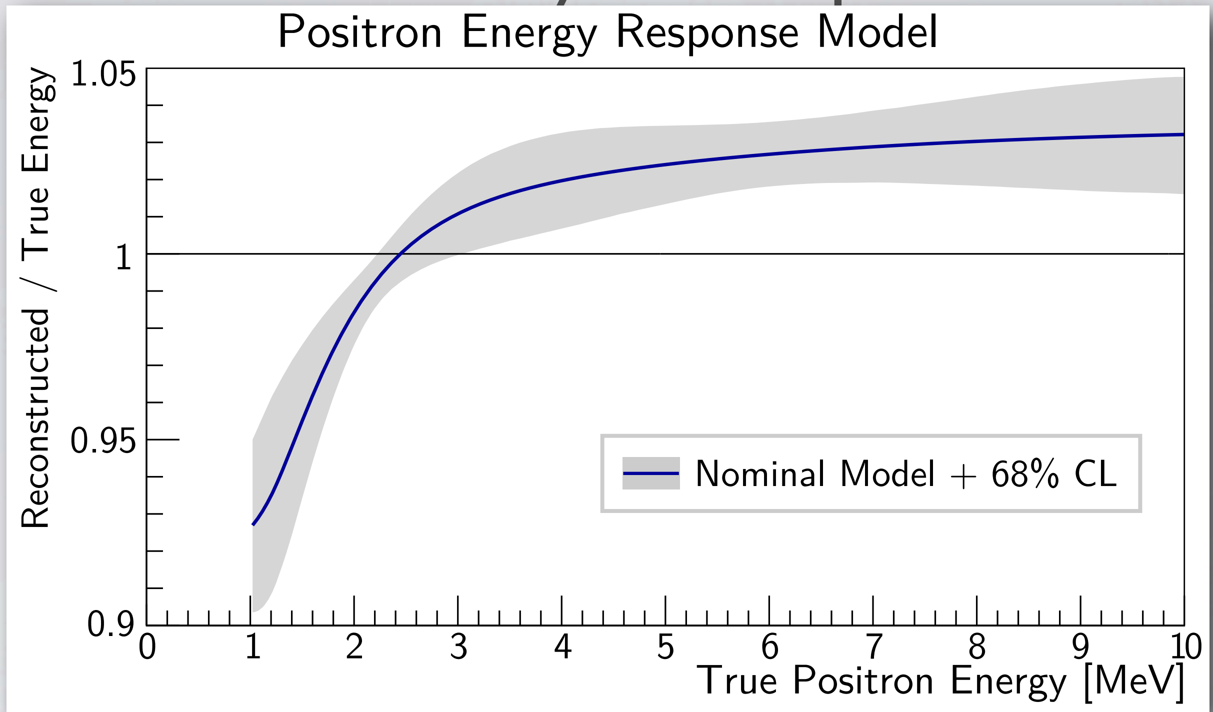

Several validated models

- Constructed based on different parameterizations/weighting of data constraints
- All models in good agreement with detector calibration data
- Resulting positron non-linearity curves consistent within $\sim 1.5\%$ uncertainty

Used combination of 5 models to conservatively estimate uncertainty

Relative Energy Scale

Crucial ingredient: Consistent energy response for all ADs

Careful calibration with in-situ data and calibration sources:

- Energy response stable to 0.1% in all detectors
- Total relative uncertainty of 0.35% between detectors

Spallation *n*Gd capture peak vs. time (after all calibration)

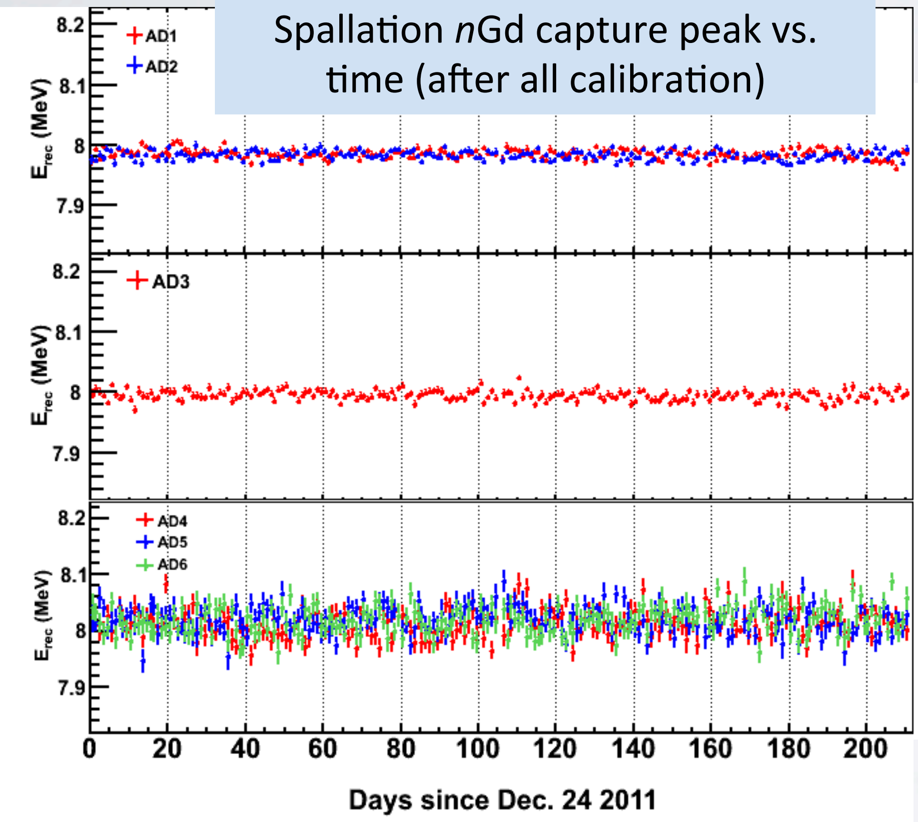

Relative energy peaks in all detectors (after calibration)

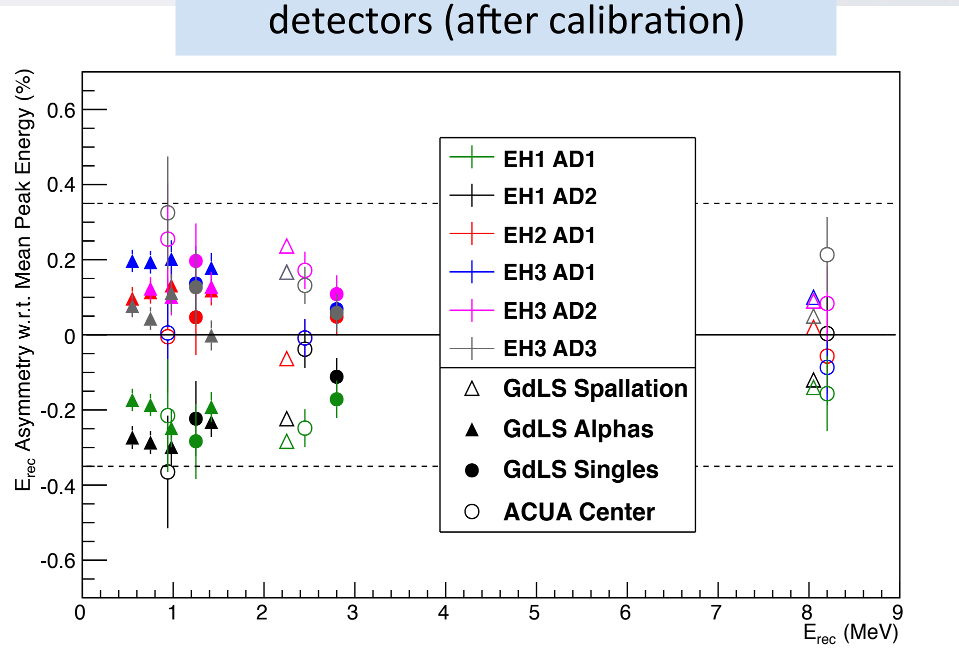

Yet, the largest source of systematic uncertainty for Δm^2_{ee}

Results

Rate only analysis

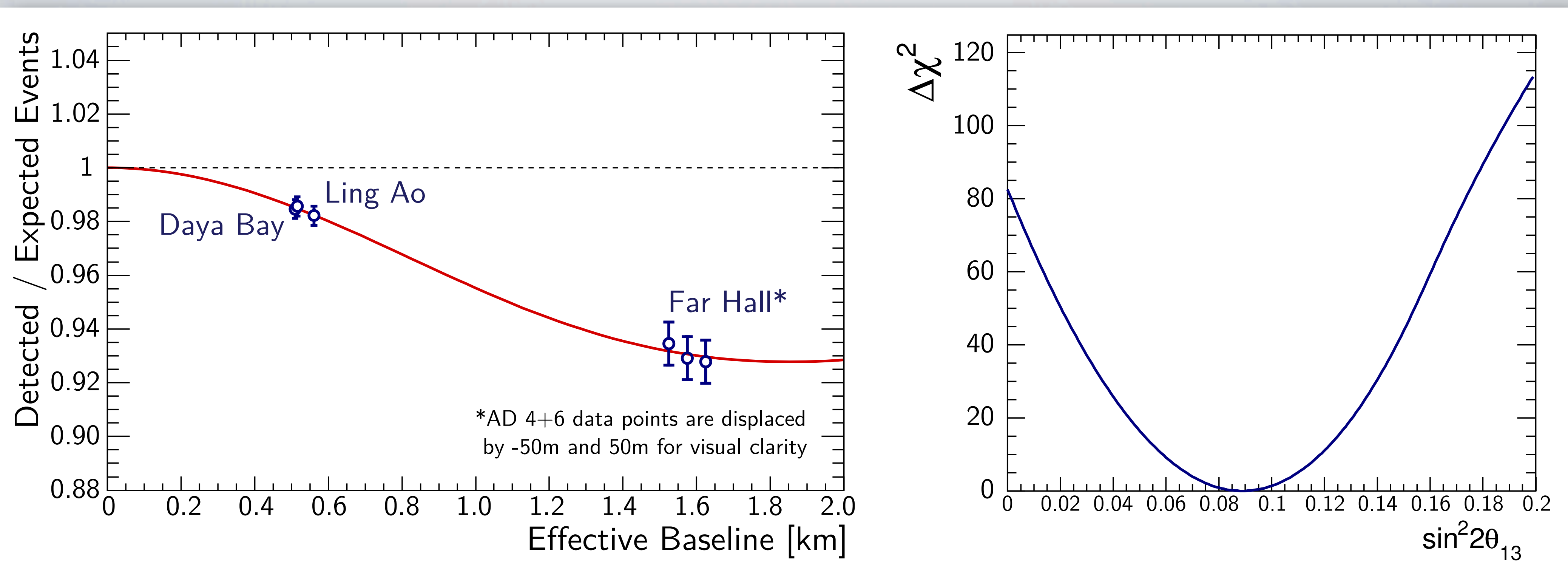

$$\sin^2 2\theta_{13} = 0.089 \pm 0.009 \quad \chi^2/N_{DOF} = 0.48/4$$

- Uncertainty reduced by statistics of complete 6 AD data period
- $|\Delta m^2_{ee}|$ constrained by MINOS result: $|\Delta m^2_{\mu\mu}| = 2.41^{+0.09}_{-0.10} \times 10^{-3}\ \mathrm{eV}^2$ PRL. 110, 251801 (2013)
- Far vs. near relative measurement: absolute rate not constrained
- Consistent results from independent analysis, different reactor models

IBD Prompt Energy Spectra

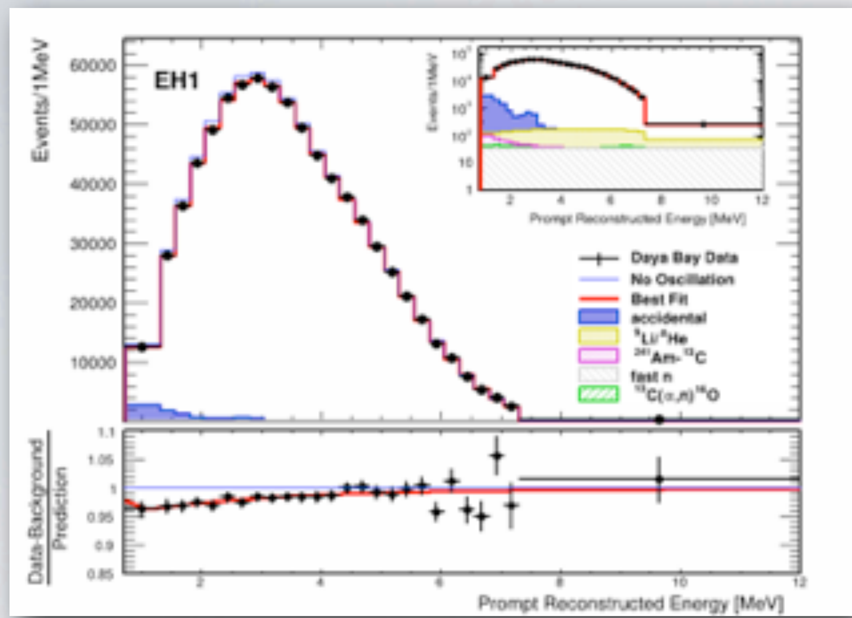

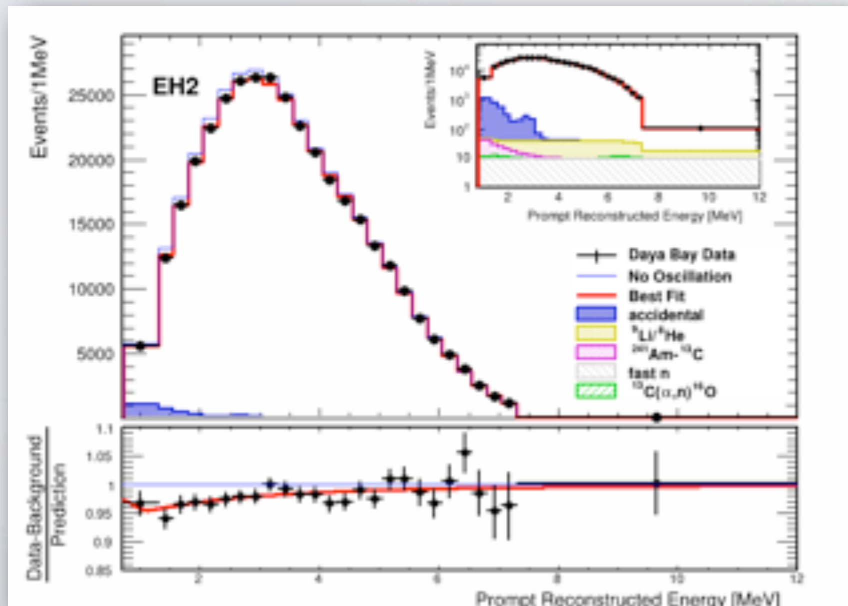

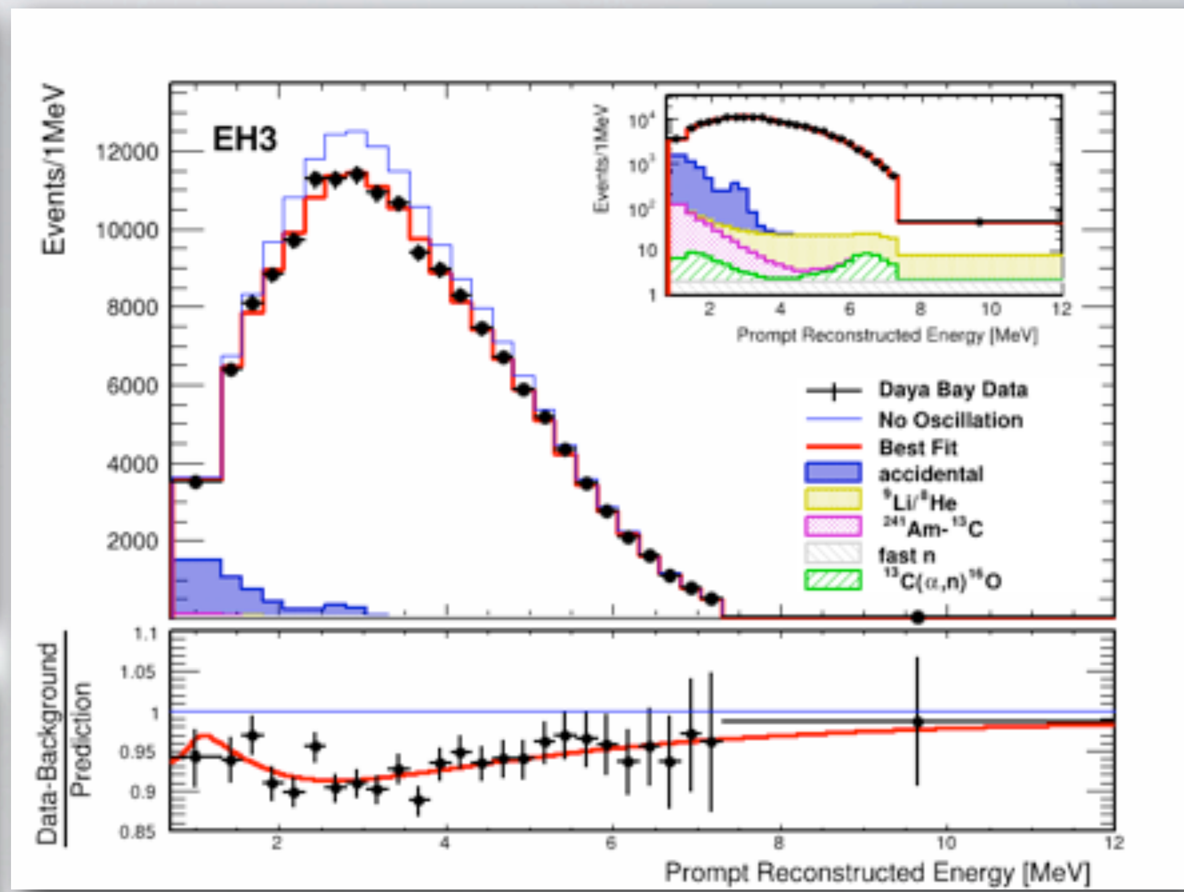

Spectral distortion consistent with oscillation

- Both background and predicted no oscillation spectra determined by the best fit
- Errors are statistical only

Rate and Shape Analysis Results

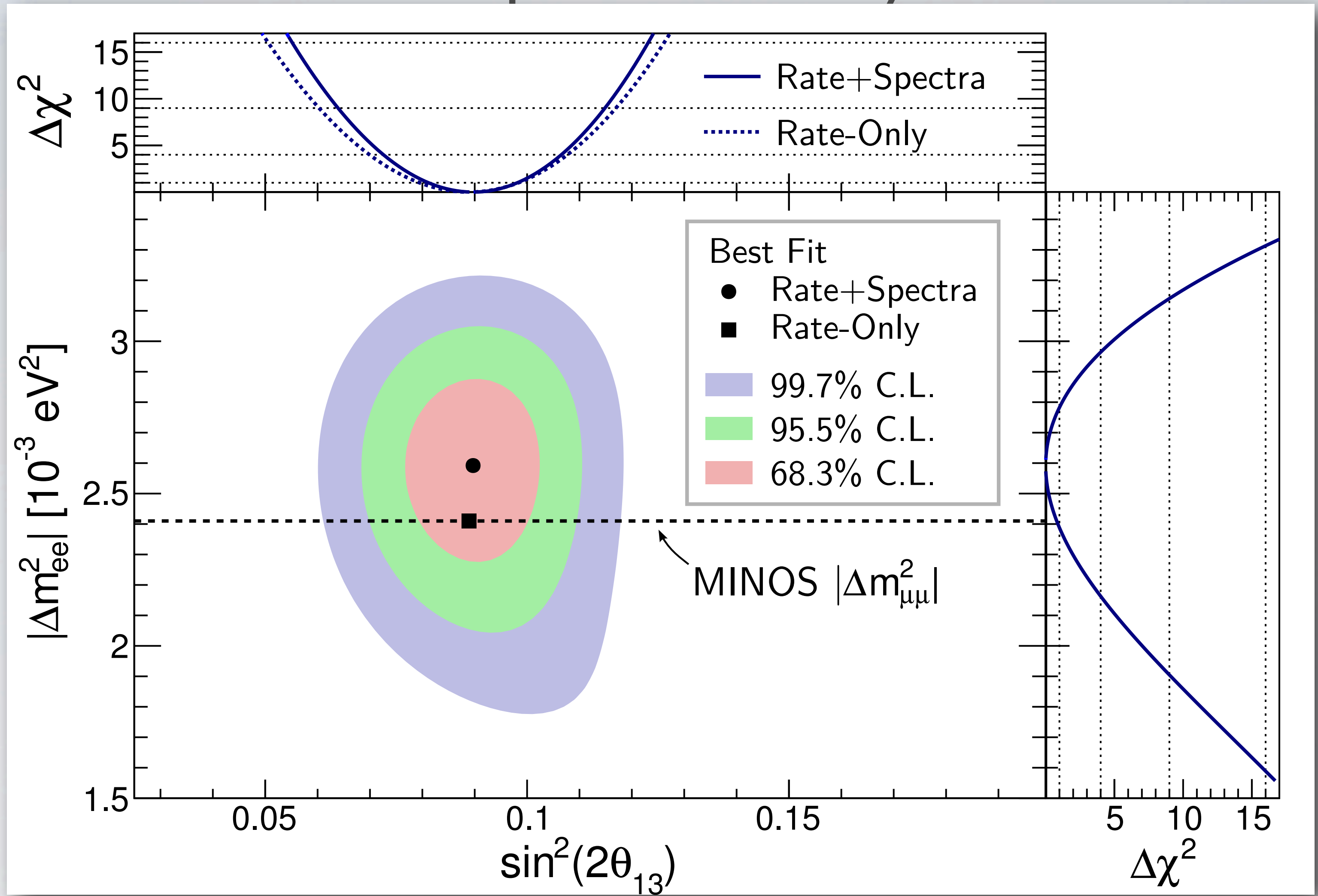

$$\sin^2 2\theta_{13} = 0.090^{+0.008}_{-0.009}$$

$\chi^2/N_{\rm DOF} = 162.7/153$

$$|\Delta m^2_{ee}| = 2.59^{+0.19}_{-0.20} \times 10^{-3}\ \mathrm{eV}^2$$

Δm^2_{ee} and $\Delta m^2_{\mu\mu}$?

$$P(\overline{\nu}_e \to \overline{\nu}_e) = 1 - \sin^2 2\theta_{13} \sin^2\left(\Delta m^2_{ee} \frac{L}{4E}\right) - \cos^4\theta_{13} \sin^2 2\theta_{12} \sin^2\left(\Delta m^2_{21} \frac{L}{4E}\right)$$

$$\sin^2\left(\Delta m^2_{ee} \frac{L}{4E}\right) \equiv \cos^2\theta_{12} \sin^2\left(\Delta m^2_{31} \frac{L}{4E}\right) + \sin^2\theta_{12} \sin^2\left(\Delta m^2_{32} \frac{L}{4E}\right)$$

- Oscillation at ~2 km governed by two mass splittings: Δm^2_{31} and Δm^2_{32}
- Insensitive to distinguish the two. → Effective mass splitting: $\mathbf{\Delta m^2_{ee}}$

Can relate to actual splittings:

$$|\Delta m^2_{ee}| \simeq |\Delta m^2_{32}| \pm 5 \times 10^{-5}\ \mathrm{eV}^2$$

+: Normal Hierarchy
−: Inverted Hierarchy

Δm^2_{ee} should be within 2-3% from the effective mass splitting for muon (anti-)neutrino disappearance $\mathbf{\Delta m^2_{\mu\mu}}$

$$P(\nu_\mu \to \nu_\mu) \simeq 1 - \sin^2 2\theta_{23} \sin^2\left(\Delta m^2_{\mu\mu} \frac{L}{4E}\right)$$

Important test of three-flavor oscillation model

Rate and Shape Analysis Results

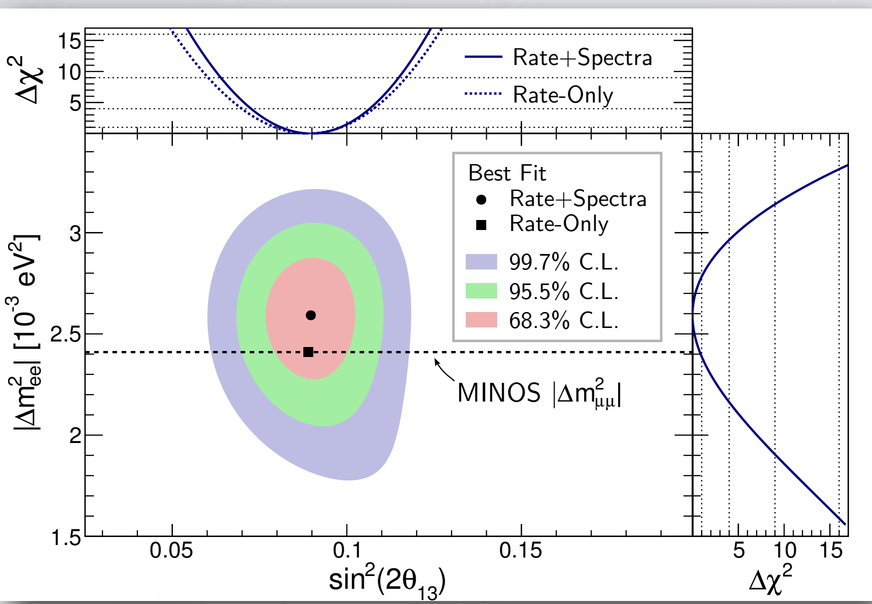

$$\sin^2 2\theta_{13} = 0.090^{+0.008}_{-0.009}$$

$$|\Delta m^2_{ee}| = 2.59^{+0.19}_{-0.20} \times 10^{-3}\ \mathrm{eV}^2$$

$$\chi^2/N_{DOF} = 162.7/153$$

Strong confirmation of the oscillation model

	Normal MH Δm^2_{32} [10^{-3}eV^2]	Inverted MH Δm^2_{32} [10^{-3}eV^2]
From Daya Bay Δm^2_{ee}	$2.54^{+0.19}_{-0.20}$	$-2.64^{+0.19}_{-0.20}$
From MINOS $\Delta m^2_{\mu\mu}$ [João, NuFact2013]	$2.37^{+0.09}_{-0.09}$	$-2.41^{+0.12}_{-0.09}$

Near vs. Far Spectrum study

Independent crosscheck with minimal reactor assumption

Predict far spectra directly from measured near site spectra

→ Minimizes impact of absolute flux and spectra prediction.

Use covariance matrices to account for systematic errors

→ Alternate method finds consistent uncertainties for neutrino parameters.

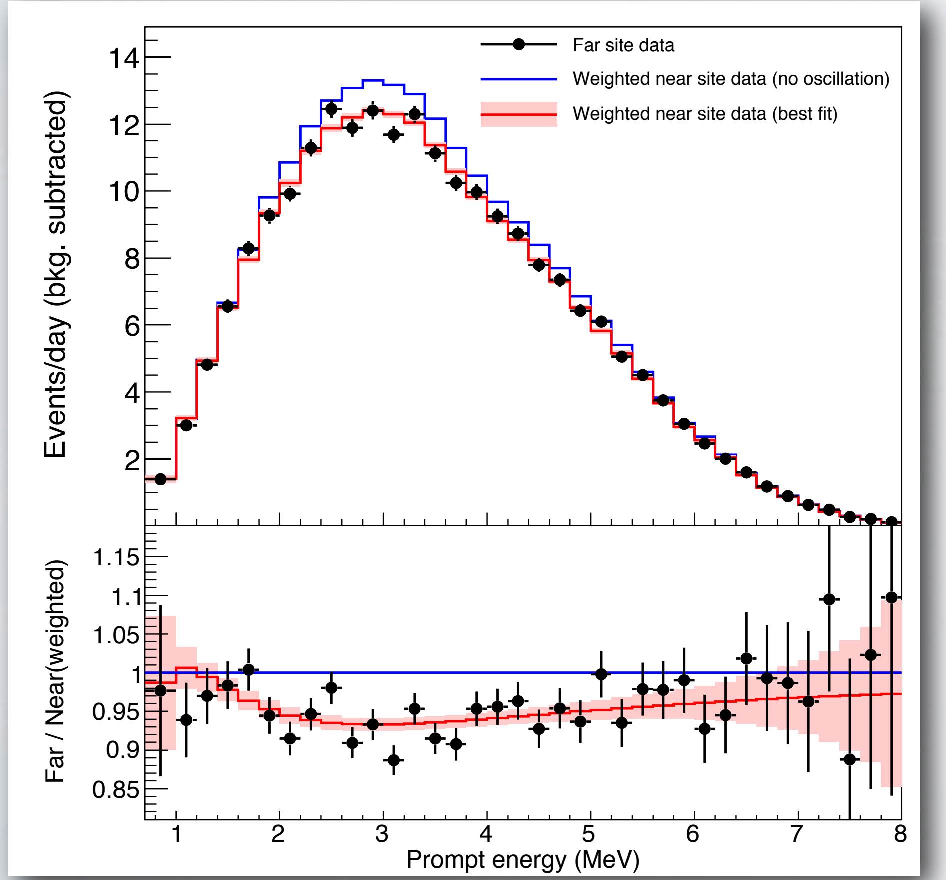

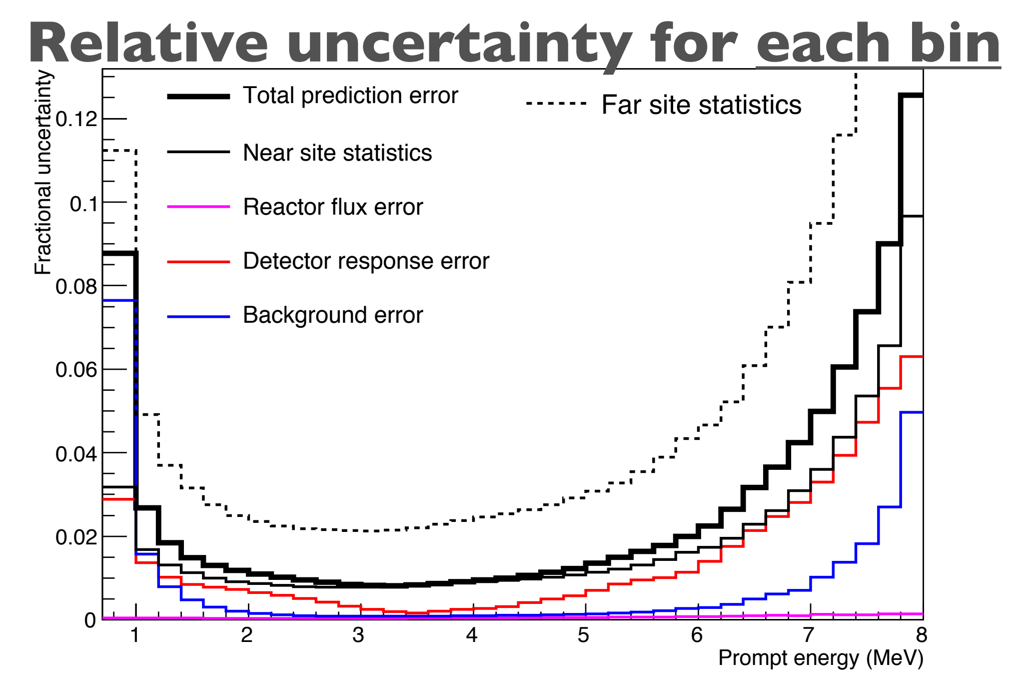

Systematic uncertainties controlled to well below statistical error

Near vs. Far Spectrum Study
Fit Result

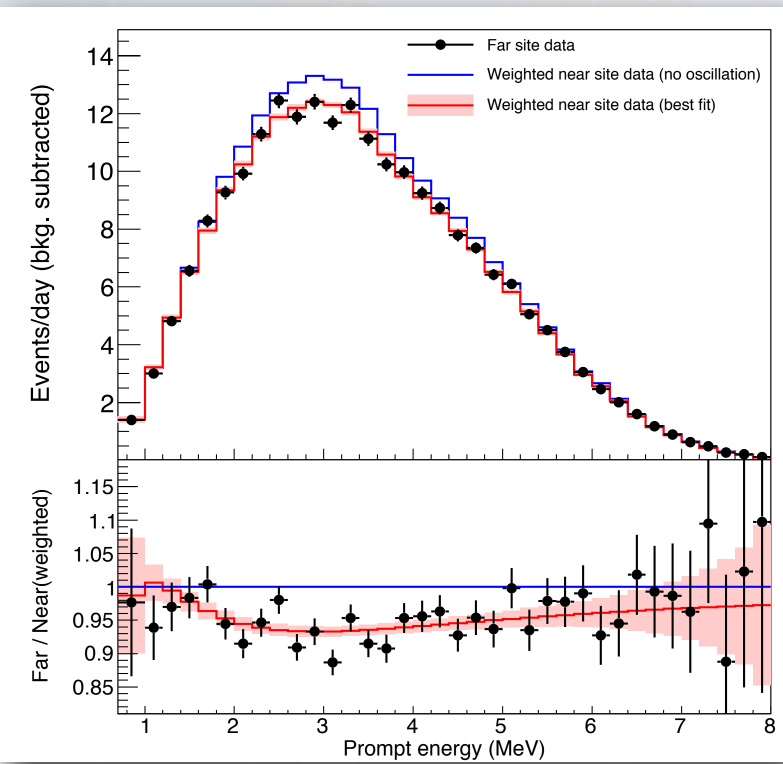

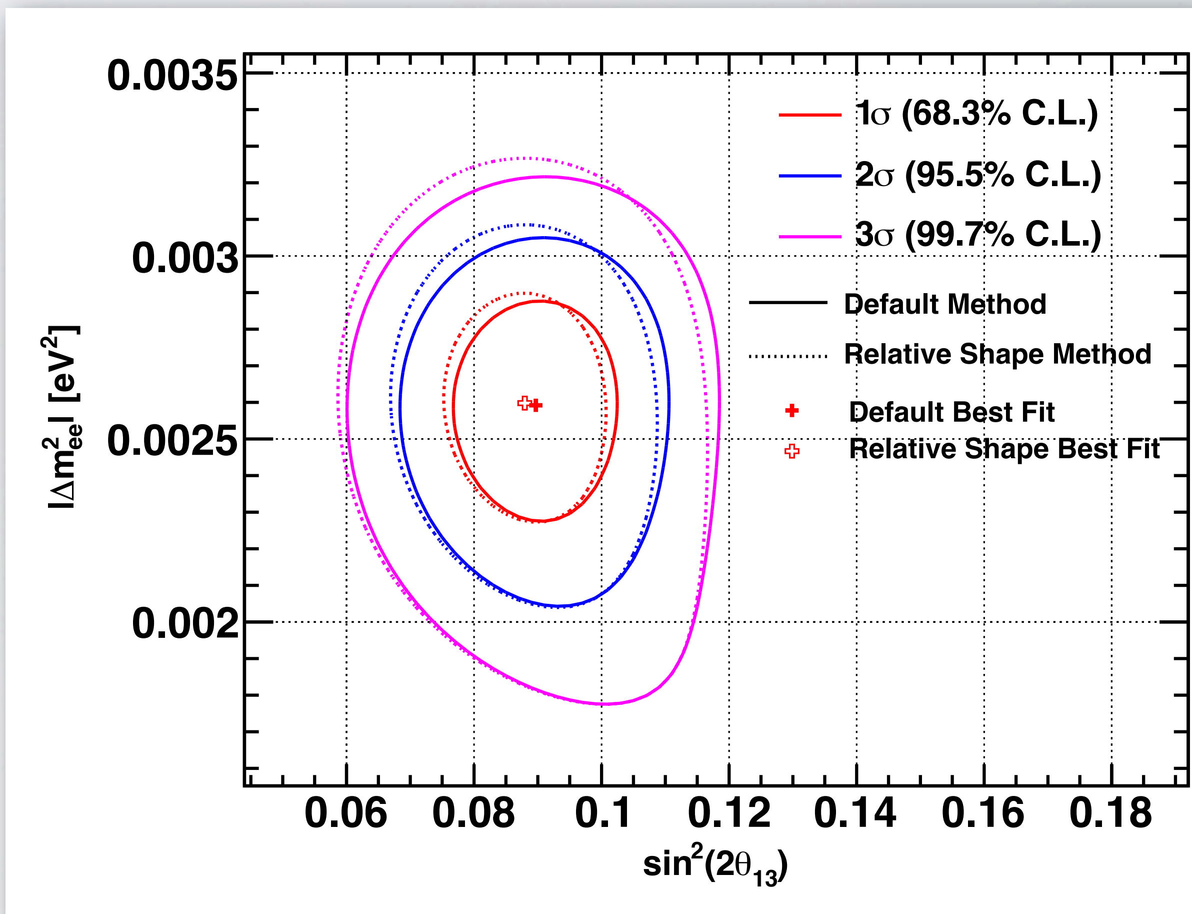

Consistent results with the default method

Neutrino Oscillates

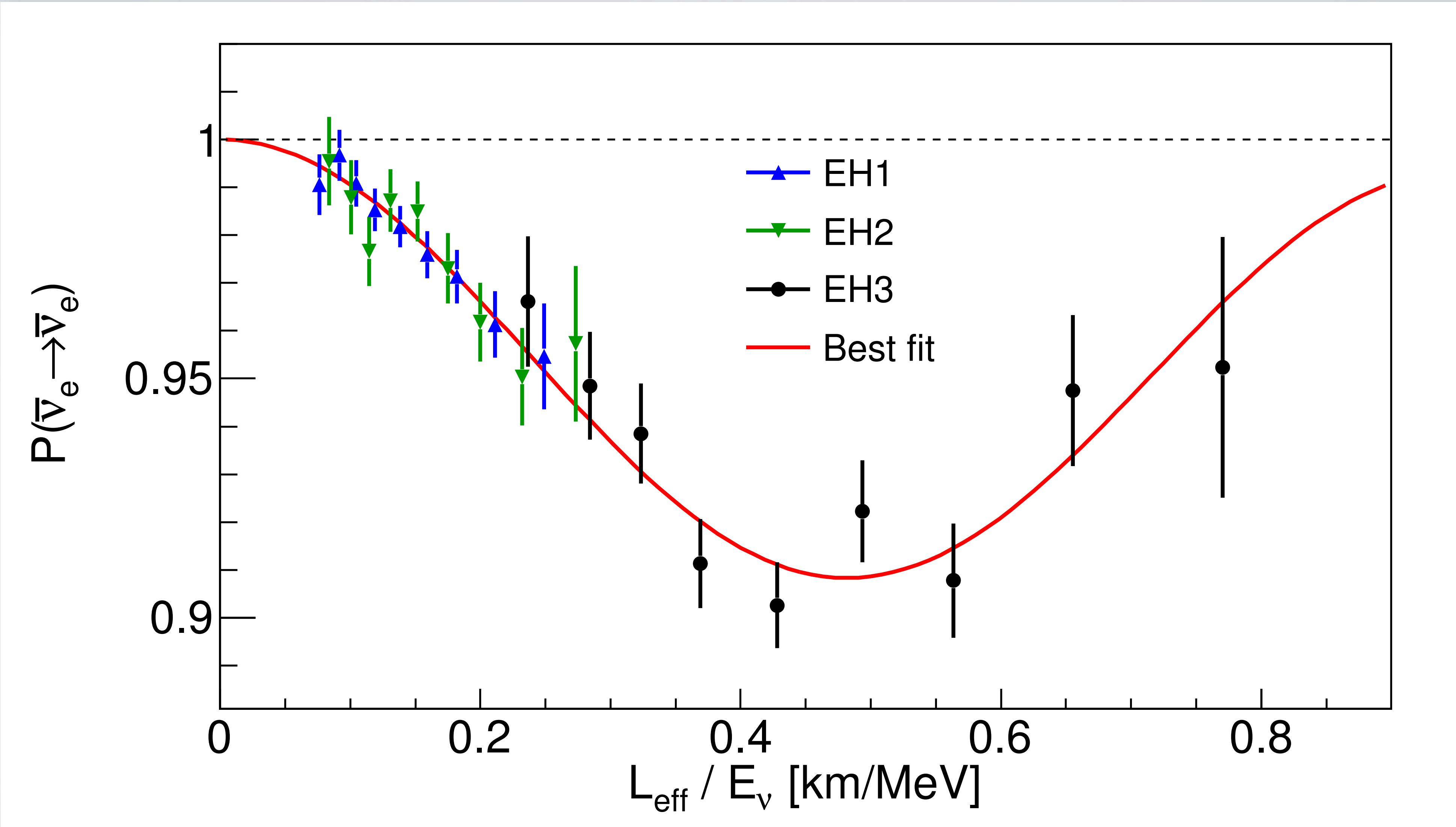

Global Comparison of θ_{13} Measurements

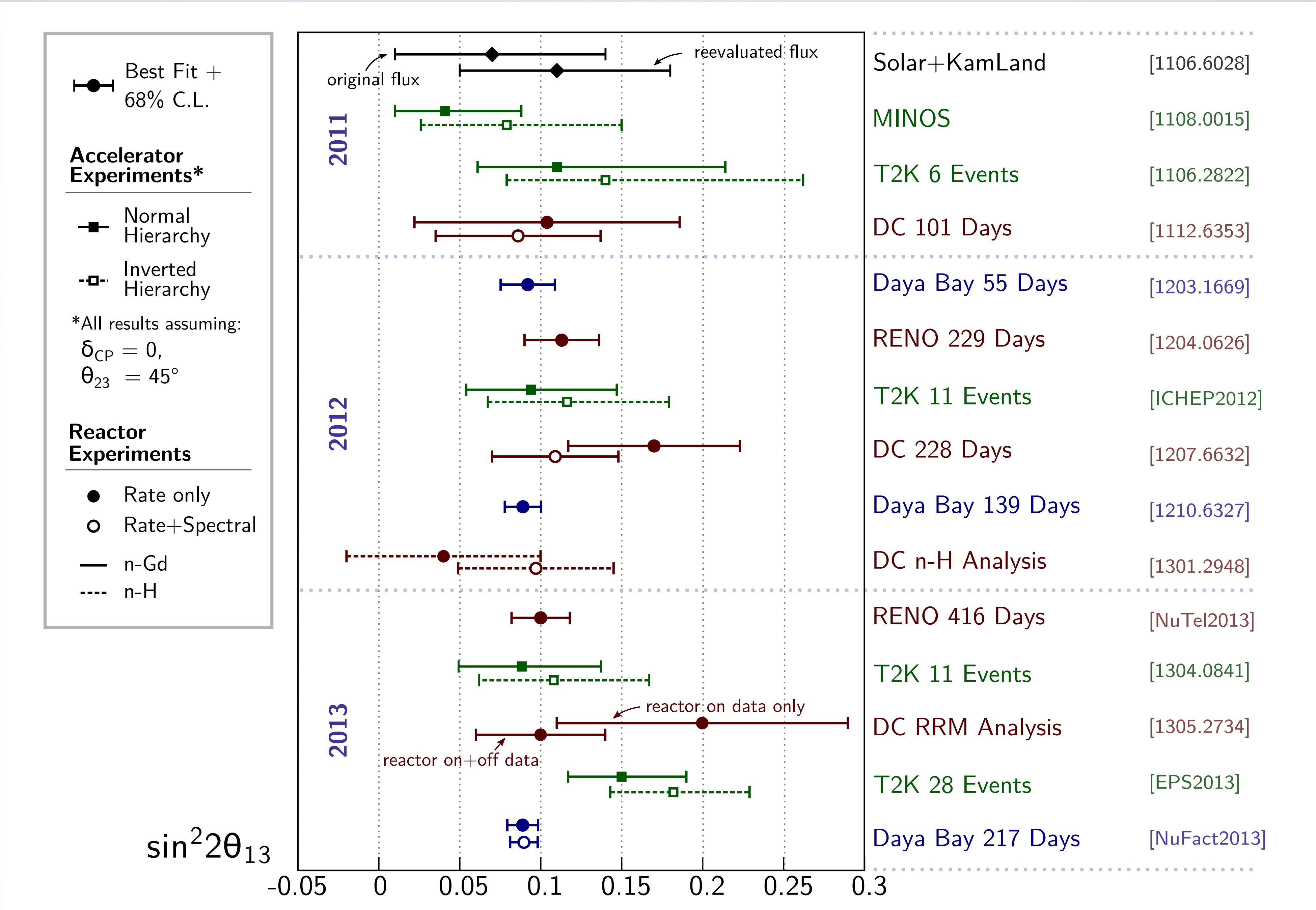

Daya Bay Onsite Progress

Final two detectors installed, operating since Oct. 2012.

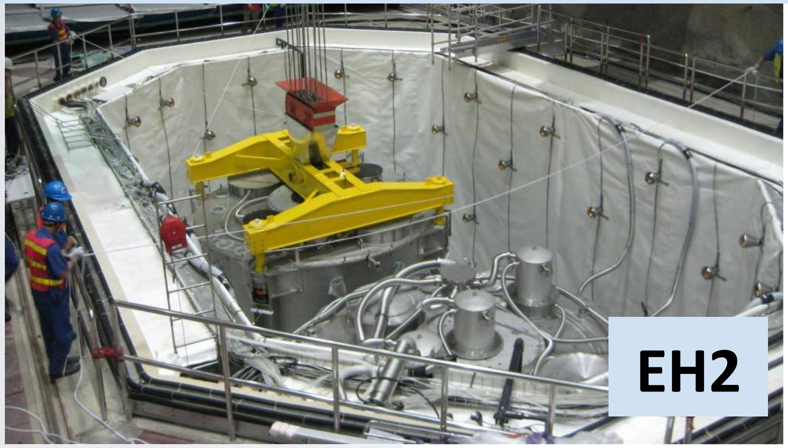

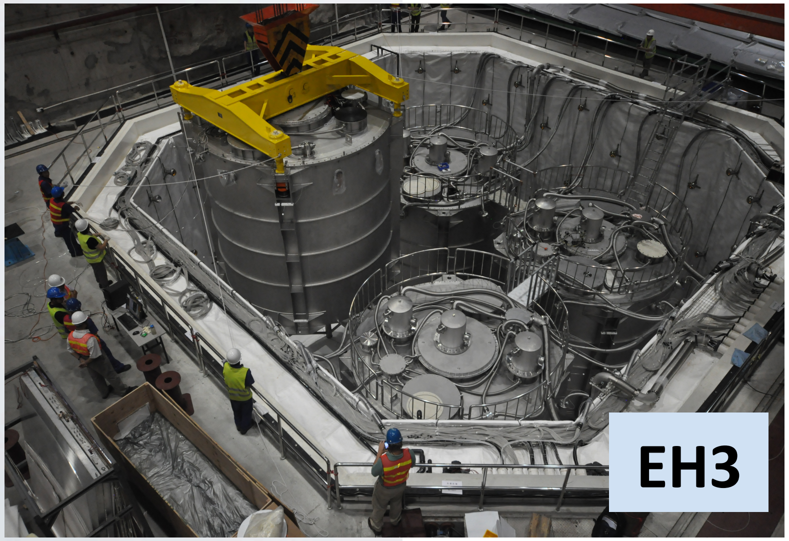

Full 4π detector calibration in Sep. 2012.

Future Sensitivity

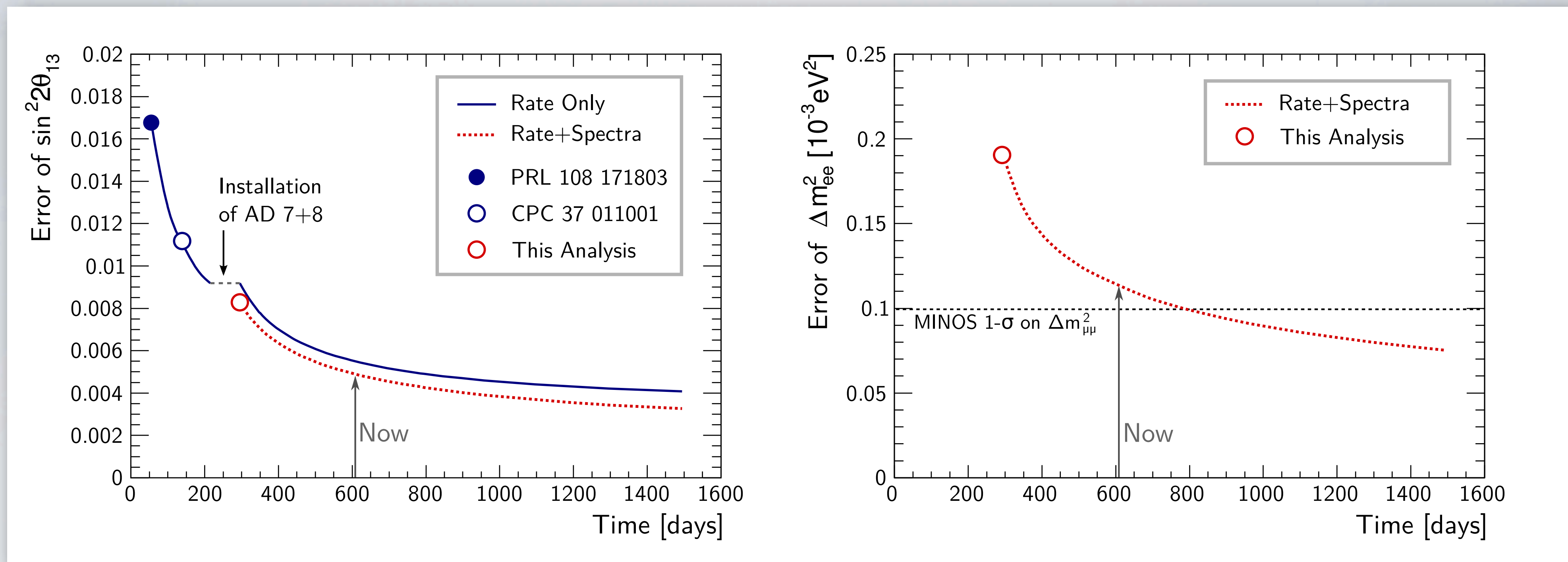

Sensitivity still dominated by statistics

- Statistics contribute 73% (65%) to total uncertainty in $\sin^2 2\theta_{13}$ ($|\Delta m^2_{ee}|$)
- Major systematics:
  - θ_{13}: Reactor model, relative + absolute energy, and relative efficiencies
  - $|\Delta m^2_{ee}|$: Relative energy model, relative efficiencies, and backgrounds
- Precision of mass splitting measurement closing in on results from μ flavor sector

How the data will look like in 2015

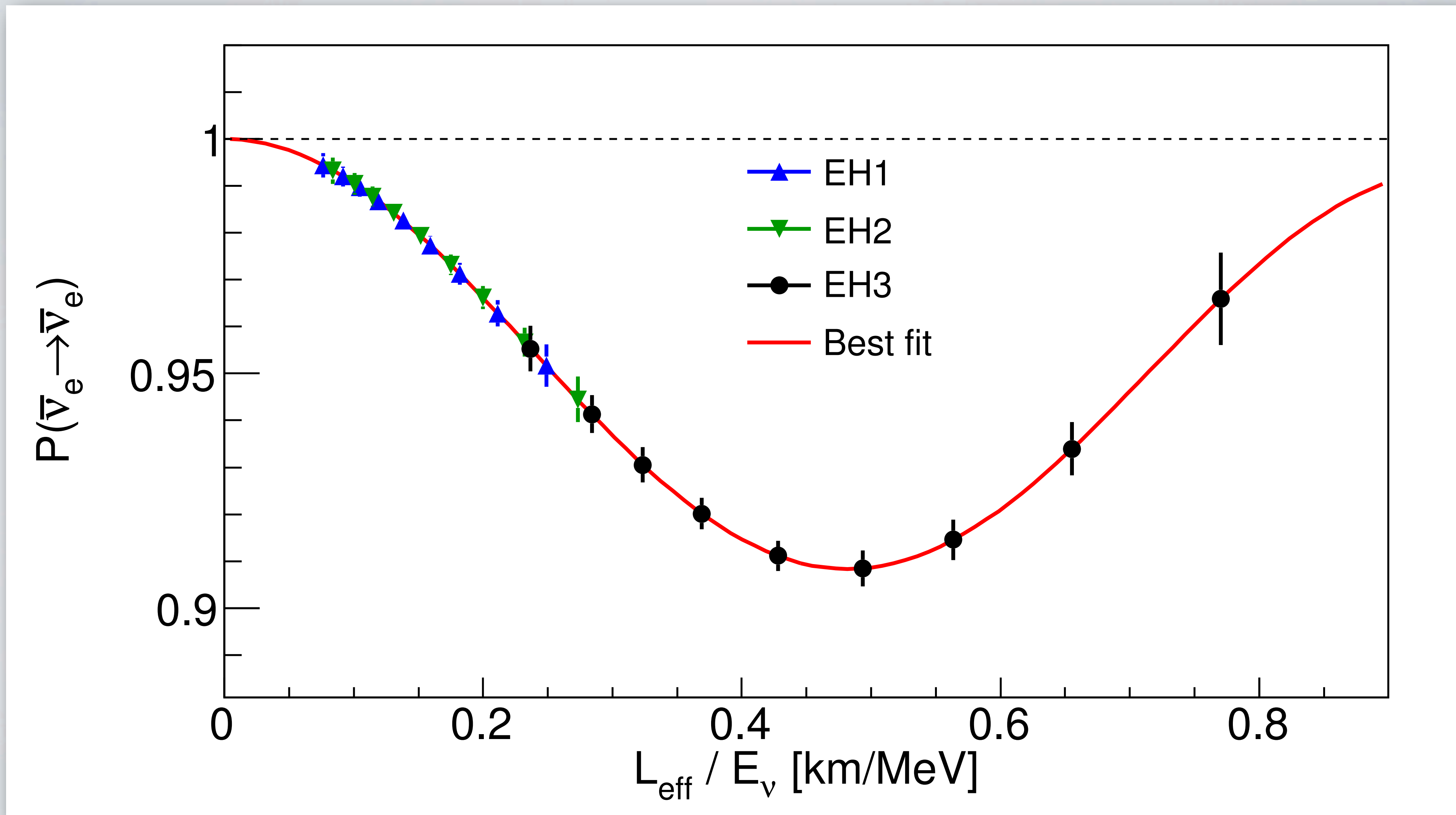

Summary

- The Daya Bay Experiment has made the first direct measurement of the short-distance electron antineutrino oscillation frequency:

$$|\Delta m^2_{ee}| = 2.59^{+0.19}_{-0.20} \times 10^{-3}\ \mathrm{eV}^2$$

- We also produced the most precise estimate of the mixing angle:

$$\sin^2 2\theta_{13} = 0.090^{+0.008}_{-0.009}$$

- Still, a lot of results coming in the near future:
  - Measurement of absolute reactor flux
  - Testing non-standard neutrino models
  - Significantly increased precision with much more statistics

Backup slides

Scintillator Response Model

Electron response

2 parameterizations to model quenching effects and Cherenkov radiation:

1) 3-parameter purely empirical model:

$$\frac{E_{\text{vis}}}{E_{\text{true}}} = \frac{1 + p_3 \cdot E_{true}}{1 + p_1 \cdot e^{-p_2 \cdot E_{\text{true}}}}$$

2) Semi-emp. model based on Birks' law:

$$\frac{E_{\text{vis}}}{E_{\text{true}}} = f_{\text{q}}(E_{\text{true}}; k_B) + k_C \cdot f_c(E_{\text{true}})$$

k_B: Birks' constant

k_C: Cherenkov contribution

Gammas + positrons

- Gammas connected to electron model through MC:

$$E_{\text{vis}}^{\gamma} = \int E_{\text{vis}}^{e^-}\left(E_{\text{true}}^{e^-}\right) \cdot \frac{dN}{dE}\left(E_{\text{true}}^{e^-}\right) dE_{\text{true}}^{e^-}$$

- Positrons connected to electron model through MC:

$$E_{\text{vis}}^{e^+} = E_{\text{vis}}^{e^-} + 2 \cdot E_{\text{vis}}^{\gamma}(0.511\,\text{MeV})$$

Simulation of individual e$^-$, e$^+$ energies due to gamma interaction in scintillator.

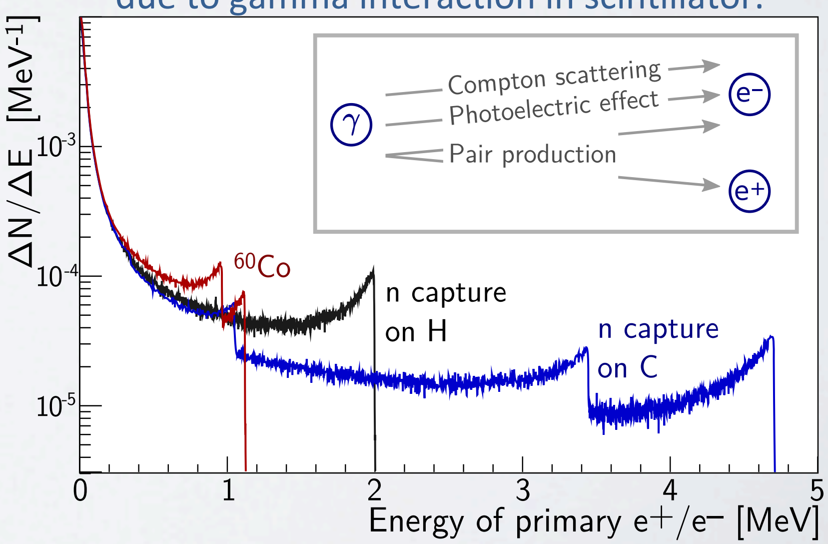

Electronics Non-Linearity Model

PMT readout electronics introduces additional biases

Electronics does not fully capture late secondary hits

- Slow scintillation component missed at high energies
- Charge collection efficiency decreases with visible light

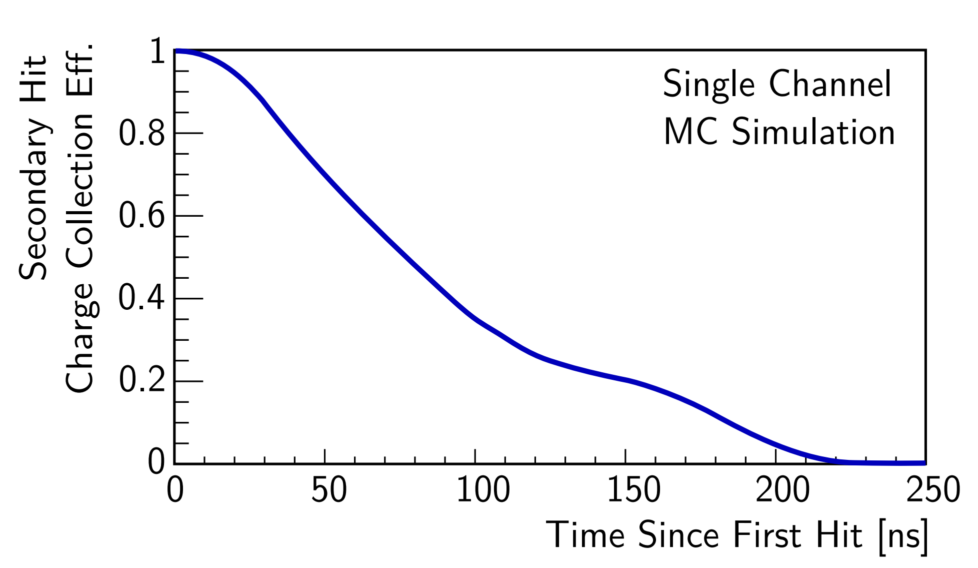

Observed non-linearity is a product of scintillator and electronics non-linearity

$$f = \frac{E_{\mathrm{rec}}}{E_{\mathrm{true}}} = \frac{E_{\mathrm{vis}}}{E_{\mathrm{true}}} \times \frac{E_{\mathrm{rec}}}{E_{\mathrm{vis}}} = f_{\mathrm{scint}}(E_{\mathrm{true}}) \times f_{\mathrm{elec}}(E_{\mathrm{vis}})$$

[1] Scintillator non-linearity → $\frac{E_{\mathrm{vis}}}{E_{\mathrm{true}}}$

[2] Electronics non-linearity → $\frac{E_{\mathrm{rec}}}{E_{\mathrm{vis}}}$

Constrained the model with full use of current existing data...

Trigger Performance

Trigger Thresholds:

- AD: >45 PMTs (digital trigger)
  >0.4 MeV (analog trigger)
- Inner Water Veto: > 6 PMTs
- Outer Water Veto: >7 PMTs
- RPC: ¾ layers in module

Trigger Efficiency:

- No measureable inefficiency >0.7 MeV
- Minimum energy expected for prompt antineutrino signal is ~0.9 MeV.

Digital Trigger (Nhit)

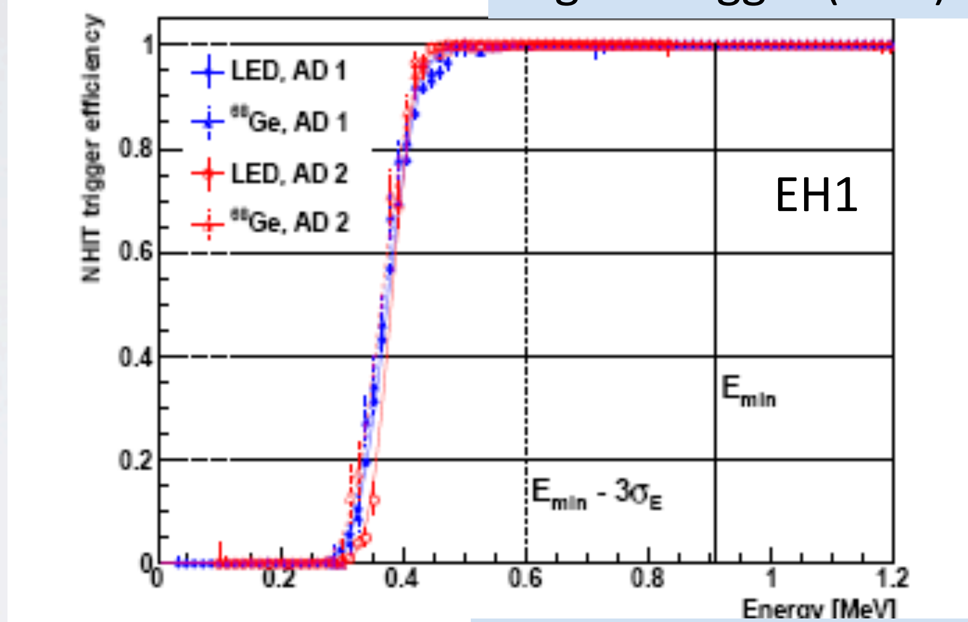

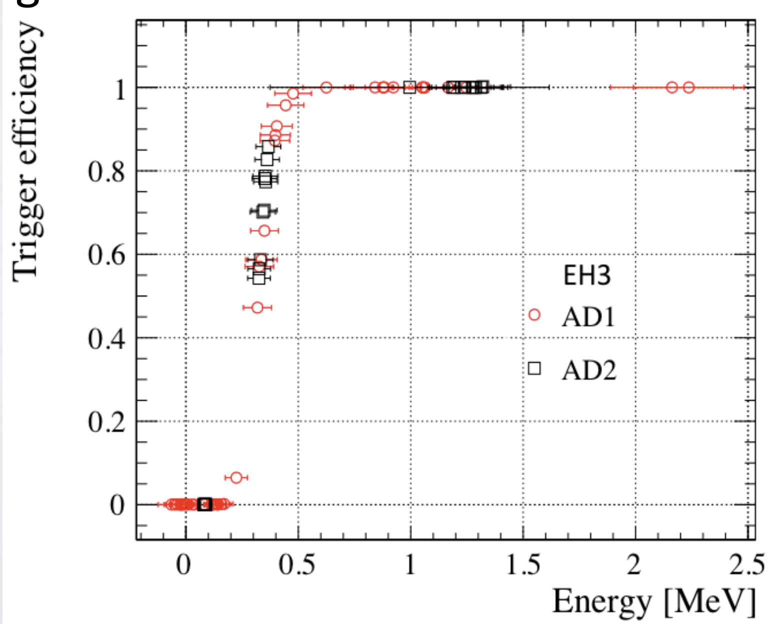

Analog Trigger (Esum)

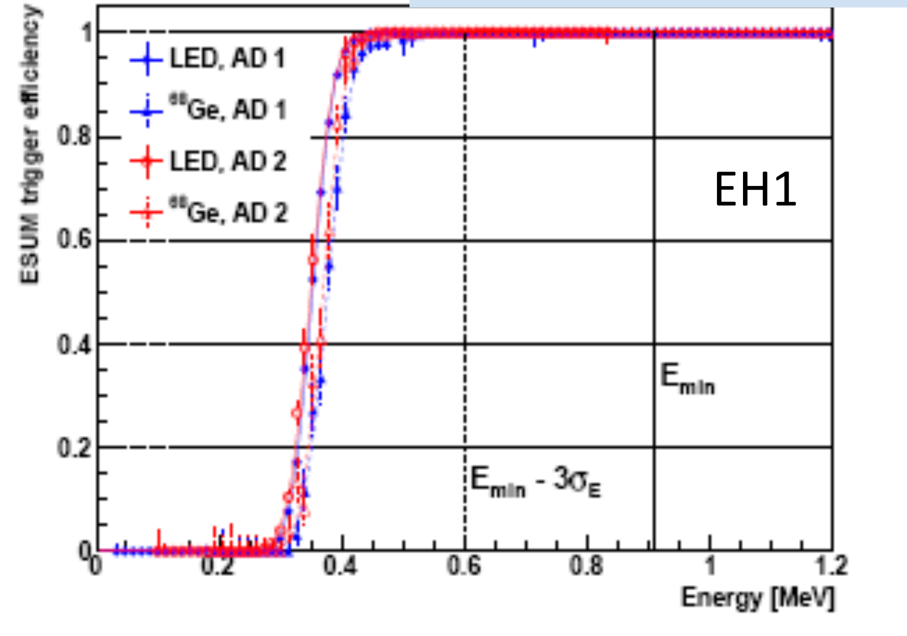

Calibration: PMT+Electronics Gain

Measure charge from single photons in-situ with data

Use out-of-time PMT signals hits to calibrate the PMT + electronics response to single photons.

Cross-check with weekly LED deployments.

Gain variation with time

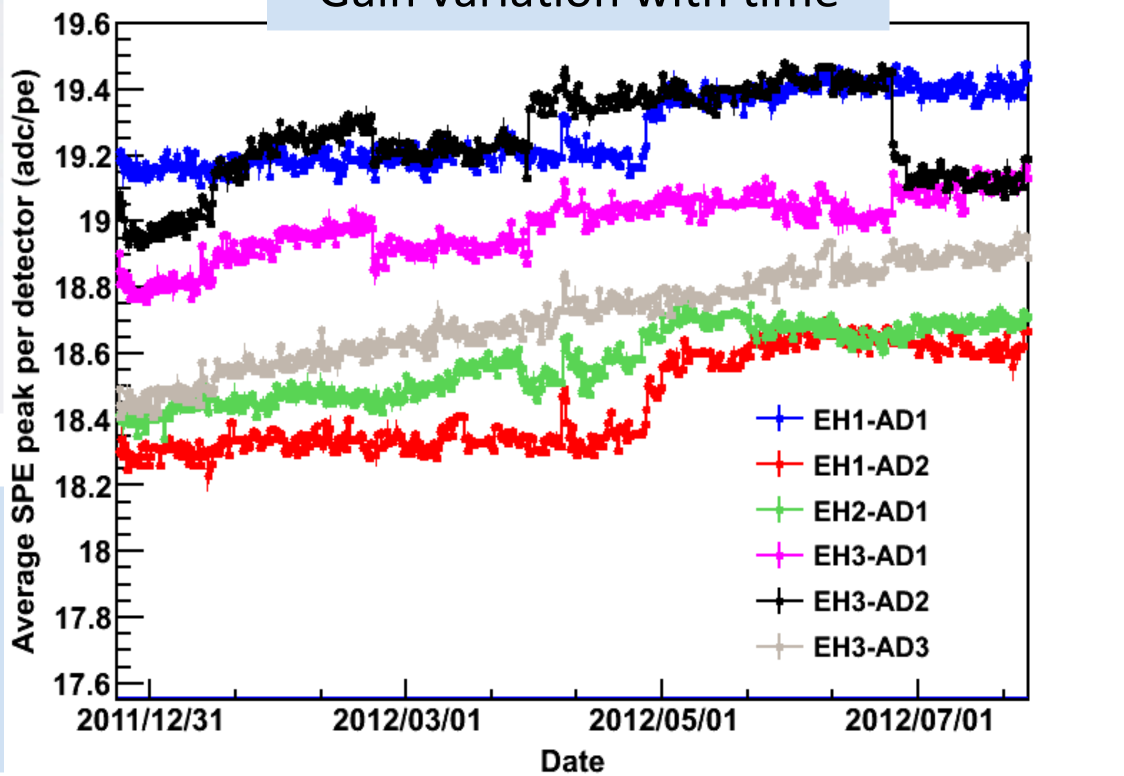

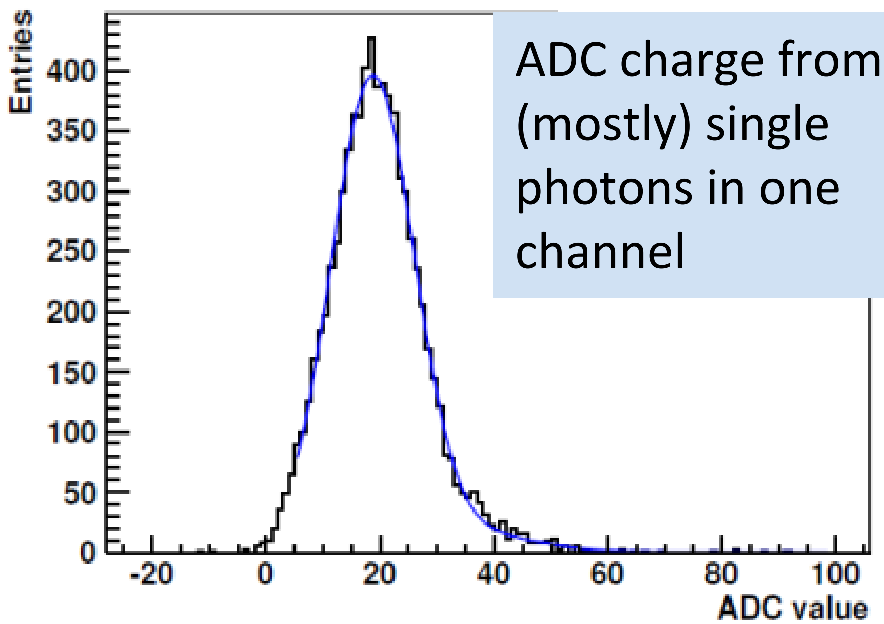

ADC charge from (mostly) single photons in one channel

Calibration driven by uncertainty in relative detector efficiency

$$\frac{N_\mathrm{f}}{N_\mathrm{n}} = \left(\frac{N_\mathrm{p,f}}{N_\mathrm{p,n}}\right)\left(\frac{L_\mathrm{n}}{L_\mathrm{f}}\right)^2\left(\frac{\epsilon_\mathrm{f}}{\epsilon_\mathrm{n}}\right)\left[\frac{P_\mathrm{sur}(E,L_\mathrm{f})}{P_\mathrm{sur}(E,L_\mathrm{n})}\right]$$

Calibration: Energy Scale

Measure energy scale in-situ with data

Calibrate charge (photoelectrons) collected per MeV in-situ using spallation nGd capture events. Also use weekly deployments of ^{60}Co source.

Spallation *n*Gd capture
(uniform throughout detector)

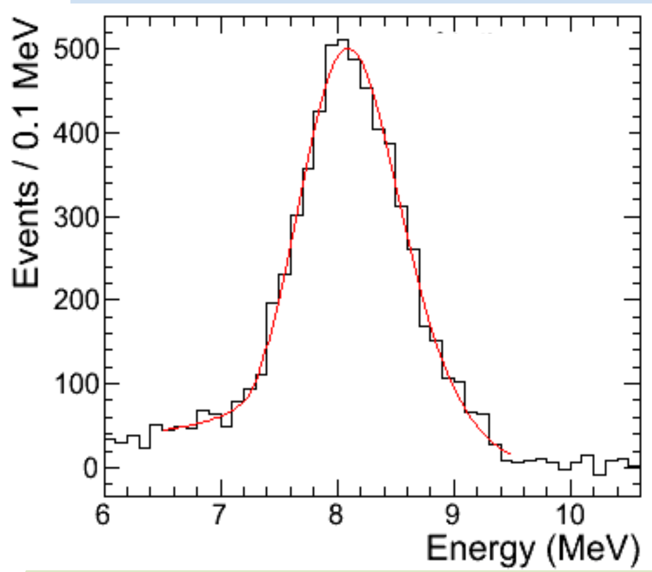

Energy Scale = Q / E

Measured charge of nGd peak

Average energy released in nGd

~1.5%/year degradation of the energy scale

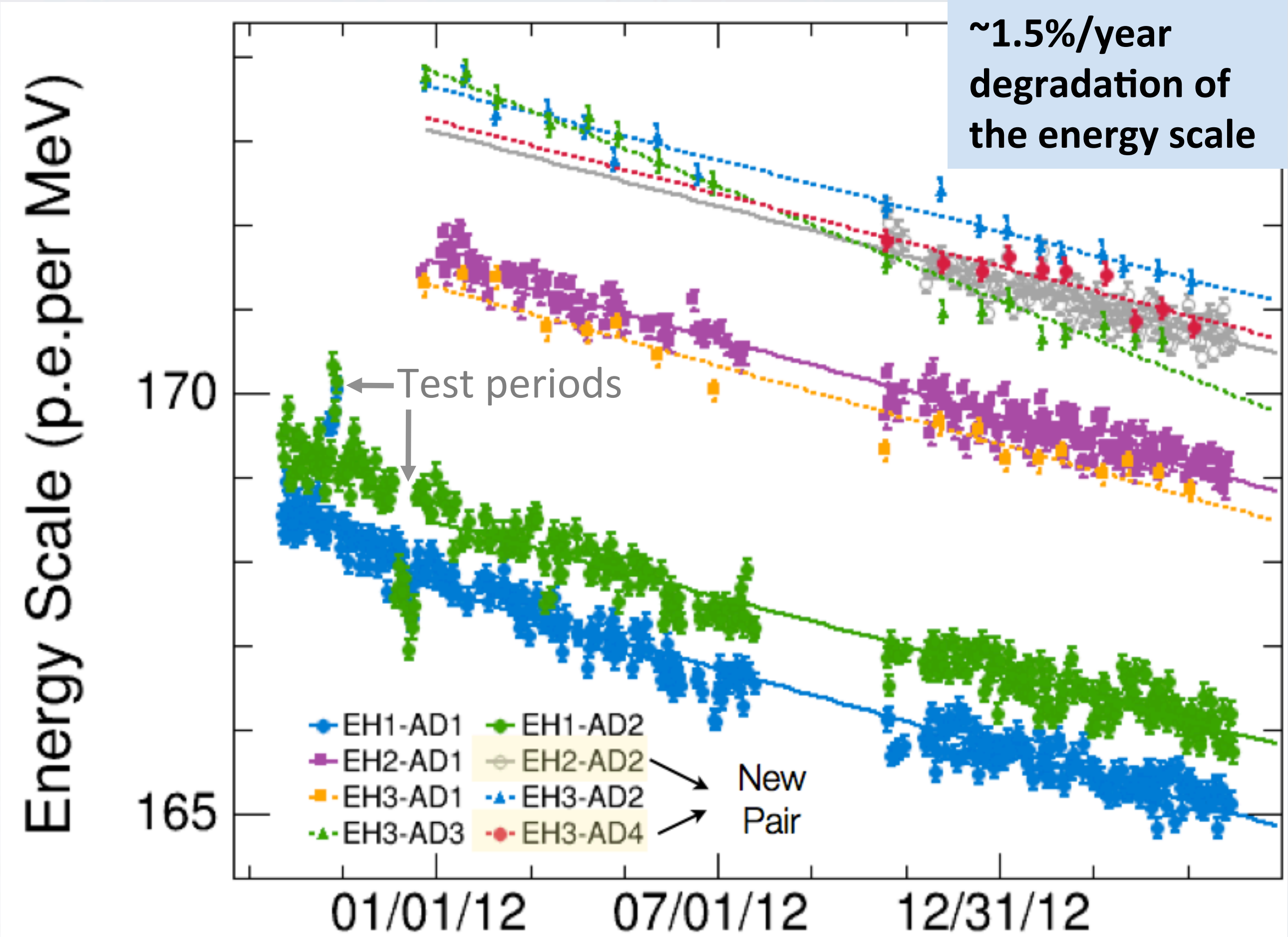

Small degradation of energy scale is seen with nGd, ^{60}Co, and other event types. Its origin is still unknown, but do not anticipate any problems in experiment's lifetime.

Calibration: Detector Uniformity

Measure uniformity with sources placed along three axes and spallation nGd events

Example: ^{60}Co

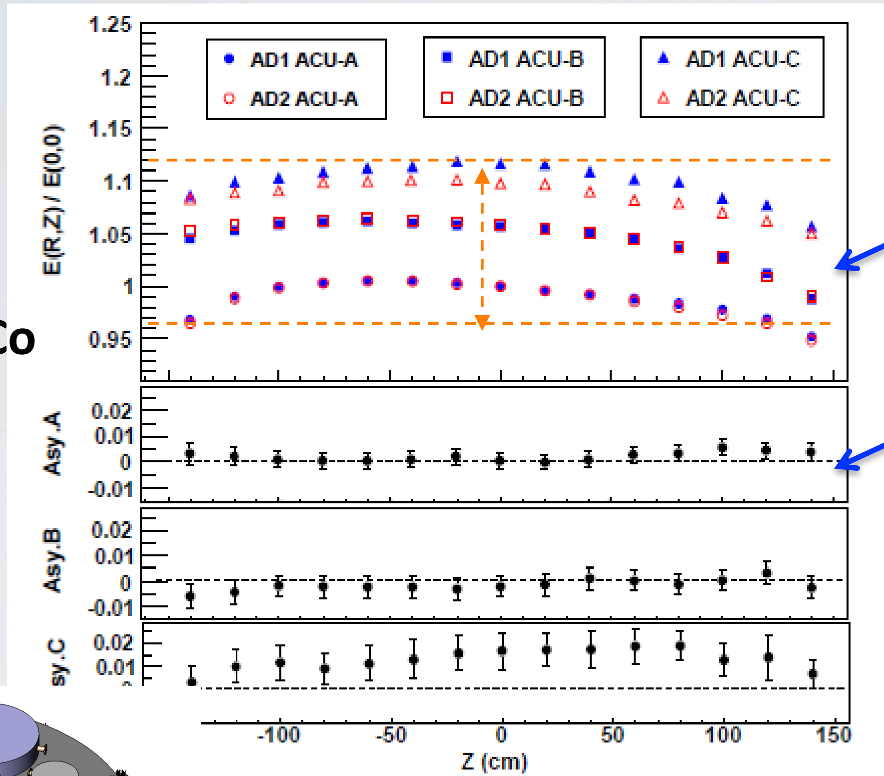

Energy response varies across detector…

…but still consistent between detectors

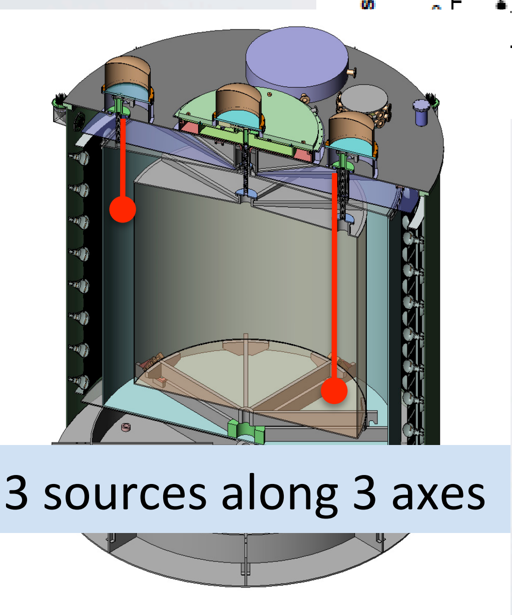

3 sources along 3 axes

After first-order correction, energy is more uniform.

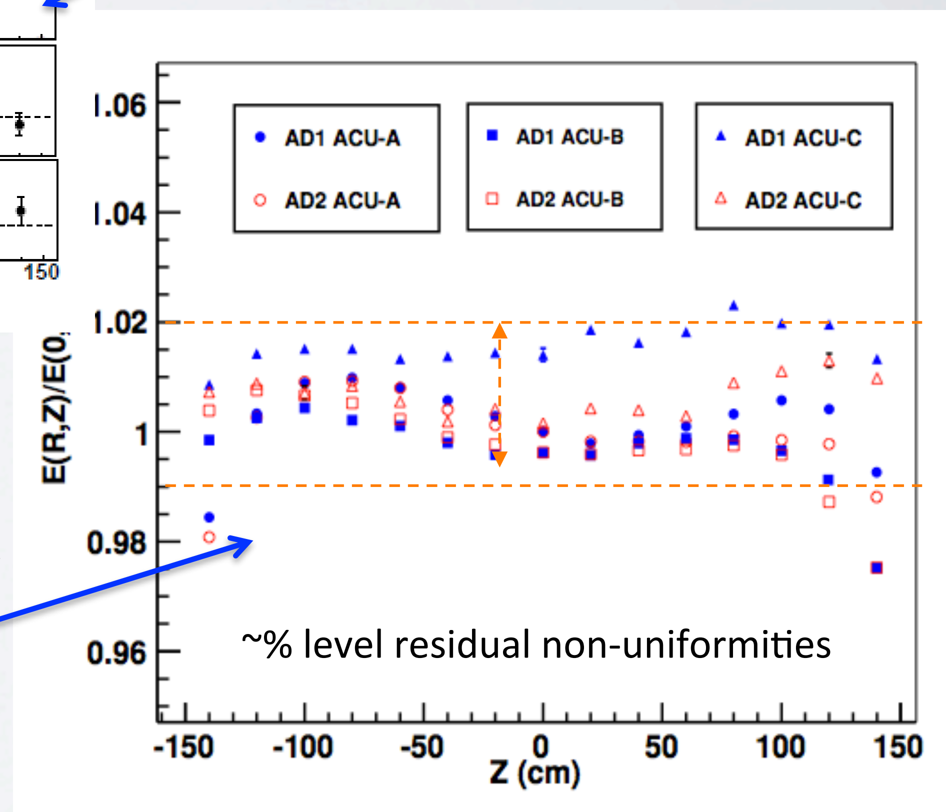

Delayed Energy Cut

Largest uncertainty between detectors

Some *n*Gd gammas escape scintillator region, visible as tail of *n*Gd energy peak.

Use variations in energy peaks to constrain relative efficiency.

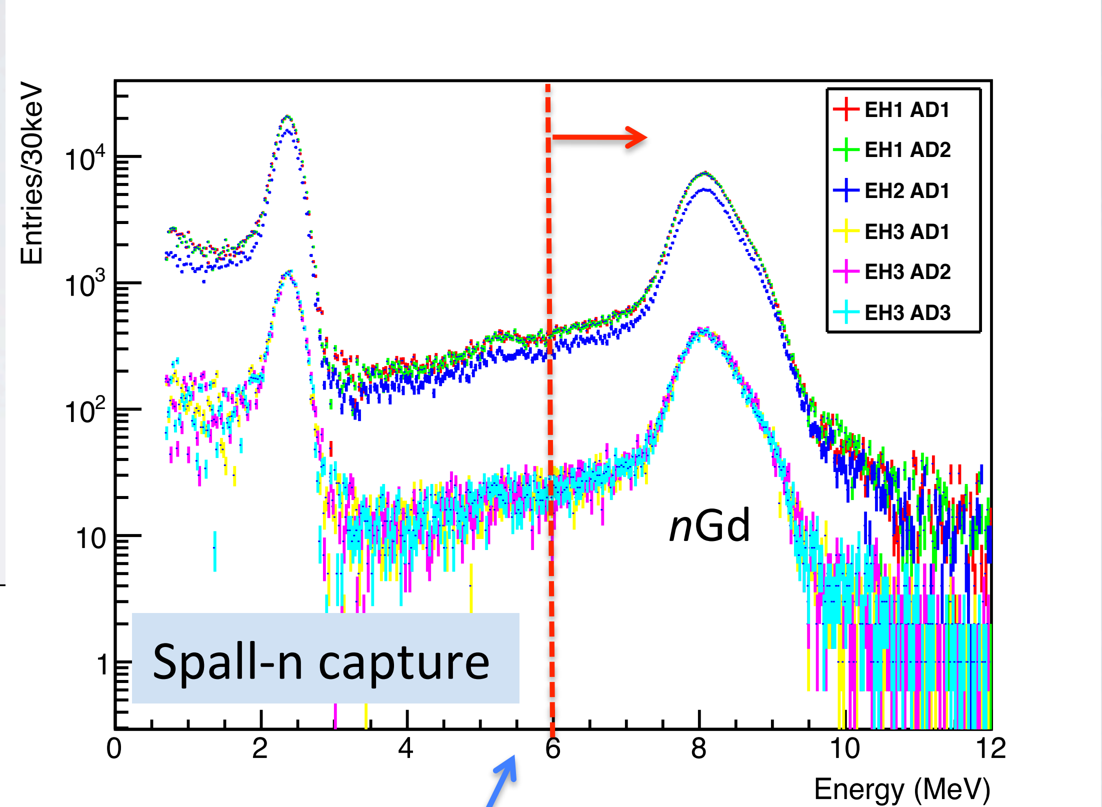

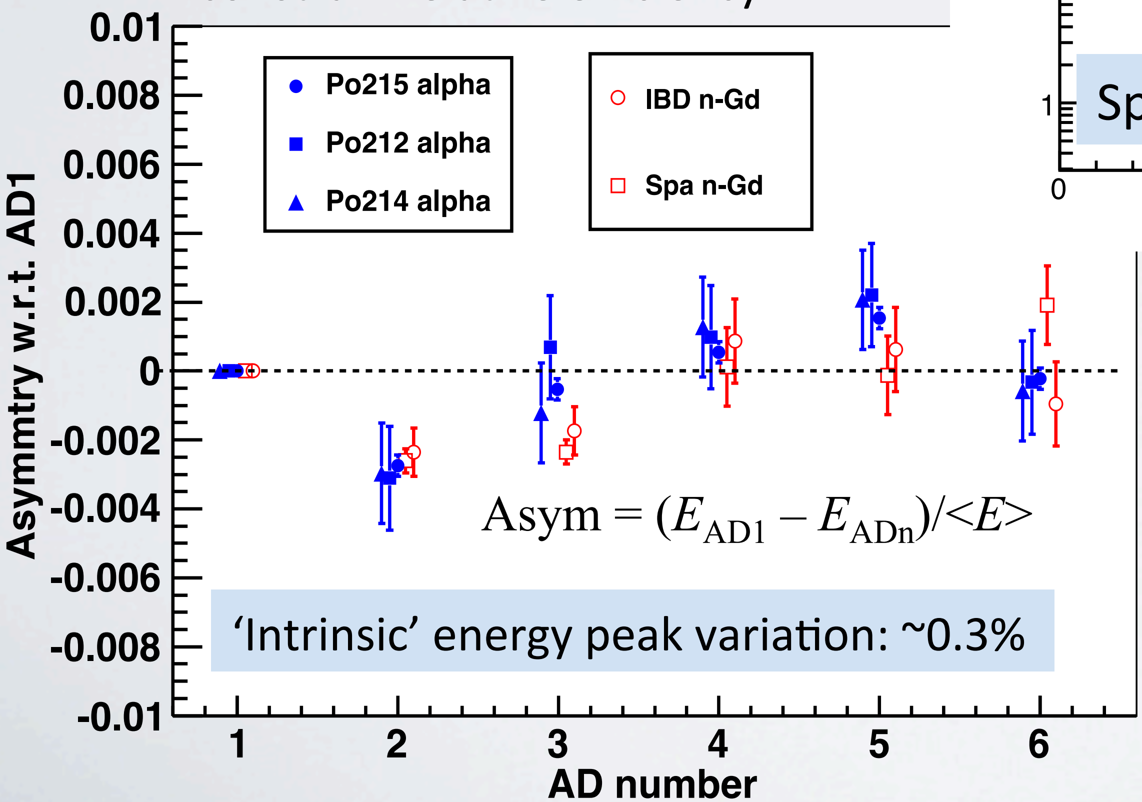

Efficiency variations estimated at 0.12%

Motivation
for
3-zone design

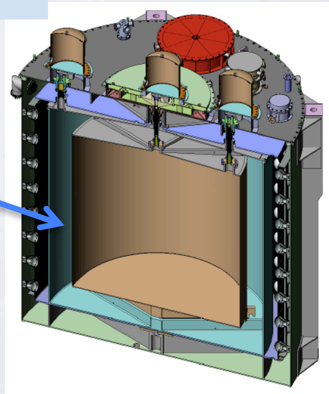

Capture Time

Consistent IBD neutron capture time measured in all detectors

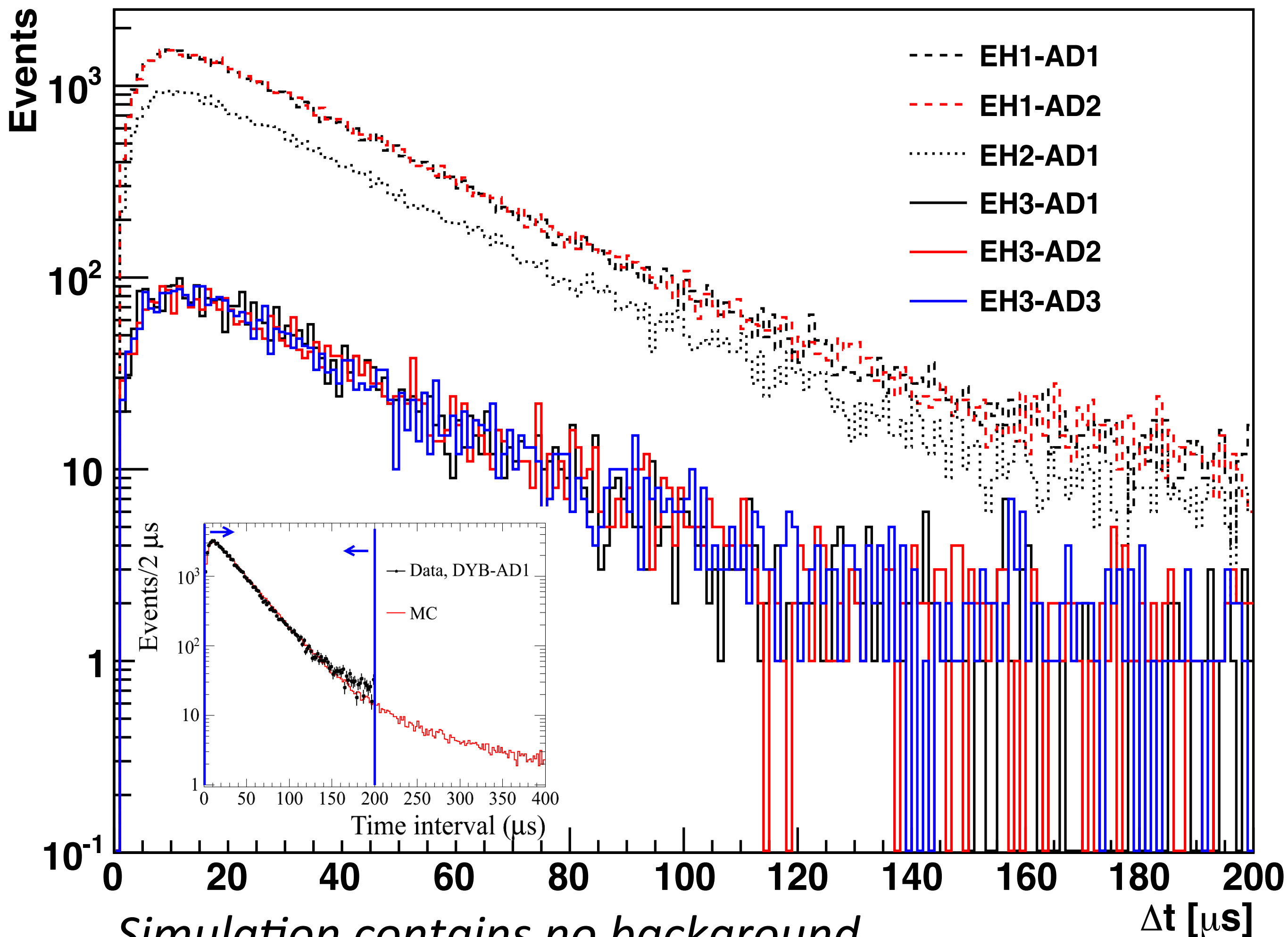

Simulation contains no background (deviates from data at >150 μs)

Capture time cut:
1μs to 200μs

Efficiency uncertainty within 0.01% between detectors.

Accidental backgrounds

Two uncorrelated signals can accidentally mimic an antineutrino signal.

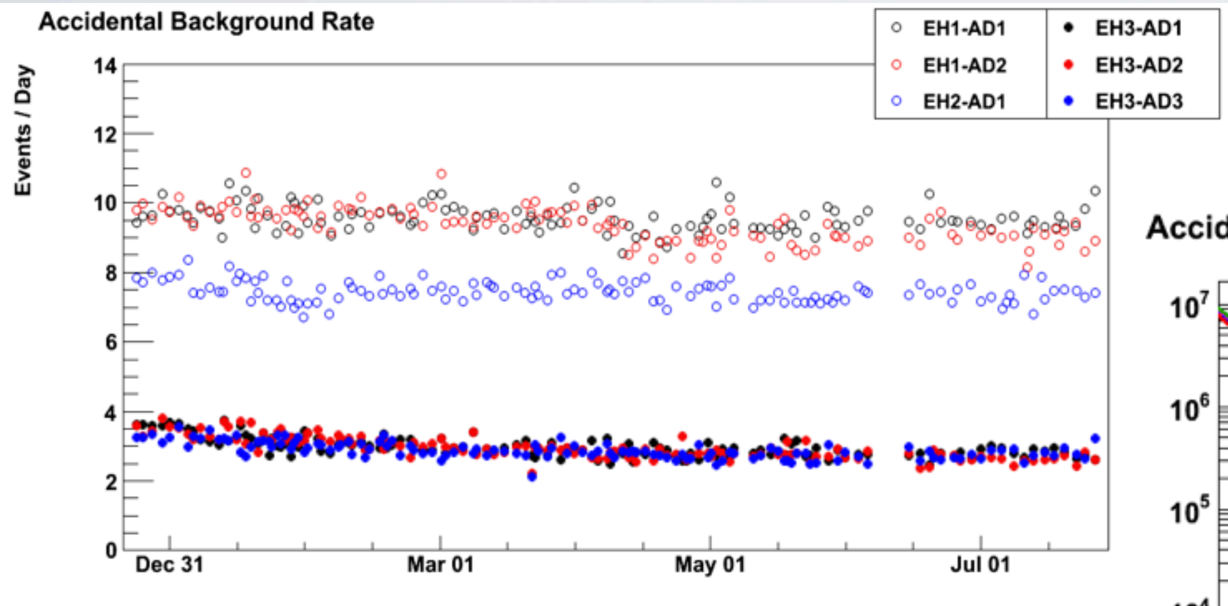

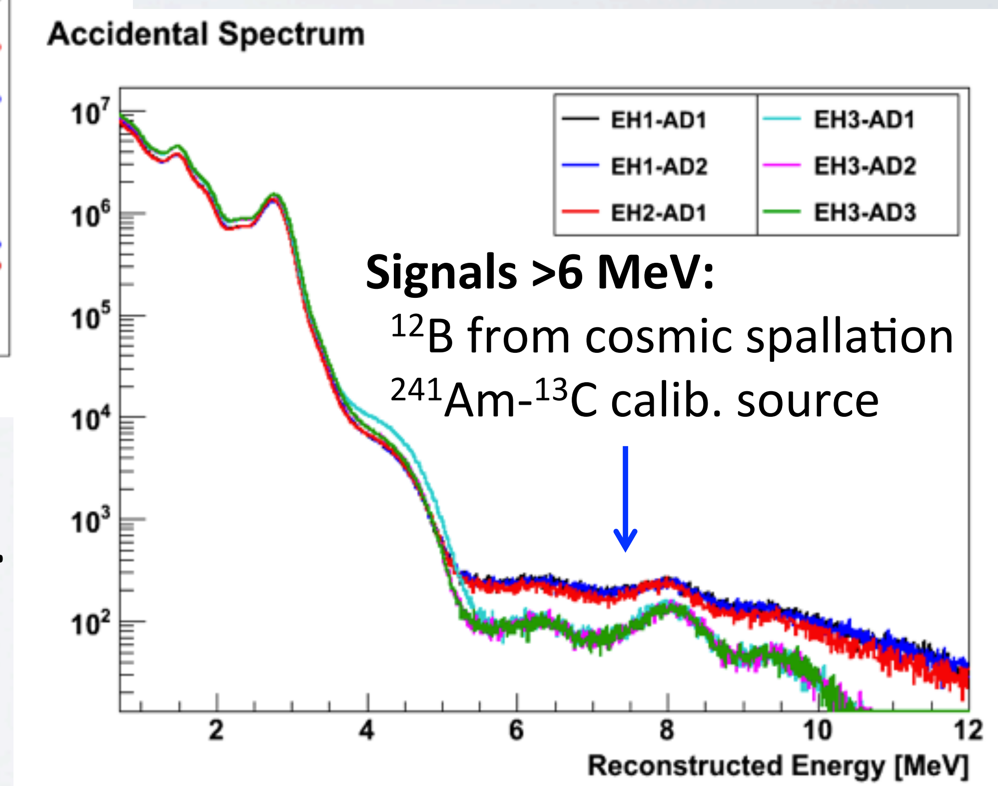

Accidental B/S is 4% (1.5%) of far (near) signal.

Accidental background be accurately modeled using uncorrelated signals in data.

➔ Negligible uncertainty in background rate or spectra.

Fast-neutron backgrounds

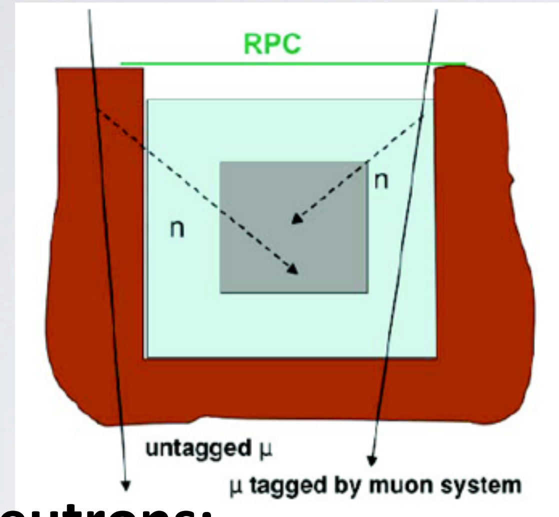

Fast Neutrons:

Energetic neutrons produced by cosmic rays (inside and outside of muon veto system)

Mimics antineutrino (IBD) signal:

- Prompt: Neutron collides/stops in target
- Delayed: Neutron captures on Gd

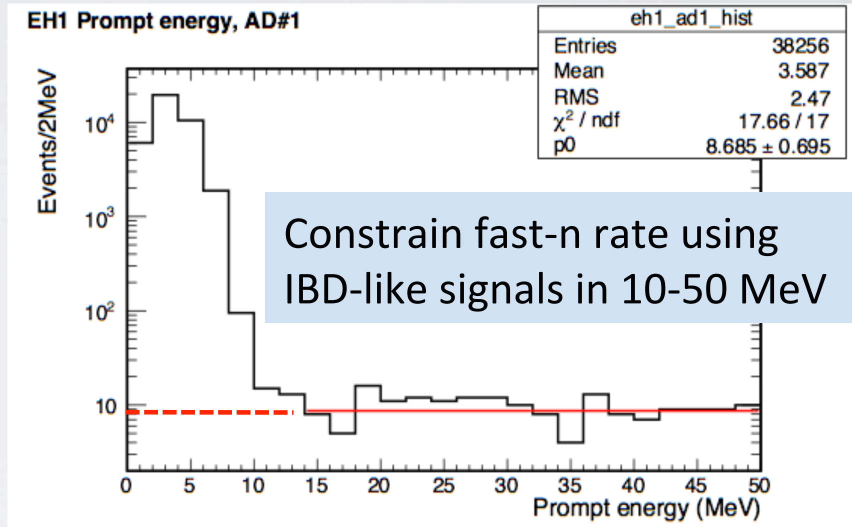

Constrain fast-n rate using IBD-like signals in 10-50 MeV

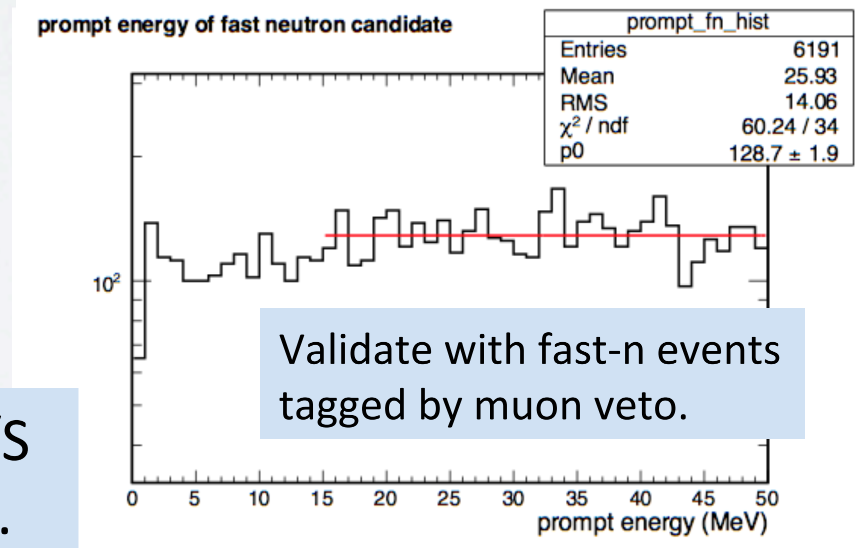

Validate with fast-n events tagged by muon veto.

Analysis muon veto cuts control B/S to 0.06% (0.1%) of far (near) signal.

Reactor Flux Models

Antineutrino flux S(E) from each reactor used to predict IBDs at each detector

	^{235}U	^{238}U	^{239}Pu	^{241}Pu
AD 1	63.3	12.2	19.5	4.8
AD 2	63.3	12.2	19.5	4.8
AD 3	61.0	12.5	21.5	4.9
AD 4	61.5	12.4	21.1	4.9
AD 5	61.5	12.4	21.1	4.9
AD 6	61.5	12.4	21.1	4.9

Approximate percentage of IBDs from each fission isotope at each detector

New/Old flux model difference in unoscillated IBD prediction by hall

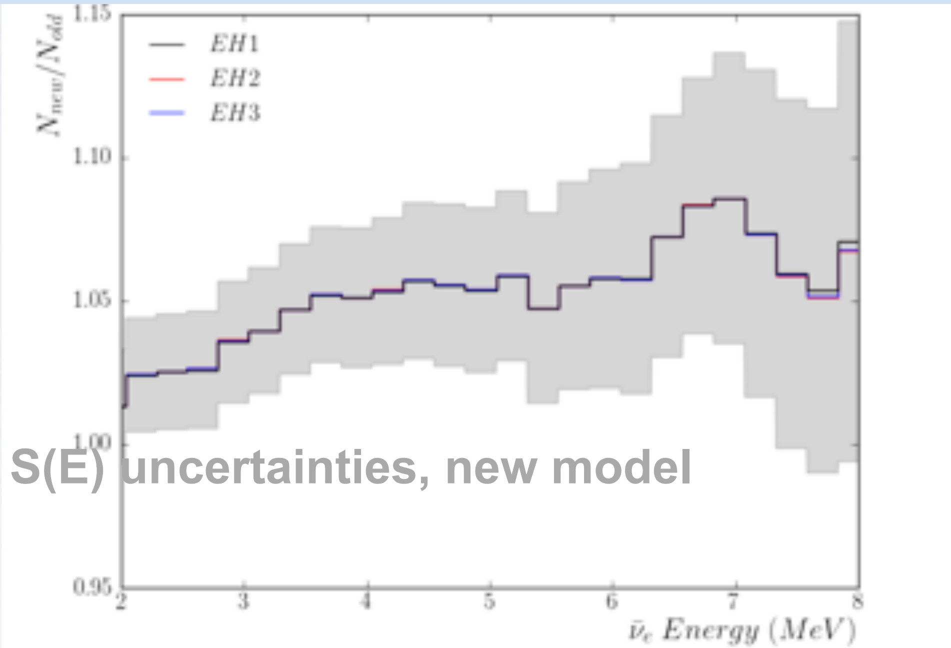

Flux model has negligible impact on far vs. near oscillation measurement

New model:

P. Huber, Phys. Rev. C84, 024617 (2011),
T. Mueller et al., Phys. Rev. C83, 054615 (2011)

Old model:

K. Schreckenbach et al., Phys. Lett. B160, 325 (1985)
A. A. Hahn et al., Phys. Lett. B218, 365 (1989)
P. Vogel et al. Phys. Rev. C24, 1543 (1981)

Rate Uncertainty Summary

Detector			
	Efficiency	Correlated	Uncorrelated
Target Protons		0.47%	0.03%
Flasher cut	99.98%	0.01%	0.01%
Delayed energy cut	90.9%	0.6%	0.12%
Prompt energy cut	99.88%	0.10%	0.01%
Multiplicity cut		0.02%	<0.01%
Capture time cut	98.6%	0.12%	0.01%
Gd capture ratio	83.8%	0.8%	<0.1%
Spill-in	105.0%	1.5%	0.02%
Livetime	100.0%	0.002%	<0.01%
Combined	78.8%	1.9%	0.2%

Reactor			
Correlated		Uncorrelated	
Energy/fission	0.2%	Power	0.5%
$\overline{\nu}_e$/fission	3%	Fission fraction	0.6%
		Spent fuel	0.3%
Combined	3%	Combined	0.8%

With near/far measurement, correlated uncertainties cancel.
Only uncorrelated uncertainties are used.

Largest systematics are smaller than far site statistics (~1%)

Uncorrelated reactor systematics reduced by far vs. near measurement.

Daya Bay Future

Improved precision on oscillation parameters

- Constrains non-standard oscillation models
- Improves reach of future neutrino experiments

Measure absolute reactor neutrino flux

- Explore the 'reactor antineutrino anomaly'
- Precise spectrum probes reactor models

Cosmogenic Backgrounds

- Measurement of cosmogenic production vs. depth

Supernova Neutrinos

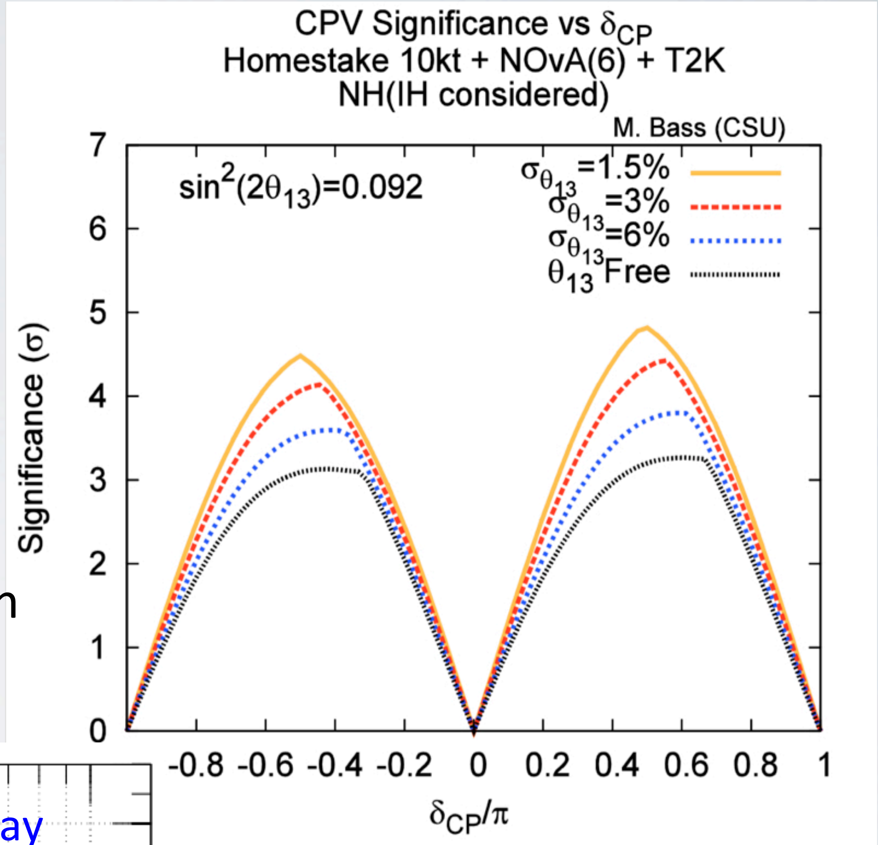

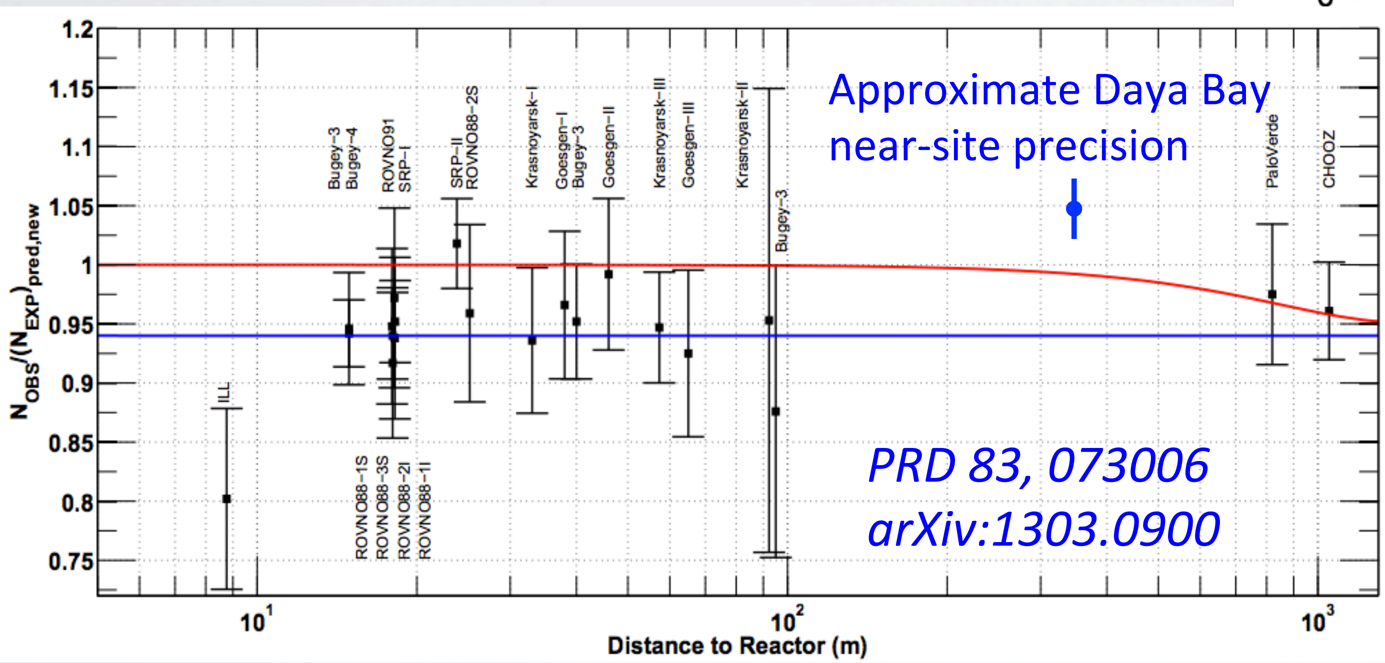

χ^2 definition

$$\chi^2 = \sum_{i}^{det\times E_p} \left[N_i^{pred}(\theta_{13}, \Delta m^2_{ee}, \vec{f}, \vec{\eta}, \vec{\epsilon}, \vec{b}), - N_i^{data} + N_i^{data} \log \frac{N_i^{data}}{N_i^{pred}(\theta_{13}, \Delta m^2_{ee}, \vec{f}, \vec{\eta}, \vec{\epsilon}, \vec{b})}\right]$$

$$+ \sum_{j}^{site\times E_p} \sum_{k}^{site\times E_p} f_j V^{-1}_{jk} f_k$$ Reactor Flux Model Constraint

$$+ \sum_{l}^{abs.E} \frac{\eta_l^2}{\sigma_l^2}$$ Energy Model Constraint

$$+ \sum_{m}^{det\times eff} \frac{\epsilon_m^2}{\sigma_m^2}$$ Detector Efficiency Constraint

$$+ \sum_{n}^{det\times bg} \frac{b_n^2}{\sigma_n^2}$$ Background Constraint

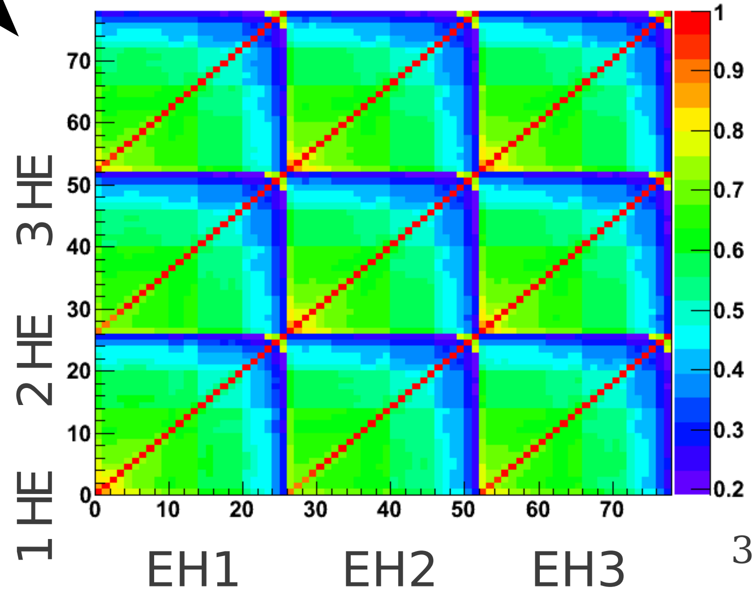

- Binned maximum likelihood method
- Constrain with the uncertainty from reactor flux model, background and relative detection efficiency.
  - Using covariance matrix to reduce number of the nuisance parameters for the reactor flux model.

Far vs. near relative measurement [No constraint on the absolute rate]

Pure Spectral Analysis

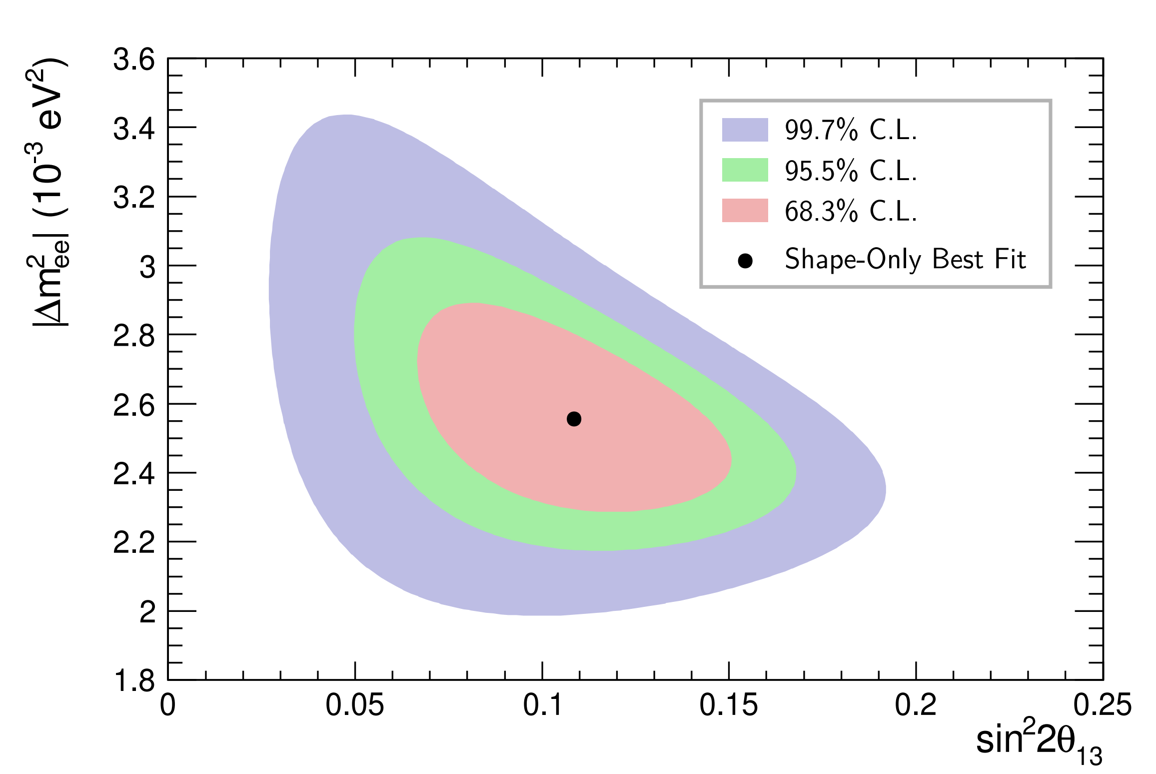

$$\sin^2 2\theta_{13} = 0.108 \pm 0.028$$

$$|\Delta m^2_{ee}| = 2.55^{+0.21}_{-0.18} \cdot 10^{-3} \mathrm{eV}^2$$

$$\chi^2/N_{\mathrm{DoF}} = 161.2/148$$

θ_{13} = 0 can be excluded at > 3σ from spectral information alone

- For each AD, total event prediction fixed to observed data:

  1. θ_{13} free-floating: $\chi^2/N_{\mathrm{DoF}} = 161.2/148$
  2. $\theta_{13} = 0$: $\chi^2/N_{\mathrm{DoF}} = 178.5/146$

$\Rightarrow \Delta\chi^2/N_{\mathrm{DoF}} = 17.3/2$, corresponding to $p = 1.75 \cdot 10^{-4}$

$\sin^2 2\theta_{13}$ sensitivity projection

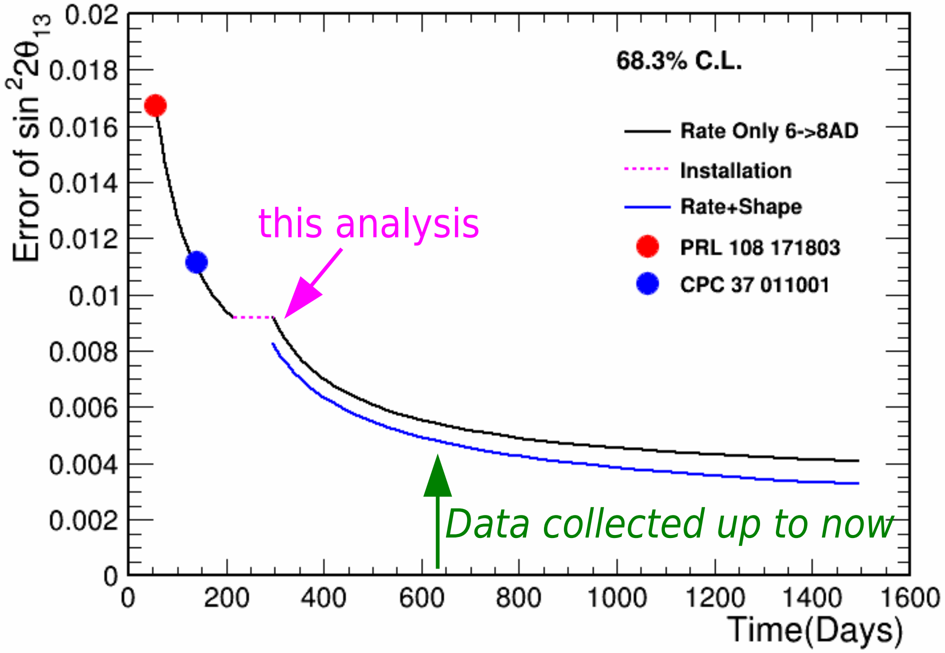

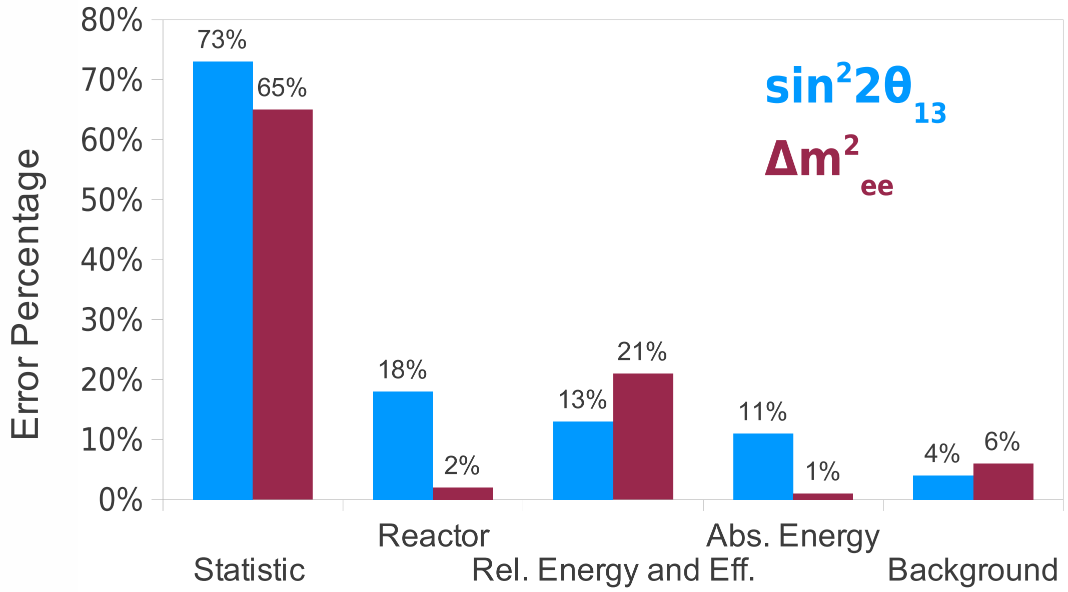

- Current errors are dominated by the statistical uncertainties (73%)
- Major systematics:
  - Reactor Model, relative+absolute energy and detector efficiency
- Daya Bay $\sin^2 2\theta_{13}$ final precision ~4%, it can be further improved by adding nH capture analysis

Δm^2 sensitivity projection

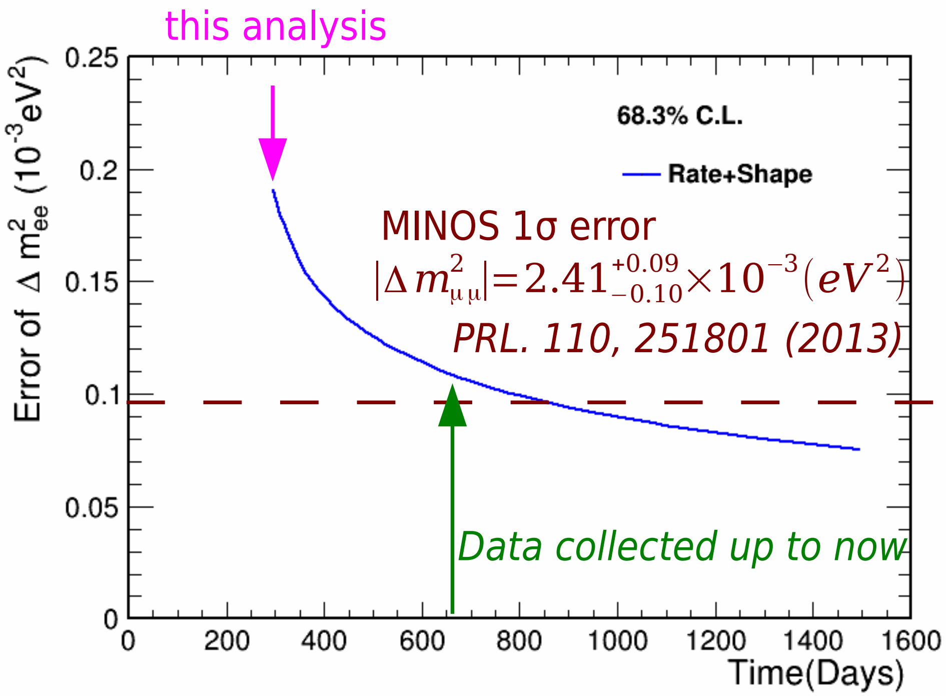

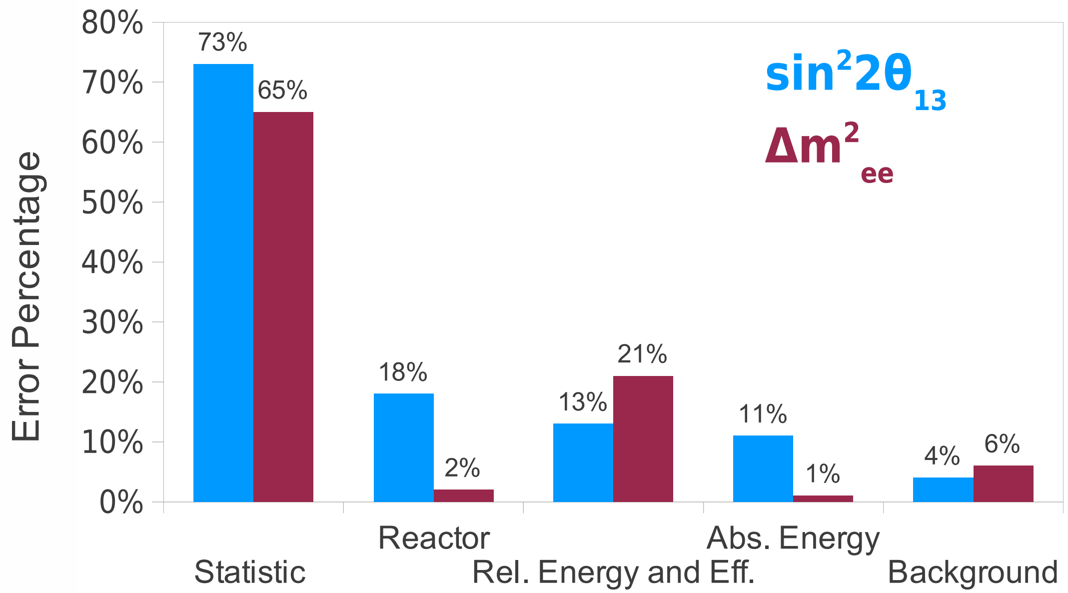

- Current errors are dominated by the statistical uncertainties (73%)
- Major systematics:
  - Relative energy and background
- Daya Bay $|\Delta m^2_{ee}|$ final precision ~0.1×10^{-3} eV^2, comparable to the results from μ flavor sector

Making a Far Site prediction from the Near Site data

From the

- relative reactor core power info
- experimental layout geometry

it is possible to determine what fraction of events in each near detector at each true energy bin originate from each core.

Each of these components is then individually extrapolated to the far site

All reactor and detector correlated systematics, including the absolute flux and shape uncertainties, **cancel to first order.**

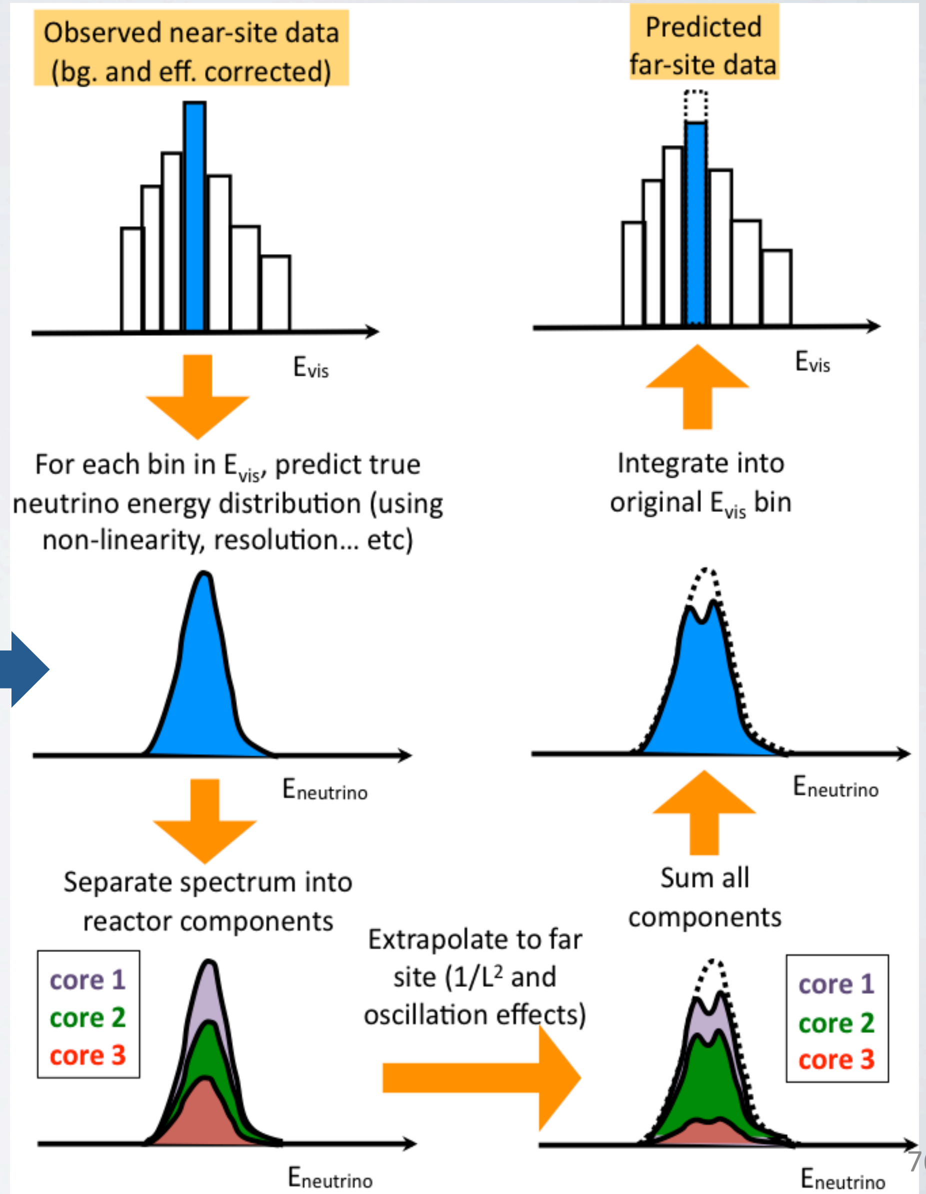

76

Δm^2_{ee}, $\Delta m^2_{\mu\mu}$ and MH

- Value of Δm^2_{ee} constrained by the effective mass splitting measured by muon (anti-)neutrino disappearance, $\Delta m^2_{\mu\mu}$.

$$P(\nu_\mu \to \nu_\mu) \simeq 1 - \sin^2 2\theta_{23} \sin^2 \left(\Delta m^2_{\mu\mu} \frac{L}{4E} \right)$$

- Reactor neutrinos can make independent measurement of Δm^2_{ee}
  - Important test of the three-flavor oscillation model
  - Need <1% precision for both Δm^2_{ee} and $\Delta m^2_{\mu\mu}$ to resolve mass hierarchy.
  - Extensively discussed in
    - PRD 72, 013009(2005) and
    - PRD 74, 053008 (2006)